Hydrocarbon migration in the Utsira High area

Master thesis
Reservoir and basin studies

ALEKSEJS FJODOROVS

UNIVERSITY OF BERGEN

DEPARTMENT FOR EARTH SCIENCE

JANUARY 2021

Abstract

The understanding of the migration routes is important for the evaluation and prediction of the position of the remaining resources on the Norwegian Continental Shelf. Various mechanisms can affect the migration and accumulation of the hydrocarbons. This can greatly affect the explorational efforts and the economic perspectivity of the prospects.

This study's goal is to investigate the possible migration routes onto and around the various fields and the discoveries in the Utsira high area. In addition, a review of the migration through the unusual, permeable basement has been conducted.

The Utsira High has been geologically mapped by the interpretation of the high-resolution 3D-seismic data. Available geological, geophysical and geochemical data from the exploration wells was collected and interpreted in order to propose migration routes and migration mechanisms that are responsible for the filling of the local structure.

The two different migration pathways with source in the South Viking Graben, have been proposed to be responsible for the filling of the fields. The migration pathways are entering the high from the west and the south-west. A possible north-western migration pathway was excluded after the review.

The Edvard Grieg and the Solveig field are most likely the first traps upon the migration from the west and south west respectively. The Edvard Grieg oil has most likely migrated towards the P-graben and the Ragnarrock discoveries, but this route has been blocked later. Due to the relative pressure differences the discoveries are thought to be leaking vertically towards the Cretaceous chalk.

As a result of the blockage of the migration towards the P-graben and the Ragnarrock, the migration continued to the Rolfsnes discovery with a possible spill towards the Johan Sverdrup field across the locally permeable basement high. The Johan Sverdrup field is believed to be the end point of this migration route. The spilling towards the northern Utsira High, Patch Bank ridge or the Ling Depression has their geological disadvantages and thus is uncertain.

The Solveig field is not in communication with the fields and discoveries to the north. The field has a complicated charge history with at least two different migration episodes. Possible

migration from the field to the north-west and to the south-east has been proposed but is highly dependent on the sealing fault properties and the continuity of good reservoir.

Acknowledgments

The study was conducted at the Department of Earth Science, University of Bergen.

First of all, I would like to thank my supervisor, Christian Hermanrud, for his excellent advices, for always being available, for quick and constructive feedback and criticism. I would also like to thank all members of the PESTOH group for valuable and interesting presentations. Philipp Müller for helping with Petrel, valuable advices and interesting discussions. I would like to also Milos Herceg for all the fun time spent together. And special thanks to Lea for being there for me in both sad and happy times.

Table of contents

Abstract II
Acknowledgments IV
1 Introduction 2
2 Geological background 4
The Paleozoic 4
The Mesozoic 5
The Cenozoic 7
3 Background theory 9
3.1 Hydrocarbon generation and migration 9
Hydrocarbon generation 9
Primary migration 9
Secondary migration 9
Spill point 10
Filling of the hydrocarbon structures 10
The fill-spill model 10
Basement reservoir properties 11
3.2 Trap integrity and leakage 12
Capillary leakage 12
Membrane fault seal 12
Fault reactivation 12
Isostatic rebound 13
3.3 Seismic amplitude variations 14
Bright spot 14
Dim spot 14
Flat spot 14
Phase reversal 14
Tuning 15
3.4 Pore pressure 15
3.5 Geochemistry 16
Pristane/phytane ratio 16
Sulfur content in oil 16
Biodegradation 16
4 Data and methodology 18
4.1 Seismic data 18

4.2 Well data 20
4.3 Geochemical data 21
4.4 Workflow and methodology 22
Preparing the data set 22
Seismic interpretation 22
Seismic attributes 22
Formation pressure 23
Fluid contacts 23
Visualization 23
4.5 Uncertainties 23
Seismic interpretation 23
Limited information 23
5 Results 25
5.1 Edvard Greig 29
Luno 30
Tellus 37
5.2 P-graben and Ragnarrock 39
Ragnarrock Basement 39
Ragnarrock Chalk 43
P-graben 43
5.3 Rolfsnes 47
5.4 Solveig 52
5.5 Johan Sverdrup: 61
North-western terrace 62
Augvald graben 64
6. Discussion 70
6.1 Migration routes onto the Utsira High 70
South-western migration route 72
Western migration route 75
North-western migration route 75
6.2 Utsira High migration models 76
6.3 Migration routes around the Utsira High 80
Route A part 1 80
Route B 82
Route A part 2 84
Route C 85
Route D 87

Route E 89
Spilling from the Johan Sverdrup 89
Summary of the migration routes 91
7 Conclusion 93
8 Proposal for future work 94
9 References 95

1 Introduction

The North Sea is a mature hydrocarbon province that has been actively explored since the first oil and gas discovery at the end of the 1960s. During the following two decades the most large and obvious structures were drilled, which lead to the discovery of a majority of the fields that are in production now. As most of the obvious traps got drilled, a relatively calm exploration period ensued. After the calm period of the 1990s until the mid-2000s, the development of new methods, technologies and new play models have resulted in the discovery of numerous smaller structures, proving that there are considerable resources yet to be found. The Norwegian Petroleum Directorate (NPD) estimates that only 49% of the resources have been produced from the NCS, with 27% as reserves and discovered resources. Around 24% of the resources are yet to be discovered, meaning that the NCS still has some economical potential (NPD,2021).

The understanding of the hydrocarbon trapping, and spilling mechanisms has been one of the corner stones of the hydrocarbon exploration since the beginning of commercial production. The “fill and spill” model proposed by Gussow (1954) is widely accepted as a realistic representation of the secondary migration. The model explains the differential entrapment of the hydrocarbons and explains the migration up-dip once the spill-point is reached. The model states that the earliest generated oil fills the deepest traps until the column reaches the structural spill point resulting in the up-dip spill to the shallower trap. As the burial and the expulsion from the source rock continues the lighter, gaseous hydrocarbons are generated. The gas displaces the accumulated oil towards a shallower trap.

The South Viking Graben is bound by the Utsira High to the east and is one of the main source kitchens in the whole North Sea (Justwan, 2006). Since the start of the hydrocarbon exploration several large discoveries have been made in the southern and the northern Utsira High, e.g. Sleipner, Grane, Balder, Heimdal, Ringhorne and Jotun fields (Mahmic et al., 2018). The central Utsira High was drilled by several wells in the early 1970s, but none of them managed to prove large hydrocarbon accumulations. The exploration on the basement highs flanking the Jurassic-Cretaceous grabens was difficult mainly due to limitations of the seismic data. In case of the Utsira High, the Cretaceous chalk deposited close over the high basement absorbed most of the energy, hiding the underlying structures, displaying the acoustic basement as a broad, flat high (Patruno and Reid, 2016). Because of this the area was largely abandoned until the 2000s, when the improved seismic resolution allowed to map the sub-chalk structures and develop new play concepts (Rønnevik and Jørstad, 2014). The

discovery of the Edvard Grieg field in 2007 has renewed the interest in the Utsira High. The ensuing exploration activity has led to the discoveries of the Johan Sverdrup, Solveig, and other fields in the area. Some discoveries were made in an unusual for the North Sea fractured and weathered basement.

Production from the fractured basement reservoirs is not uncommon globally. Significant production areas with this type of reservoir include the Arabian shield basement reservoirs of Yemen and the Tertiary basement granites offshore Vietnam (Gutmanis, 2009). Prior to the Tellus discovery on the Utsira High the crystalline and metamorphic basement has been regarded as the lower limit of the hydrocarbon-bearing formations (Riber et al., 2015). The discovery has opened a possibility for hydrocarbon migration through the basement towards the interior part of the high or even to be used as a migration route across the high to fill the grabens that are cutting into the Utsira High.

The area around the Utsira High has seen large commercial interest for around the last 15 years, but there is still a huge potential for the discovery of new commercial accumulations. This can be observed, for example, from the last three awards of predefined areas (APA) in which large areas around the high have been awarded to different companies (NPD, 2021). Despite fairly recent exploration efforts as well as ongoing commercial interest, the geological constrains on the accumulations and migration routes have not been presented in the scientific literature.

The aim of the study is to investigate the geological constrains on the migration routes both to the Utsira High and around the individual fields within it. This was done by conducting a detailed seismic interpretation of the area together with the collection of different geochemical and petrophysical data. The depths of the contacts were identified together with likely migration pathways and migration mechanisms. The analyses of these structures included the investigation of pore pressure data, geochemical signatures of the fluids and the establishment of likely migration routes based on the observations and available literature.

2 Geological background

The Paleozoic

The North Sea is located between the shores of mainland Norway to the north-east, Denmark to the east, the Benelux countries to the south and the UK to the west. The central part of the sea is that of a failed trilete Late Jurassic rift basin (Ziegler 1992; Coward et al. 2003). The present-day tectonic framework of the North Sea basin holds evidence of a complex and long basin history. The compressional tectonics established during the Caledonian (460-400 Ma) and Variscan (400-300 Ma) orogenies formed ENE-WSW and NE-SW oriented lineaments in the crystalline basement, beneath the upcoming North Sea Basin (Whipp et al., 2014).

In the Early Ordovician, the Caledonian orogeny was initiated due to subduction along both margins of the Iapetus Ocean. The result of the subduction was the collision of two continents, Baltica and Laurentia. The collision between the two continents started in the Mid Silurian to Early Devonian (Coward et al., 2003). The dating of the crystalline basement rocks from the Utsira High, has shown these rocks to be between 409 and 482 Ma. These rocks are believed to represent magmatic and volcanic episodes related to the closure of the Iapetus Ocean and the continent-continent collision of the Baltica and Laurentia (Frost et al. 1981; Slagstad et al. 2011, Lundmark et al. 2013; Riber et al. 2015) The closure of the Iapetus Ocean led to a shift in the tectonic regime from the compressional to the extensional. This resulted in the collapse of the Caledonian orogeny in the Early Devonian. In Devonian and Carboniferous times, the earlier mentioned ENE-WSW and NE-SW oriented lineaments were reactivated as normal faults due to the post-orogenic crustal relaxation (Ziegler, 1990). These lineaments acted as zones of crustal weakness, imposing geometric constraints on both the evolution of the subsequent Mesozoic rift system and the conditions of Cenozoic thermally driven subsidence (Whipp et al., 2014).

The Devonian extensional collapse of the Variscan mountain range initiated in the start of the thermal subsidence and the extension associated with multidirectional rifting and volcanism that was at its largest in the Early (Glennie, 1995; Lundmark, Sæther and Sørlie, 2013). Several volcanic activity events helped to define the border between the Utsira high and the Permian basin to the south of the high. This activity may date the earliest North Sea graben system development, including the development of grabens on the Utsira High as well as the earliest uplift of the Utsira high (Glennie et al., 2003). The following more regional subsidence has resulted in the deposition of the thick Permian sequences filling in the topography around the structural highs (up to 1,2km) and much thinner (up to 100m)

sequences on the structural highs like the Utsira High. This indicates that the high was a stable block already in the Permian (Zanella and Coward, 2003, Sorento, Stemmerik and Olaussen, 2018). The Permian basins experienced rapid subsidence (Glennie, 1998)., During the following phase of thermal subsidence, the sandstone continued to fill up the basins (Zanella and Coward, 2003). As a result of the melting of the Permo-Carboniferous ice cap on the Gondwana and the opening of the seaway from southern North Sea to the Arctic ocean, the Late Permian North Sea experienced a glacio-eustatic sea-level rise. The transgression that was caused by this rise formed the Zechstein sea in which up to several kilometers of evaporites, carbonates and shales were deposited (Coward et al., 2003). The differential uplift and erosion of the Zechstein group occurred prior to the deposition of the Triassic strata. Because of that on the Utsira High the Zechstein is slightly folded in contrast to the overlying Triassic (Sorento, Stemmerik and Olaussen, 2018).

The Mesozoic

During the Mesozoic, the North Sea has been subjected to two major rifting events in the Permo-Triassic and Middle-Late Jurassic. The structural imprints of the two rifting events differ significantly, due to a change in the orientation of the extensional stress field (Færseth, 1996). At the transition from the Permian to the Triassic the North Sea experienced the first episode of extension. The propagation of the Norwegian- Greenland Sea rift in the North Sea area resulted into the brake up of the Pangea and onset Late Permian- Early Triassic rift phase (Ziegler 1992). The east-west extension resulted in the creation of wide fault-bounded basins, consisting of the Viking Graben, the Moray Firth Basin and the Central Graben. In the northern North Sea, the Viking Graben was the dominating sedimentary depocenter, with major faults most likely penetrating the entire crust (Færseth, 1996; Whipp et al., 2014). The Viking Graben cut through the older Caledonian structural elements, as well as the axes of the pre-rift sedimentary basins developed throughout the Middle to Late Paleozoic (Ziegler, 1992). On the Utsira high this activity resulted in a Triassic reactivation of the Rotliegend fault system. This created the characteristic grabens and the wedge-shaped geometry of the Triassic strata dipping towards the graben bounding faults (Sorento, Stemmerik and Olaussen, 2018).

At the same as the rifting, the depositional environment in the area changed. The Zechstein Sea regressed, which established continental deposition conditions in the North Sea area (Nystuen et al. 2014). Sediments deposited during the Early Triassic corresponding to the Skagerrak Formation are dominated by alluvial and/or lacustrine semi-arid environments,

including aeolian dunes and flash flood deposits (Nystuen et al. 2014; Mahmic et al. 2018). Later into the Late Triassic there was a shift towards semi-humid climate, are dominated by fluvial sandstones, meandering rivers and an increase in smectite and kaolinite weathering products due to the shift towards a semi-humid climate (Nystuen et al. 2014; Mahmic et al. 2018). Meanwhile, since at least the Late Triassic the Utsira high was exposed to subaerial weathering. The basement has developed different weathering profiles indicative of different climatic conditions or topographic levels (Riber et al. 2015).

The period of active rifting finished in the Early Triassic, followed by the continuation of the thermal subsidence. During the Early Jurassic, a narrow connection was created between the southern Tethys Ocean and the northern Boreal Sea. The following transgression resulted in the deposition of the marine shales and sandstones of the Dunlin group. These shales and sandstones are widely preserved around the northern and central North Sea with exception of the southern Utsira high (Vollset & Dorè, 1984). During the Middle Jurassic the central North Sea has experienced thermal doming. During this time the uplift of the central North Sea together with a global regression resulted in the blocking of the seaway connection between the Tethys Ocean and the Boreal Sea. This caused a deep erosion in the Early Jurassic and older sediments (Ziegler, 1992). Consequently, there is no evidence of the Early Jurassic sediments on the southern Utsira high. This is marked by a Mid-Cimmerian unconformity separating the Triassic from the overlying Late Jurassic sediments (Jackson et al., 2010).

The synrift development during the Middle-Late Jurassic in the Viking Graben area reduced the influence of the North Sea dome and reestablished the connection between the Boreal and Tethys seas (Ziegler, 1992). This interplay between the tectonics and the eustatic sea level rise favored the deposition of marine sands around the topographic highs. These Late Jurassic sandstones are interbedded with the Draupne and Heather formation shales (Olsen, Briedis and Renshaw, 2017). At the Utsira high these can be observed as adjacent to the main bounding faults of the Augvald and the Luno grabens and can indicate the subaerial exposure of the high throughout the Late Jurassic. These sandstones are overlain by the Draupne formation shales (Riber et al. 2015).

The final and brief subaerial exposure of the Utsira high happened in the Early Cretaceous and is marked by the shallow-marine sandstones of the Åsgard formation. As the second phase of the North Sea rift has ceased, the region has experienced rapid thermal subsidence and burial (Ziegler, 1992; Cowards et al, 2003). During the Cretaceous there was a continuous

global sea level rise (Nøttvedt et al., 2008). The Early-Middle Cretaceous claystones, siltstones and marlstones of the Cromer Knoll group were deposited. The base of the Cromer Knoll group is often marked by an erosive contact that represents the Base Cretaceous Unconformity (BCU). On the Utsira high the BCU is the boundary between the underlying Viking group/Skagerrak Fm/basement and the overlying Cromer Knoll group (Copestake et al., 2003). This was followed by the deposition of the carbonates, marls and siltstones of the Shetland group. In the Late Cretaceous the combination of the high sea level and the low topographic relief resulted into a wide and shallow epicontinental shelf sea (Surlyk et al., 2003).

The Cenozoic

In the Paleocene, the depositional environment changed from the gradual infill of an already existing rift relief to the deposition, due to an uplift of the western and easter margins of the North Sea basin. The repeated basin uplift and subsidence resulted in the deposition of the submarine-fan systems of the Rogaland group. These fan complexes are interbedded with hemipelagic shales of the same group (Isaksen & Tonstad, 1989).

In the Early Eocene, the opening of the North Atlantic Ocean marked the end of the extensional setting initiated by the Devonian collapse of the Caledonian orogeny (Isaksen & Tonstad, 1989). The extension, uplift and volcanism caused by the continental break-up and the opening of the North Atlantic Ocean affected the North Sea and the north-eastern Atlantic margin (Fyfe et al, 2003). The region continued undergoing steady subsidence, while the sediment supply was steady due to the margin uplift (Coward et al., 2003). In the late Eocene there was an onset of regional compression because of the seafloor spreading to the north-west. The relative sea-level fell, allowing the submarine fans to transport sands to the central parts of the basin. This episode is marked by the sandy formations withing the mostly shaly Hordaland group (Isaksen & Tonstad, 1989).

The Eocene-Oligocene boundary was marked by the global shift from the greenhouse to the icehouse climate. Throughout the Oligocene the sedimentation was mainly represented by the mud with some episodes of coarse clastic gravity flows deposited in the periods of the margin uplifts (Fyfe et al, 2003; Gregersen and Johannessen, 2007).

During Mid-to-Late Miocene the uplift of the margins and climatic cooling resulted in the shallowing of the North Sea that was accompanied by the progradation of the deltaic complexes draining from the Shetland Platform and the Scandinavia (Fyfe et al, 2003). The

basin subsidence continued into the Pliocene, resulting in the deposition of thick packages of the argillaceous sediment due to an increased input from the European delta systems (Fyfe et al., 2003; Gregersen and Johannessen, 2007).

The Quaternary is mainly characterized by global cooling, subsequent glaciations and the eustatic sea-level drop. Glaciations resulted in erosional unconformities and removed the upper parts of the prograding Pliocene deposits. The post-glacial isostatic rebound contributed to the continued elevation of the North Sea margins (Gregersen and Johannessen, 2007). It is well documented that the Scandinavian Ice Sheet has extended across the North Sea to the Scottish Highlands and Northern Ireland as late as the Last Glacial Maximum (LGM) (Lambeck et al., 2010). The effects of the glacial tilting and the subsequent leakage has been shown by Horstad and Larter (1997) on the example of the Troll Eastern oil province. Stoddard et al. (2015) have modeled the effects of the ice sheet at the LGM. The modelling has shown that due to variations in the ice thickness there is a regional tilt towards the NE with varying tilt magnitudes. Also, it was shown that faults at the reservoir depths (ca. 2000m) show tensile and shear stresses which could facilitate redistribution and leakage of oil from the Johan Sverdrup field.

3 Background theory

3.1 Hydrocarbon generation and migration

Hydrocarbon generation

Hydrocarbons are generated from sedimentary rocks with sufficient amount of organic material. The generation happens when the rock, usually organic rich shale or coal, is buried and heated. Different hydrocarbons are generated at different temperatures. Most fractions of oil are occurring at temperatures between 100ºC and 150ºC. Gas generation occurs at temperatures between 150ºC and 220ºC. If the reservoir temperatures exceed 150ºC the oil starts to naturally crack into gas (Quigley and Mackenzie, 1988).

Primary migration

The primary migration is a process in which the hydrocarbons are expelled from the source rock into the adjacent porous and permeable carrier bed (Chapman, 1972). Organic rich source rocks usually are not homogenous. Thin, porous and permeable beds can work as initial conduits within the source rock. If the permeable beds are absent or the fluids cannot escape through these beds, the pressure will start to rise resulting in the hydraulic fracturing of the source rock with following expulsion along the microfractures (Barnard and Bastow, 1991). A second theory proposed by Ungerer et al. (1984) suggests that primary migration can occur by diffusion along the continuous oil wet kerogen laminae.

Secondary migration

The secondary migration is a process by which the hydrocarbons migrate through permeable carrier beds. The secondary migration is governed by the buoyancy forces and is believed to start after sufficient amount of the hydrocarbons enter the pore space at the interface between the carrier bed and the source rock (Barnard and Bastow, 1991). The hydrocarbons continue migrating along the upper part of the carrier beds until they meet some sort of barrier. When the barrier is reached the accumulation can ensue. In the instances when migration is not affected by any barrier the hydrocarbons will eventually reach the surface. Faults often act as barriers for the hydrocarbon flow. Fault sealing or across fault juxtaposition of the reservoir sandstone against the impermeable shale are the most common migration barriers in the heavily faulted areas. In Jurassic reservoirs hydrocarbons often migrate up-dip following the strike of the faults (Johnsen et al., 1995).

Spill point

The spill point is defined as the structurally lowest point in a trap that can retain the hydrocarbons. The spill point can be controlled by a fault or by the geometry of the structure. The fault-controlled spill point is the shallowest point at which the reservoir is juxtaposed to another reservoir. The spill point controlled by the structural geometry is the shallowest point of the top of the reservoir along the synclines hinge line.

Filling of the hydrocarbon structures

A filled structure is defined as a structure that is filled down to it maximum potential (spill point). The overfilled structure contains the hydrocarbon column down to a deeper level than the interpreted spill point. This can be explained by the presence of a sealing mechanism along the fault axis that is preventing the migration of the hydrocarbons. The underfilled structure contains the hydrocarbon column down to a shallower level than the interpreted spill point. Such a situation can occur either due to a leaking top seal, fault intersection or limited charge of the hydrocarbons. Some underfilled structures may contain residual hydrocarbons shows beneath that coincides with the interpreted spill point, meaning that previously the trap was filled to spill.

The fill-spill model

If the migration into the trap is continuous, the initial trap will be filled and the leakage with the further up-dip migration will occur. Gussow (1954) proposed a model in which several traps are put into one system with continuous generation at different times. Figure 3.1.1 shows this model with an early and late stage of the generation.

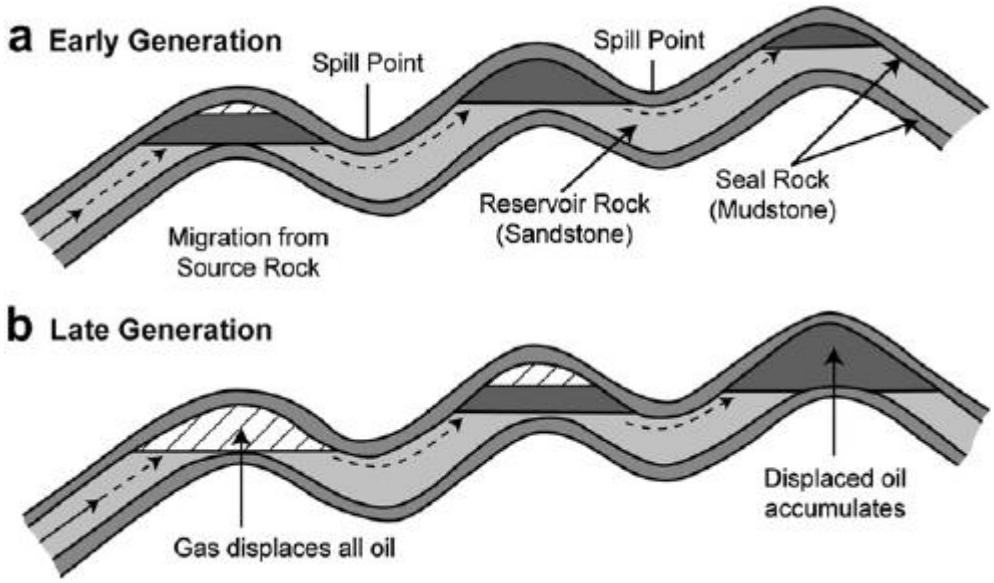

Figure 3.1.1: Gussow's (1954) fill to spill model. Modified from Fustic et al (2012)

The early stage of generation would mostly result in expulsion of oil with some minor gas as the source rock is buried within the oil window. The deepest structure is filled to the spill point spilling the oil into the middle structure. Once enough oil migrates into the middle structure it also reaches the spill point and the accumulation in the shallowest structure begins. In an early stage of the generation some gas can appear. But due to higher buoyancy it will be trapped in the deepest structure. With the increasing burial depths and thus temperatures, the source rock will enter the late generation phase in which mostly gas will be generated. The gas will displace all of the oil from the deepest reservoir and will start filling the middle one while the shallowest accumulation will continue filling to its spill point. Summarized, the fill to spill model explains that the shallowest traps are oil-filled while the deepest traps are gas-filled (Gussow, 1954)

Basement reservoir properties

Since the crystalline basement is essentially tight, the reservoir properties of the basement are mainly dependent on the secondary porosity created as result of fracturing, weathering or chemical alteration and dissolution of the minerals. Gutmanis (2009) has collected and reviewed the main controls on the basement reservoir quality.

The lithology and type of rock can greatly affect the fracture height, density, and dimension. In the metamorphic rocks, on the one hand, fractures tend to be constrained by the layering, resulting in worse reservoir properties due to bad interconnectivity. On the other hand, in the massive and homogenous rocks such as granites, the fracture networks are blockier and more interconnected.

In contrary to clastic reservoirs the faults in the basement tend to increase the permeability by generating very high fracture densities within the damage zones around the fault planes. At the same time, the permeabilities within the fault plane itself tend to decrease (see membrane fault seal in 3.2)

Present and past stress is important for the fracture reactivation. Previously sealed fractures can break the seal as a result of reactivation. Lastly, the secondary alteration by the hydrothermal activity can both cause precipitation of minerals within the fractures reducing the porosity, and dissolve minerals within and around the fractures.

3.2 Trap integrity and leakage

Capillary leakage

Capillary leakage of the hydrocarbons can occur when the buoyancy of the hydrocarbons exceeds the capillary entry pressure of the water wet top seal. This means that the leakage can in theory happen without the presence of the fluid conduits like faults or permeable beds. The capillary entry pressure is controlled by the cap-rocks pore throats largest radius (Berg, 1975).

$$P_{ce} < (p_w - p_{hc})*g*h:$$

where the P_{ce} = the capillary entry pressure, p_w = water density, p_{hc} = hydrocarbon density, g = gravitational constant and h = height of the hydrocarbon column.

Membrane fault seal

Membrane fault seal stands for a type of fault sealing that can leak in specific cases. Several mechanisms have been identified whereby the fault plane can act as a seal (Watts, 1987; Knipe, 1992; Yielding et al., 1997).

1) Juxtaposition of reservoir sands against low-permeability shale with high capillary entry pressure. In this case the hydrocarbon column pressure would have to exceed the capillary entry pressure of the shale as described above.
2) Clay smear or entrainment of fine-grained material into the fault plane, creating a high capillary entry pressure within the fault plane itself.
3) Cataclasis, in which crushed coarse-grained grains will produce clay into the fault plane, creating a high capillary entry pressure.
4) Diagenesis in which a cementation along the permeable fault plane might partially or fully remove the porosity and thus sealing the fault.

Fault reactivation

Fault reactivation in the northern North Sea in the Visund field was investigated by Wiprut and Zoback (2000, 2002). Three factors were suggested to control the fault reactivation:

- Locally elevated pore pressure due to buoyant hydrocarbons bordering the faults
- Fault orientations that are optimally oriented for frictional slip at the present-day stress levels
- Compressional stress caused by post-glacial rebound.

Considering that the pore pressure is close to hydrostatic in all of the fields within the study area, only the preferable fault orientation and the stress by the post-glacial rebound are applicable to the Utsira High.

Wiprut and Zoback (2000, 2002) suggest that the faults that are critically stressed in the current stress field are permeable, while the faults that are not critically stressed are sealing. Several fluid migration studies seem to confirm the critically stressed fault hypothesis (Barton et al., 1998; Wiprut and Zoback, 2000).

The glacial loading is assumed to have affected the fault reactivation. The ice-sheet thickness has fluctuated throughout the Quaternary, resulting in isostatic subsidence and rebound. The glacial loading may have reduced the compressive stresses and stopped active faulting in the northern North Sea when the glacial ice sheet was present (Wiprut and Zoback, 2002).

Isostatic rebound

In addition to effects on the faults the isostatic rebound may play an important role in the charge history of the Utsira High (Stoddart et al., 2015). Besides the induced stresses on the fault the glacial rebound affected the tilting of the area. Horstad and Larter (1997) proposed that the glacial tilting may have played a crucial role in the filling of the Eastern Troll field. The model for the migration model is shown in figure 3.2.1. Considering that some of the fields in the study area have good oil shows beneath the OWC and that the OWC throughout the fields is varying, Stoddart et al. (2015) suggest that tilting might have played a crucial role in the migration around the high as well as leakage from the structures.

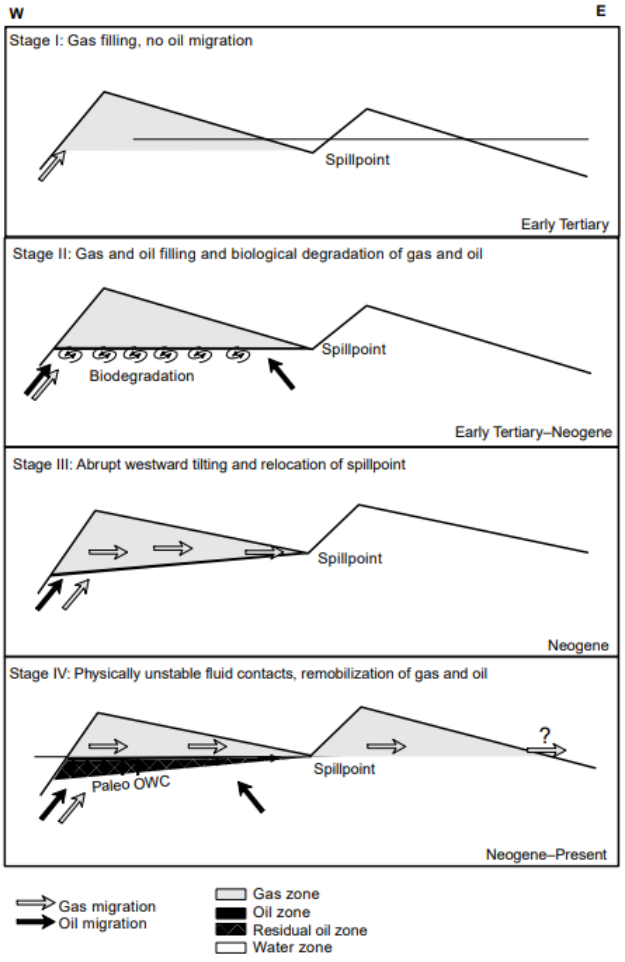

Figure 3.2.1: Stages of migration and filling of the Troll field. From Horstad and Larter (1997).

3.3 Seismic amplitude variations

Bright spot

Bright spot is a seismic amplitude anomaly that is defined as local increase in the positive or negative amplitude along a reflection related to a local increase or decrease in acoustic impedance. The negative amplitude bright can be related to a locally different fluid in the porous rock. The gas or oil saturated sandstone will have a different reflection coefficient than the water saturated sandstone (Ligtenberg, 2005; Løseth et al., 2009). Figure 3.3.1 shows a typical bright spot.

Dim spot

Dim spot is a local decrease in the positive or negative amplitude along a reflection related to local increase or decrease in acoustic impedance. The decrease in amplitude is very typical for a gas saturated reservoir in which the gas presence cancels the lithological impedance contrast (Ligtenberg, 2005; Løseth et al., 2009). Figure 3.3.1 shows a typical dim spot.

Flat spot

Flat spot is a horizontally flat seismic reflection that stand with an angle on the stratigraphic reflections. Flat spot usually shows a fluid change (contact) within the reservoir. Gas- water contacts (GOC) are especially prone to crease flat spots due to large difference in acoustic impedance between the two fluids (Ligtenberg, 2005; Løseth et al., 2009). Figure 3.3.1 shows a typical flat spot.

Phase reversal

Phase reversal is a 180º phase shift along a continuous reflection so that through becomes a peak and vice versa. Phase reversal can indicate the presence of hydrocarbons if the overlying shales have lower acoustic impedance than the water saturated sandstones, but both have a higher impedance contrast than the hydrocarbon saturated sandstone resulting in an increase in acoustic impedance instead of a decrease (Ligtenberg, 2005; Løseth et al., 2009). Figure 3.3.1 shows a typical phase reversal separated by a flat spot (fluid contact).

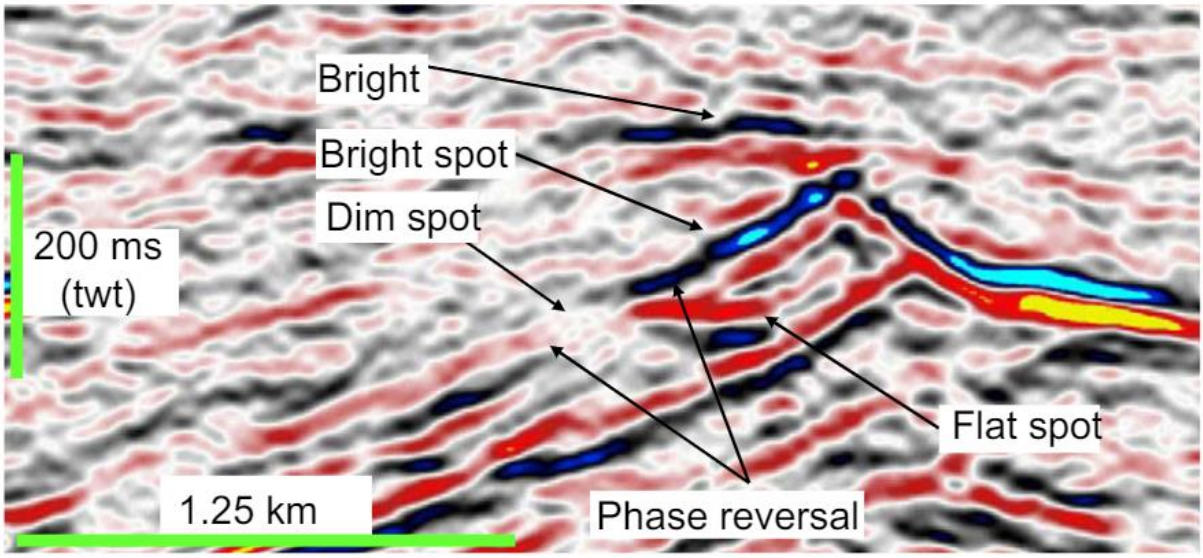

Figure 3.3.1: Direct hydrocarbon indicators in a seismic section. From Løseth et al., (2009).

Tuning

Tuning is an amplitude anomaly that is associated with thin beds resulting in an increase or a decrease of seismic amplitude because of a constructive or destructive interference between the reflectors. The thickness at which the interference occurs is called the tuning thickness. The Tuning thickness is defined to be ¼ of a wavelength (Roden et al., 2017).

3.4 Pore pressure

The pore pressure or the formation pressure is a pressure within the reservoir pores. The pore pressure is often referred to the hydrostatic pressure. The hydrostatic pressure is a pressure of the water column weight from the surface if that water column is in communication (Moss et al., 2003). Within the reservoir pressure barriers can occur resulting in the buildup of extra pressure creating an overpressure situation as well as the escape of excess pressure creating an underpressure. Both over- and underpressure are calculated in relation to the hydrostatic pressure (Buhrig, 1989).

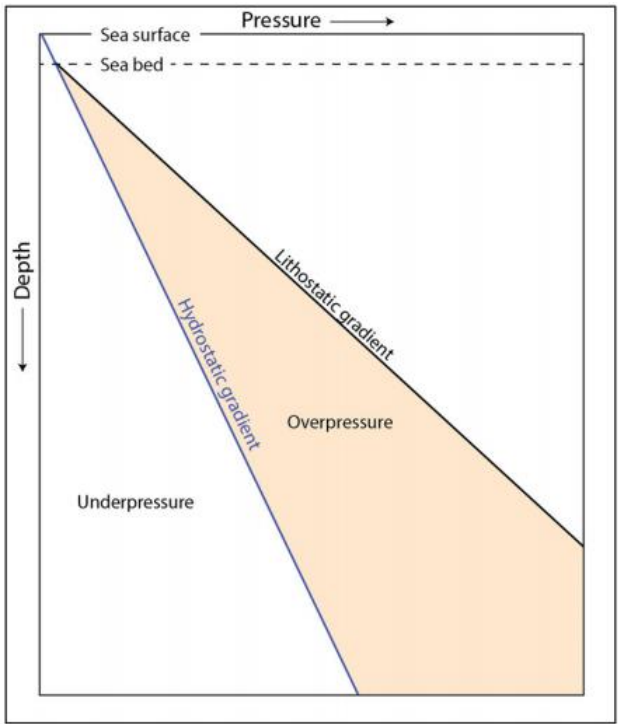

Figure 3.4.2: An idealized pressure vs depth model showing relationship between the hydrostatic pressure, overpressure and the underpressure. Derived from Moss et al. (2003)

Overpressure occurs in reservoirs with restricted or no communication to the overlying formations. Several mechanisms can cause the overpressure. If the formation is rapidly buried the formation water will take some of the overburden weight. Because of the water incompressibility the pressure will start building up given that the excess pressure cannot escape into the overburden. Another process that can result in the overpressure is the temperature increase that will result in the pressure build up. The addition of extra fluids in form of generated hydrocarbons and the effects of compaction can also lead to overpressure (Buhrig, 1989; Moss et al., 2003).

Underpressure is less common than overpressure. It is mostly formed because of rapid uplift and/or overburden erosion resulting in lower pressure than the surrounding formations (Osborne and Swarbrick, 1997).

3.5 Geochemistry

Pristane/phytane ratio

Pristane/phytane (Pr/Ph) is a ratio of abundance of pristane in comparison to phytane. The Pr/Ph ratio is considered to indicate the degree of oxygenation in the depositional environment and thus can be used to distinguish between source rock facies (Justwan 2005; Hermanrud, pers. con). Pristane and phytane are not much affected by the biodegradation (Head et al., 2010). The ratio can be used to compare light to medium biodegraded oil.

Sulfur content in oil

Sulfur-rich source rock intervals are associated with sulfur contents greater than 1% (Waldo et al., 1990). Sulfur content can be used as an important biomarker to distinguish between different source rock facies when other parameters such as Pr/Ph ratio are not applicable. In case of the Utsira High the anomalously high contents of sulfur in oil and water in the Johan Sverdrup field may indicate different facies of Draupne fm source rock (Hermanrud, pers. con). At the same time, the increased sulfur content may be a result of in situ dissolution of evaporitic sulfides and a subsequent diffusion of the sulphate rich water and the oil (Ramstad et al., 2016)

Biodegradation

Biodegradation is a process during which the microorganisms chemically dissolve hydrocarbons. The biodegrading organisms have a preference to remove specific compounds from the oil and gas. With the degradation the oil is depleted of the saturated hydrocarbons first, leaving heavy polar and asphaltene components in the reservoir (Head et al., 2010). This

decreases the API gravity while increasing the viscosity, sulfur content and acidity of the oil. The biodegradation can occur at the temperatures that are less than 80 °C (Connan, 1984).

4 Data and methodology

Chapter 4 gives an overview of the seismic data, exploration wells, methods and workflow used to commence this study, including related uncertainties.

4.1 Seismic data

The seismic dataset in form of the Petrel E&P Software Platform project consists of one merged seismic cube ST12M02 provided by the license partners: Equinor Energy AS, Lundin Energy Norway AS, Petoro AS, Aker BP ASA, Total E&P Norge AS. The location of the dataset is shown in figure 4.1.1.

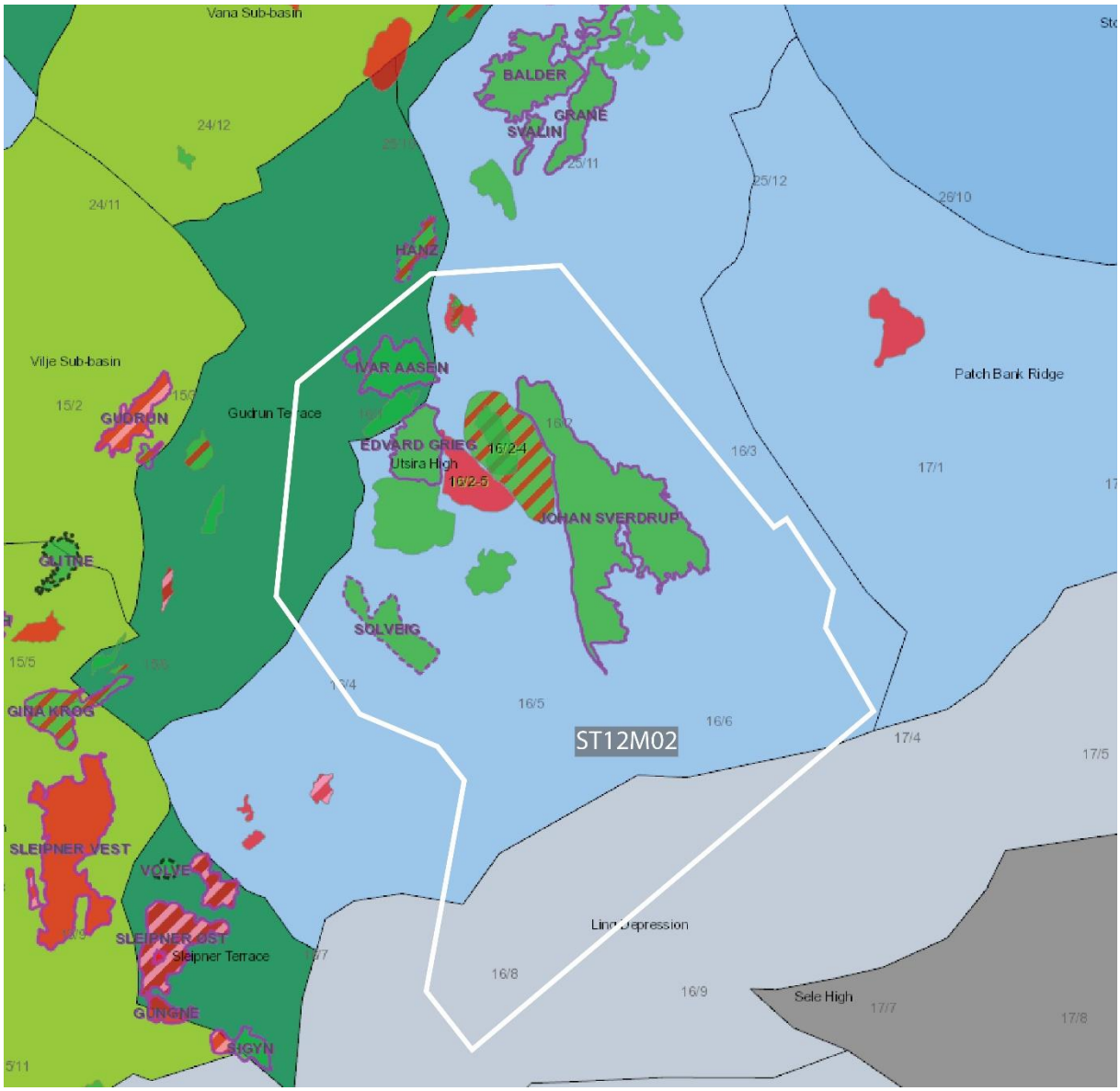

Figure 4.1.1: The extent of the seismic cube ST12M02 illustrated by white polygon with field outlines. Modified from the NPD, 2021.

The seismic survey is time migrated to zero phase (wavelets are symmetrical about zero time). All the seismic cubes are in the time domain with a vertical axis given in TWT in ms. A downward increase in acoustic impedance is associated with a peak and represented by a blue reflection in the seismic. A downward decrease in acoustic impedance is represented by a red through. An important observation is that the BCU was changing polarity depending on its position. Within the grabens the BCU represented shale to sand boundary resulting in decrease in acoustic impedance. On the basement high the BCU was at the basement representing shale to crystalline basement boundary, resulting in the increase in acoustic impedance due to higher wave velocities in the basement (figure 4.1.2)

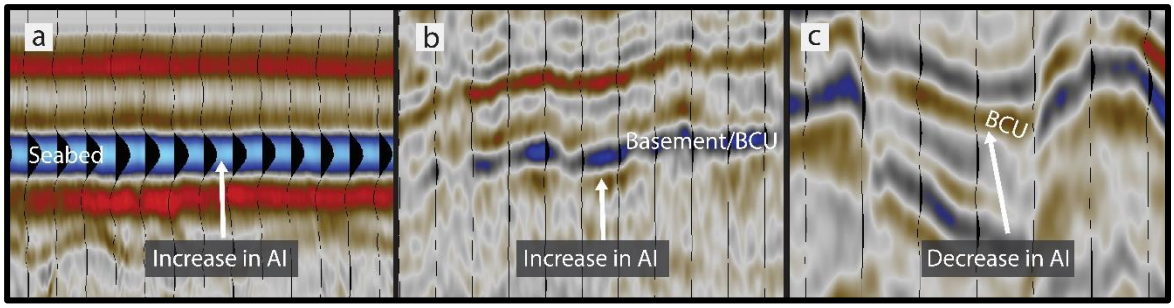

Figure 4.1.2: Illustration of the polarity of the seismic survey with blue representing the acoustic impedance increase and red representing acoustic impedance decrease.

An approximation of the seismic resolution was made using the wavelet toolbox in Petrel to estimate the dominant frequency range in the depths of interest in the cube. Within the same range the seismic velocity was calculated using the sonic log from the representative well. Equations used are presented in figure 4.1.3. The seismic cube information summary is shown in table 4.1.4.

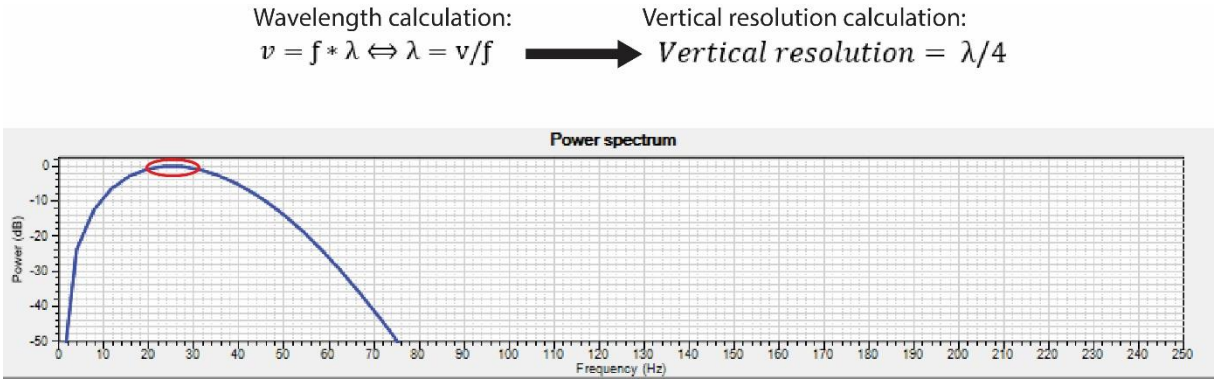

Figure 4.1.3: Formulas used for the calculation of the vertical resolution where v = velocity, f = frequency and lambda = wavelength) and power spectrum with dominant frequencies in red circle. Modified from the Petrel's wavelet toolbox.

Table 4.1.4: Summary of the information about the seismic cube.

Seismic cube	*Phase*	*Polarity*	*Resolution at target depth*	*Line orientation*	*Line spacing*
ST12M02	Zero	Normal	Ca. 50m	Inline = SW-NE Xline = SE-NW	12,5 12,5

4.2 Well data

Some wells were included in the project provided by Equinor. These wells included the well location and the trajectory, and they were adjusted for checkshots to fit the seismic cubes time domain. For some of the wells conventional logs were present (caliper, gamma ray, sonic etc.). Throughout the seismic interpretation information from more well was required and thus necessary data, including well paths and checkshots, was downloaded into the Petrel from The Norwegian National Data Repository for Petroleum data (Diskos). Formation tops were downloaded from the NPD's online Factpages. Additional information from other wells, including outside of the study area was used to complete the study. Also, NPD's press releases were used for information for the wells that are not yet publicly available. Table 4.2.1 shows all the wells that were used for the study (besides those that are not publicly available), while figure 4.2.2 shows the position of the wells that were used for seismic interpretation.

Table 4.2.1: All wells that were used in this study

Area	*Wells*						
Edvard Grieg	16/1-8	16/1-10	16/1-13	16/1-15	16/1-18	16/1-23 S	16/1-27
Solveig	16/4-6 S	16/4-8 S	16/4-9 S	16/4-11	16/5-5		
Rolfsnes	16/1-12	16/1-25 S	16/1-28 S				
P-graben	16/1-17	16/2-5					
Ragnarrock	16/2-3	16/2-4	16/2-18 S				
Johan Sverdrup	16/2-6 16/2-14 16/3-7	16/2-7 A 16/2-15 16/5-2S	16/2-8 16/2-16 16/3 T2	16/2-9 S 16/3-2 16/5-4	16/2-10 16/3-4	16/2-11 16/3-5	16/2-12 16/3-6
Other	16/1-2 16/4-1 16/7-2	16/1-5 16/4-2 16/7-10	16/1-14 16/4-3 25/11-17	16/1-24 16/4-5 25/11-28	16/1-29S 16/4-7 25/11-29S	16/2-20S 16/4-10	16/2-22S 16/5-1

The pressure data was acquired from the RFT (repeat formation tester) and the MDT (modular formation dynamics tester) measurements in the available well reports found in Diskos or provided by Equinor.

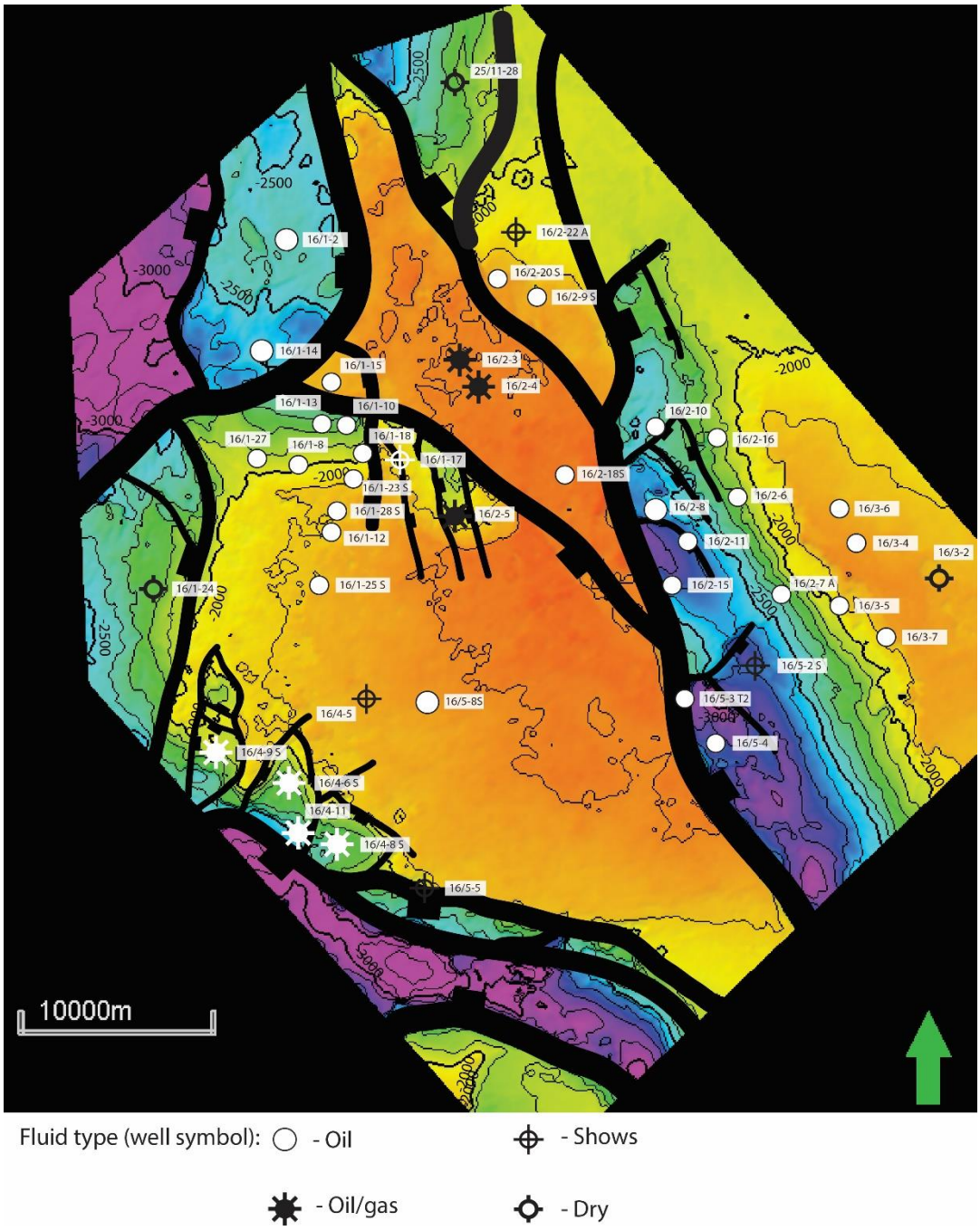

Figure 4.2.2: Top Basement map of the study area with faults and positions of all wells that were used for seismic interpretation.

4.3 Geochemical data

Geochemical reports were downloaded from Diskos or provided by Equinor. The geochemical reports that were used:

1) Final geochemical interpretation reports → used for general information about the hydrocarbons like source rock, source rock maturity, biodegradation etc.
2) Reports on the composition analysis of MDT reservoir fluid samples → used to search for the Pr/Ph ratios and SO_4 concentration of the formation water.

3) Sampling and trace reports → used to search for the SO_4 concentration of the formation water.
4) Oil and reservoir core analyses reports → used to search for the Pr/Ph ratios.

4.4 Workflow and methodology

Preparing the data set

The project provided by Equinor was already setup from the beginning. The only manipulation with the data cube was that it was set in one of the Equinor's internal coordinate systems resulting in the incorrect display of imported wells. The coordinate system was later changed for ED50 UTM31M.

Seismic interpretation

Petrel E&P 2019 was used to perform the seismic interpretation. A detailed regional interpretation of selected formation tops was executed. Selected formations or groups were top Basement, top reservoir (BCU), top Shetland and top Cromer Knoll. Also, in graben areas internal formations or groups such as top Zechstein/Permian and top Skagerrak. The top Basement was picked on an increase in acoustic impedance (blue reflection). The top reservoir or BCU was picked on a decrease in acoustic impedance (red reflection) in the graben areas and on the same reflection as basement over the structural highs. Due to polarity reversal the surfaces representing top BCU maps were merged post interpretation. The top Shetland was picked at an increase in acoustic impedance (blue reflection). The top Cromer Knoll was picked at a decrease in acoustic impedance (red reflection).

The interpretation was carried out using a combination of the manual interpretation, guided autotracking and the seeded 3D autotracking tools. Manual interpretation was mainly used for interpretation of the basement within the grabens where reflections were extremely chaotic. Guided autotracking was used to interpret internal reflections in the grabens. Seeded 3D autotracking was used over areas with clear and continuous reflections were present, for example above the basement highs. Random composite lines were used for fault interpretations as well as in the structurally difficult areas. The line increment varied from 4-128 lines depending on the structural complexity and data quality. The interpretation of the formation tops was used to generate surface maps. These maps were further used for a visualization of the reservoir geometry and interpretation of the migration routes.

Seismic attributes

RMS amplitude and variance were used to enhance stand-out features and aid the observations. The RMS amplitude calculates the square root of the sum of the squared

amplitudes in a specific vertical amplitude. It maps amplitude anomalies that can help with mapping the geological features. The RMS amplitude was mainly used to map the locations of the Permo-Triassic grabens along the top reservoir surface. The variance attribute calculates the amplitude variance along the surface it is extracted from. It was mainly used to visualize faults.

Formation pressure

Formation pressures from the MDT and the RFT measurements were plotted using Excel. The reservoir pressures were compared between the wells and with reference to the hydrostatic pressure. Oil and water gradients were calculated for the different wells. The fluid gradient is measured pressure per unit of length. It is calculated performing a linear regression of the pressure points. The hydrostatic pressure represents a weight of water column with depth given that the pores are connected. The hydrostatic pressure can be calculated with the following equation: $P = r * g * h$. P = pressure, r = density of the seawater (1027,3 kg/m^3), g = gravitational constant (9,81 m/s^2) and h = height (or in this case depth) in TVD MSL.

Fluid contacts

Fluid contacts have been mainly retrieved from the NPD's online Factpages. When not present online the final well reports or discovery evaluation reports were used. For several wells the fluid contact was not mentioned and thus the intersections between the oil and water gradients were calculated.

Visualization

The Adobe Illustrator CS6 was used to create figures, 2D seismic cross-sections as well as annotate on specific features of the maps. All 2D seismic cross-sections have 5 times vertical exaggeration to enhance structural features.

4.5 Uncertainties

Seismic interpretation

The seismic data used for this study is of good quality. At the same time, the seismic interpretation is dependent on the experience of the interpreter as well as their scientific background. This can lead to different interpretations from different interpreters. The checkshots were used to quality control the interpretation.

Limited information

Due to the ongoing exploration and the commercial potential of the area, little studies have been published to aid the analysis. Some information that could help is still not available

publicly. Because of that, much of the migration route interpretation had to rely on the established rules of geology as well as logic. The interpretation of migration routes into the study area has been done without the help of the interpreted seismic. Because of that published maps had to be utilized at the expense of interpretation accuracy.

5 Results

This chapter will present the observations and seismic interpretations from the fields and discoveries studied in this thesis. The area is split into several sub-chapters divided by the fields. Figure 5.0.1 shows a regional map of the main geological structures in the central North Sea with an outline of study area. The study area is divided into different chapters due to structural and lithological differences. 6 fields/discoveries are described with focus on their seals and contact depths.

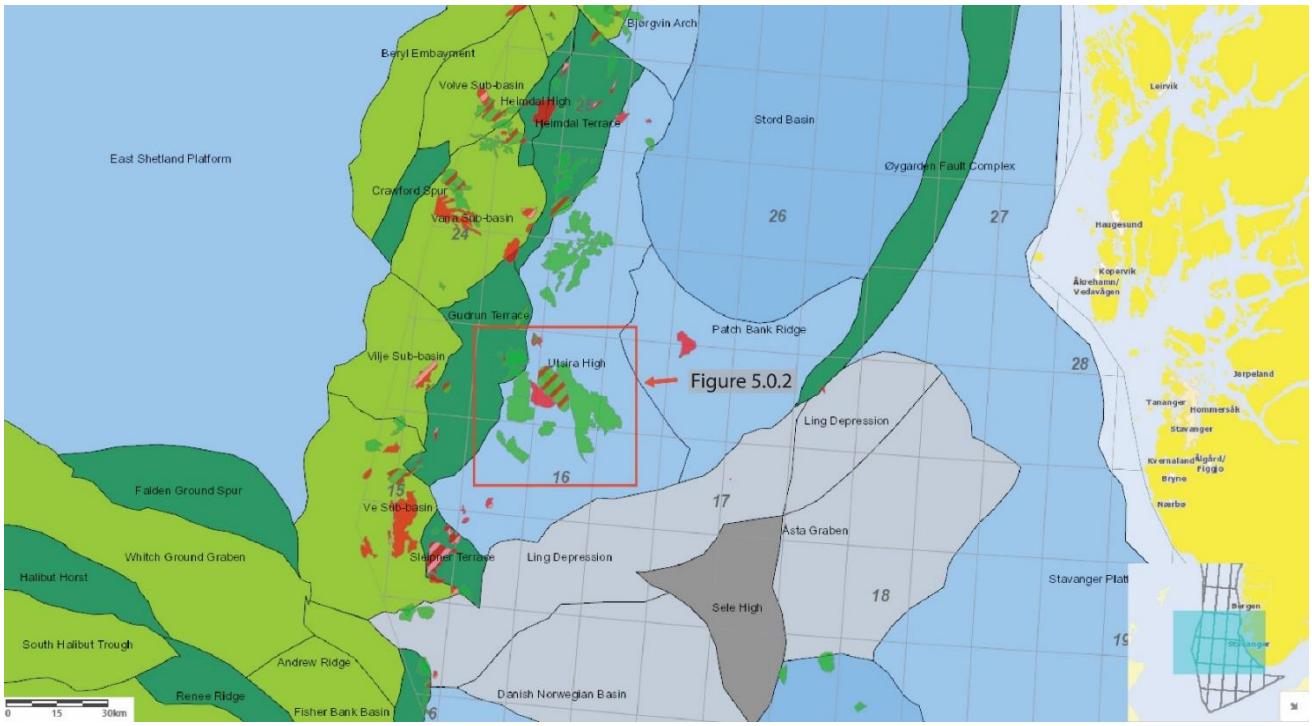

Figure 5.0.1: Regional map of the main structures in the central North Sea, with the study area outlined as figure 5.0.2. The map is retrieved and edited from NPD's home page.

The Utsira High is situated between the Gudrun Terrace to the west and the Ling Depression to the east. The area encompasses several hydrocarbon fields such as Johan Sverdrup, Edvard Grieg and Solveig. The area is still undergoing exploration with new discoveries that were made while this thesis has been done (f.ex.: 16/5-8 – Goddo, which cannot be used in this thesis due to unavailability of the exploration data). The main clastic reservoirs in the area are Jurassic Intra Draupne fm and Triassic Skagerrak fm. Another important reservoir unit that makes the Southern Utsira high unique on the NCS is the weathered basement. In one of the discoveries (Ragnarrock) the hydrocarbons have been detected at several stratigraphic levels. In addition to the basement reservoir the hydrocarbons have been observed in the chalks of the Late Cretaceous Shetland gp.

The structural framework is described by figures 1.0.2 a,b and c, showing the basement high that is subdivided into smaller highs (the Haugaland and Avaldsnes highs) by several Permo-Triassic half-grabens (the Augvald, Luno and Solveig grabens). It is important to note that some of the structures such as Luno and Solveig Grabens, do not have an official name or name in the literature like other structures (Olsen *et al*, 2017; Riber *et al*, 2015). The names are based on the most prevalent discoveries or features that are located there. The whole area can be described as one megaclosure where the top of the reservoir (BCU level) has a 4-way dip from the shallowest point of the basement high, creating a dome-like structure (figure 1.0.2d). The main bounding faults in the area are the west bounding, Johan Sverdrup and Luno master faults (figure 1.0.2a). These faults are cutting through the Southern Utsira High and confine a series of minor isolated or partially interconnected mini basins. Mini basins are generally asymmetric with deeper parts closer to the bounding fault.

All the structures can be described as a structural-stratigraphic trap (sub-unconformity) where the top seal is Cromer Knoll gp shales above the BCU. The lateral sealing is dependent on the reservoir type. For the clastic reservoir, the lateral sealing is related to the continuity of the reservoir (pinch-out) and the sealing capacity of the bounding faults. The lateral sealing in the basement reservoir is related to the reservoir quality mainly due to tight areas where tight "pockets" of basement form by precipitation of clay minerals in the fractures reducing permeability. The bottom sealing is absent in some structures, while in others underlying shales or tight basement seal from the base. In basement reservoirs magnitude of weathering decreases with depths resulting in bottom seals.

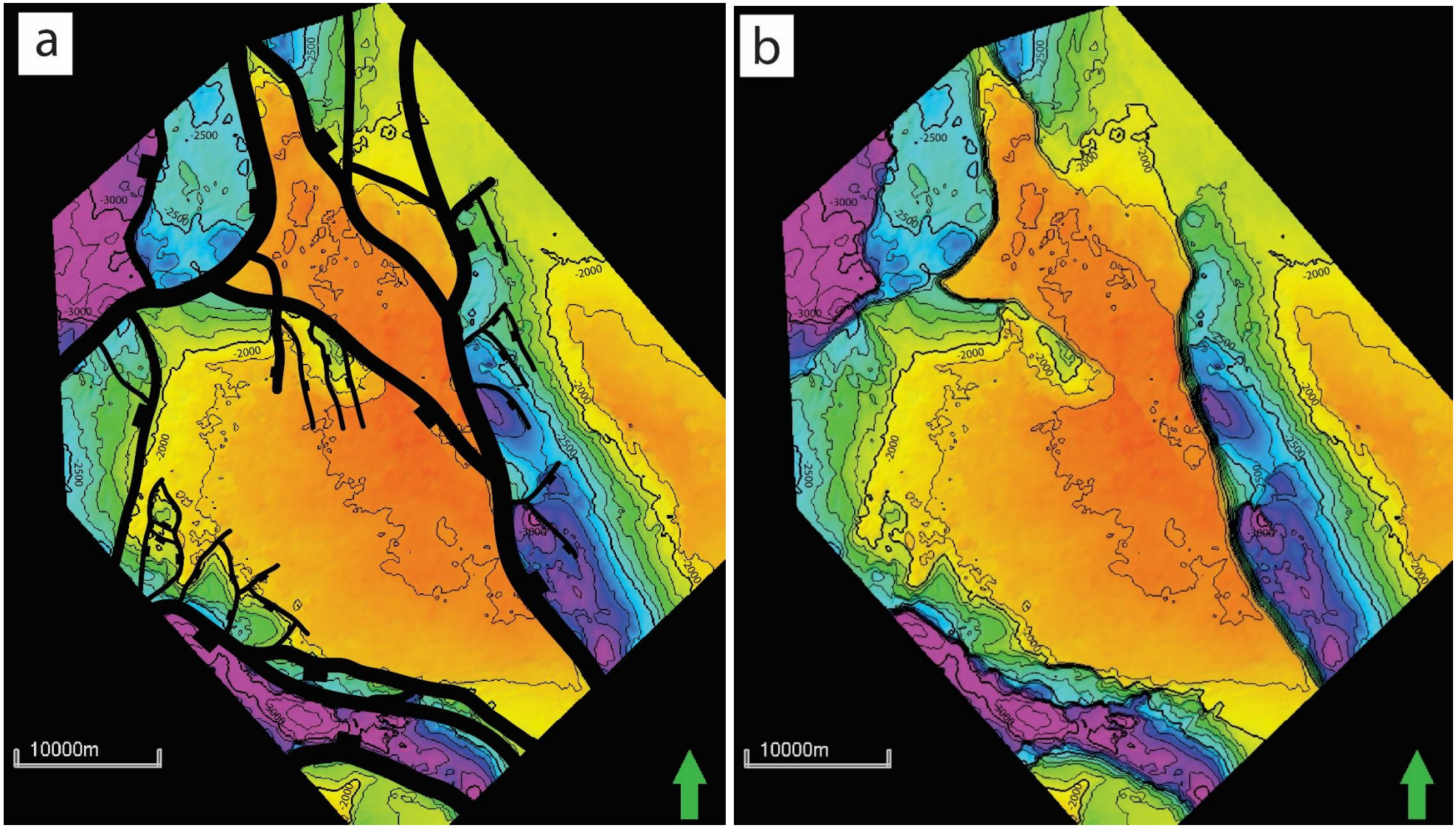
a
b
10000m
10000m
-2000
-2500
-3000

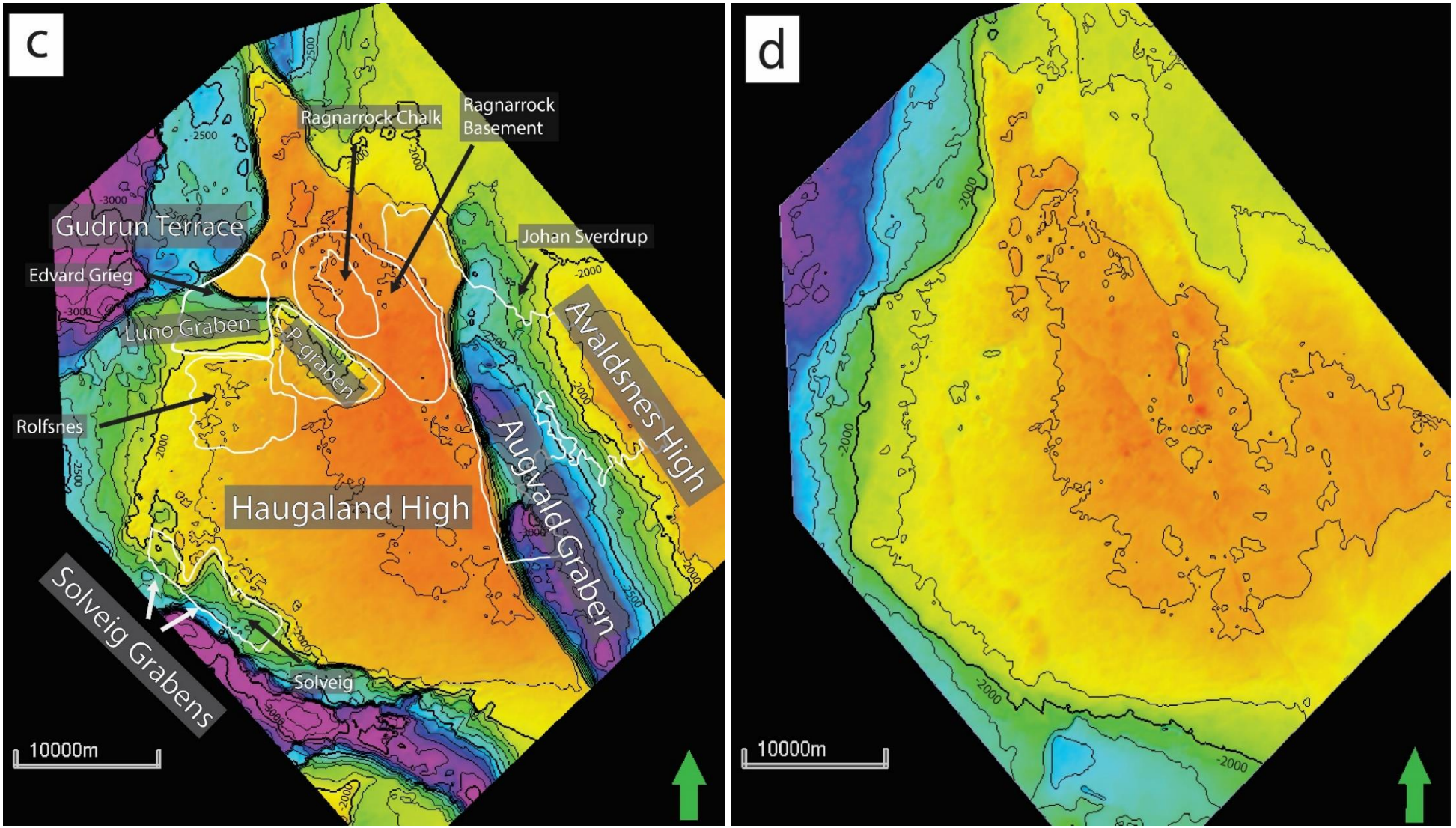

Figure 5.0.2: Overview of the Utsira High presented by top Basement surface with (a) and without (b) fault interpretations, (c) showing main structures with white field outlines and (d) BCU surface map showing the shallowest point of the BCU in the central part of the study area

5.1 Edvard Grieg

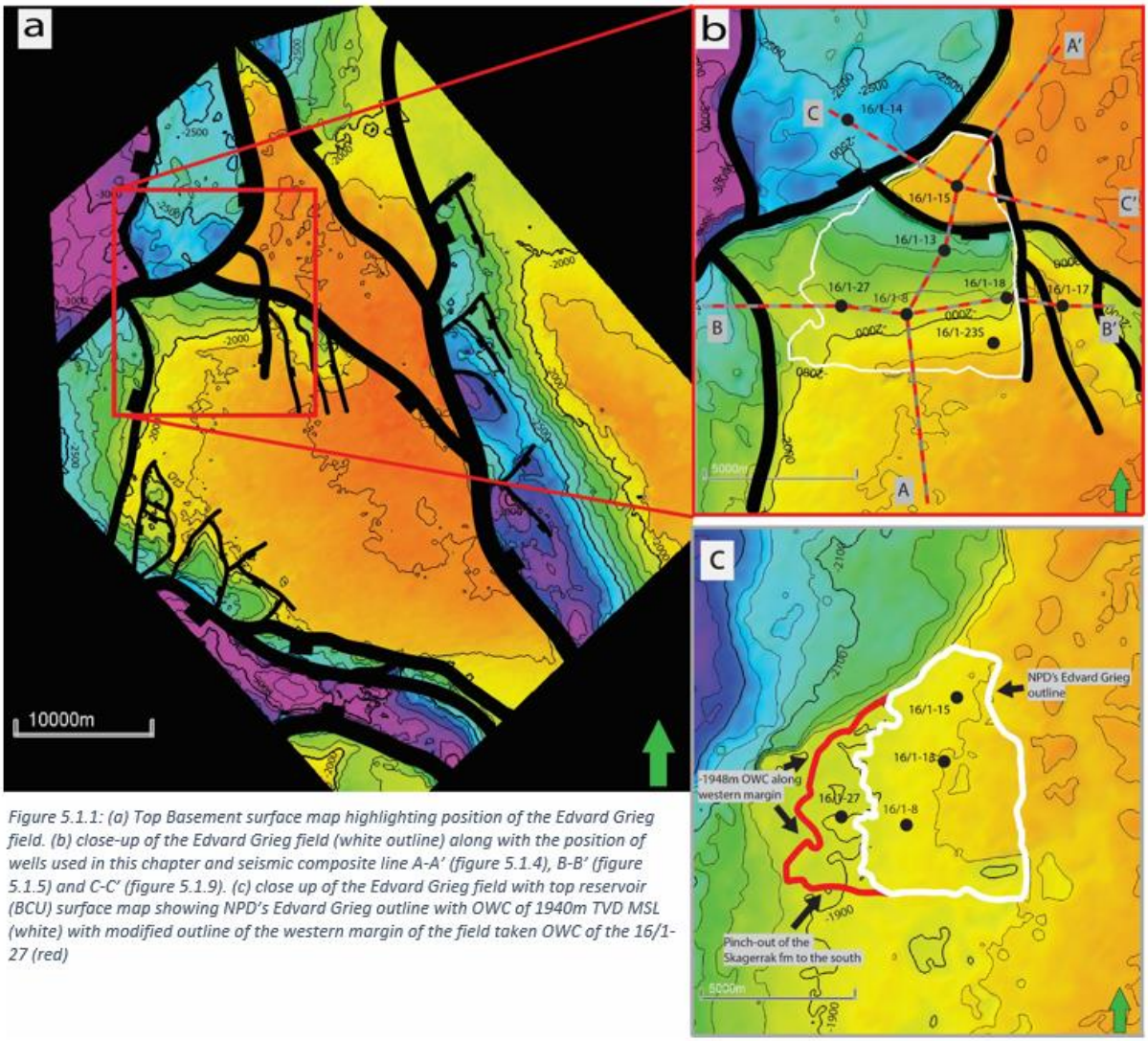

Figure 5.1.1: (a) Top Basement surface map highlighting position of the Edvard Grieg field. (b) close-up of the Edvard Grieg field (white outline) along with the position of wells used in this chapter and seismic composite line A-A' (figure 5.1.4), B-B' (figure 5.1.5) and C-C' (figure 5.1.9). (c) close up of the Edvard Grieg field with top reservoir (BCU) surface map showing NPD's Edvard Grieg outline with OWC of 1940m TVD MSL (white) with modified outline of the western margin of the field taken OWC of the 16/1-27 (red)

The Edvard Grieg is an oil field that is in the western part of the Utsira High (Figure 5.1.1). In the exploration and early appraisal phase the field was referred to as two separate discoveries, Tellus (basement reservoir discovery) and Luno (clastic reservoir discovery). Later, in the appraisal phase it was discovered that both share similar pressures regimes and oil families, resulting in them to be referred as one field. The field has been in production since 2015.

The Edvard Grieg structure can be described as a structural stratigraphic trap where the top seal is represented by Cromer Knoll gp marls overlying the BCU. To the south the field is sealed by pinch-out of the reservoir. In Tellus, the west bounding fault is sealing by the juxtaposing reservoir against the Cromer Knoll gp marls. The east bounding fault is sealed to the east and north-east. The field is comprised of two types of reservoirs: Early-Cretaceous to Late- Triassic clastics (Luno) and weathered pre-Devonian basement (Tellus).

Table 5.1.2: Summary of lithologies and oil-water contacts for wells used in this sub-chapter.

Well	Discovery (drilling year)	Reservoir Group/Formation	HC- water contact TVD MSL (m)	Top of the reservoir TVD MSL (m)
16/1-8	Luno (2007)	Intra Draupne fm, Skagerrak fm	1939	1900
16/1-10	Luno (2008)	Intra Draupne fm, Skagerrak fm	1940	1872,9
16/1-13	Luno (2009)	Intra Draupne fm, Skagerrak fm	1939	1890,1
16/1-15	Tellus (2011)	Åsgard fm, Basement	1940	1892
16/1-15AT2	Tellus (2011)	Åsgard fm	1940	1893,5
16/1-18	Luno (2014)	Skagerrak fm	ODT 1926	1864,1
16/1-23S	Luno (2015)	Åsgard fm, Skagerrak fm	1933,5	1901
16/1-27	Luno (2017)	Åsgard fm, Skagerrak fm	1947,7	1932,8
16/1-17	P-graben (2013)	Skagerrak fm	Shows at 1856, 1867 and 1917	1843,4

As it can be seen from table 5.1.2, the oil- water contact is calculated from pressure data to be at around 1939 m TVD MSL with two exceptions in the southern and eastern part of the field (wells: 16/1-23 S and 16/1-27).

Luno

The Luno discovery is in a Permo-Triassic half-graben with bounding W-E trending normal fault to the north (figure 5.1.3). It was first drilled by well 16/1-8 which encountered oil in Intra Draupne and Skagerrak fm. Subsequently, five appraisal wells were drilled to delineate the discovery. The results from wells drilled are shown in table 5.1.2. Table 5.1.2 shows that the lithologies are represented by Skagerrak fm, Intra Draupne fm and Åsgard fm. The Skagerrak fm is comprised by the terrestrial (lacustrine and alluvial) Triassic sandstones and conglomerates. Jurassic Intra Draupne fm is comprised of non-marine alluvial sediments, mainly due to the lack of trace fossils suggesting a non-marine environment. Late Cretaceous Åsgard fm is comprised of shallow-marine sandstones.

Seismic composite line A-A' (figure 5.1.4) shows (a) an uninterpreted and (b) interpreted seismic section from south to north showcasing the Luno half-graben. The figure illustrates the half-graben's master fault separating Luno and Tellus discoveries and shows a pinch-out of the Skagerrak fm to the south. Similar pressures (and OWC) in Tellus and Luno suggest that the master fault is not sealing (figure 5.1.3).

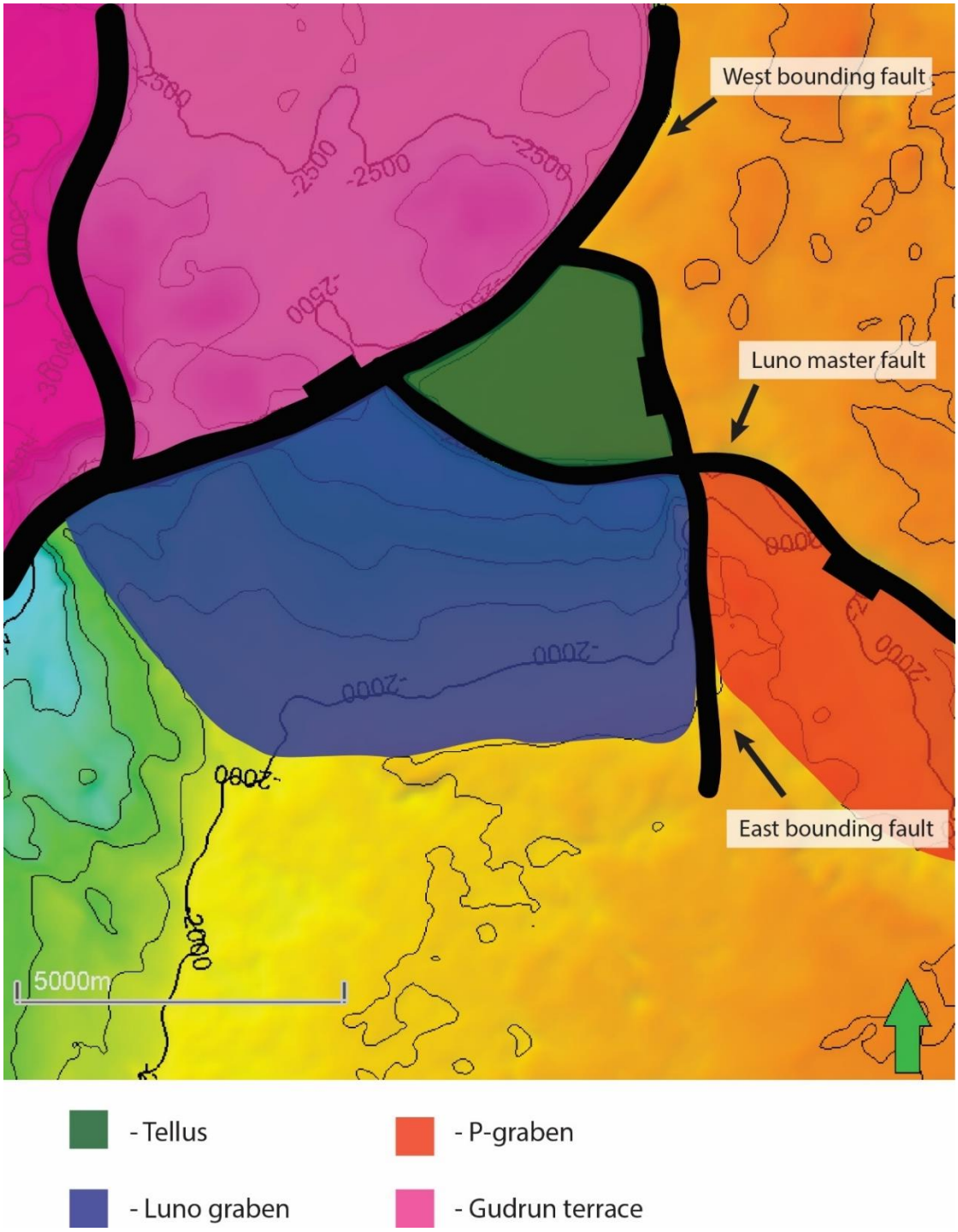

Figure 5.1.3: Top basement surface map showcasing main areas and faults around the Edvard Grieg field that are referenced in this chapter.

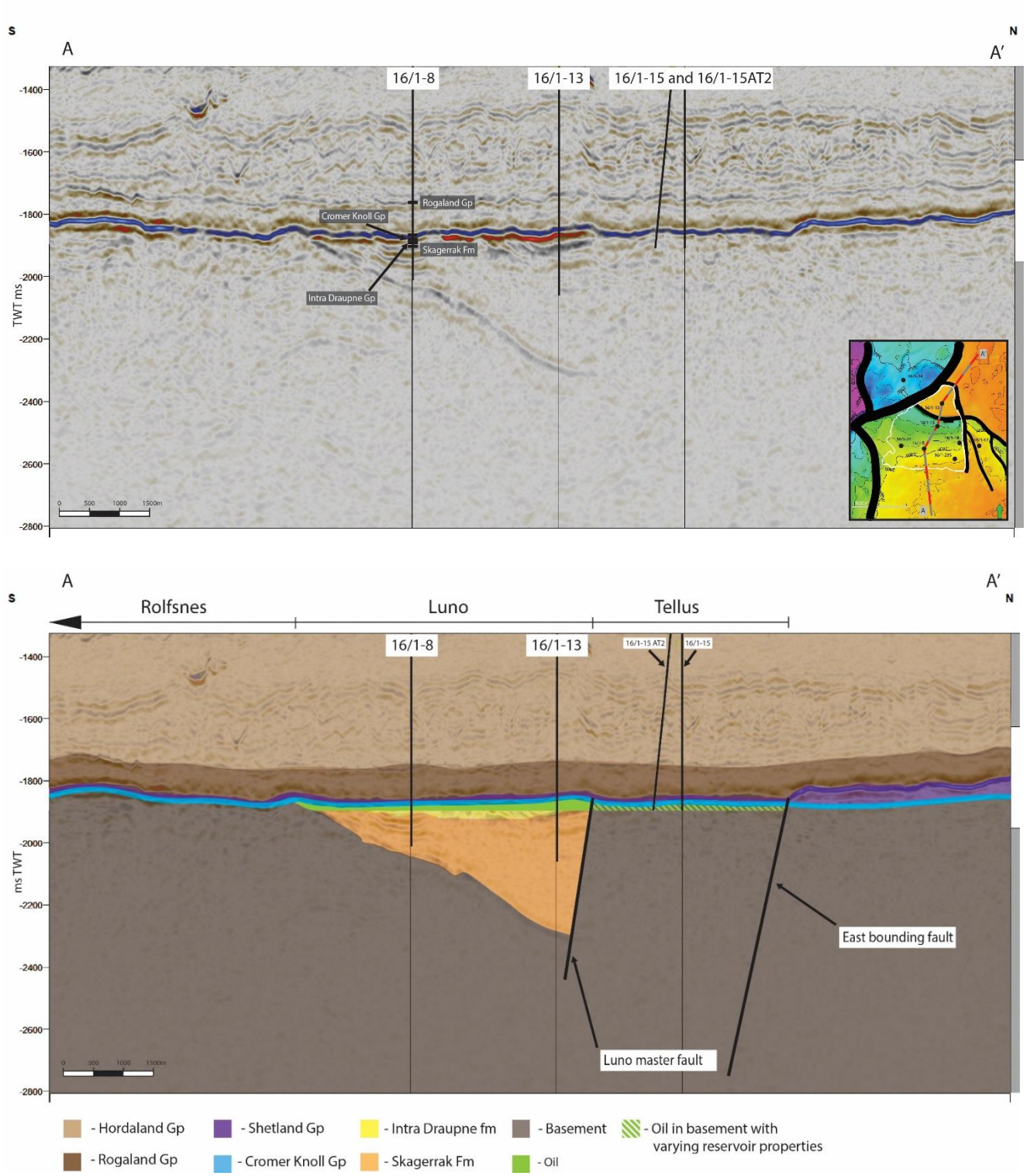

Figure 5.1.4: Uninterpreted (a) and interpreted (b) S-N seismic section of the Edvard Grieg field

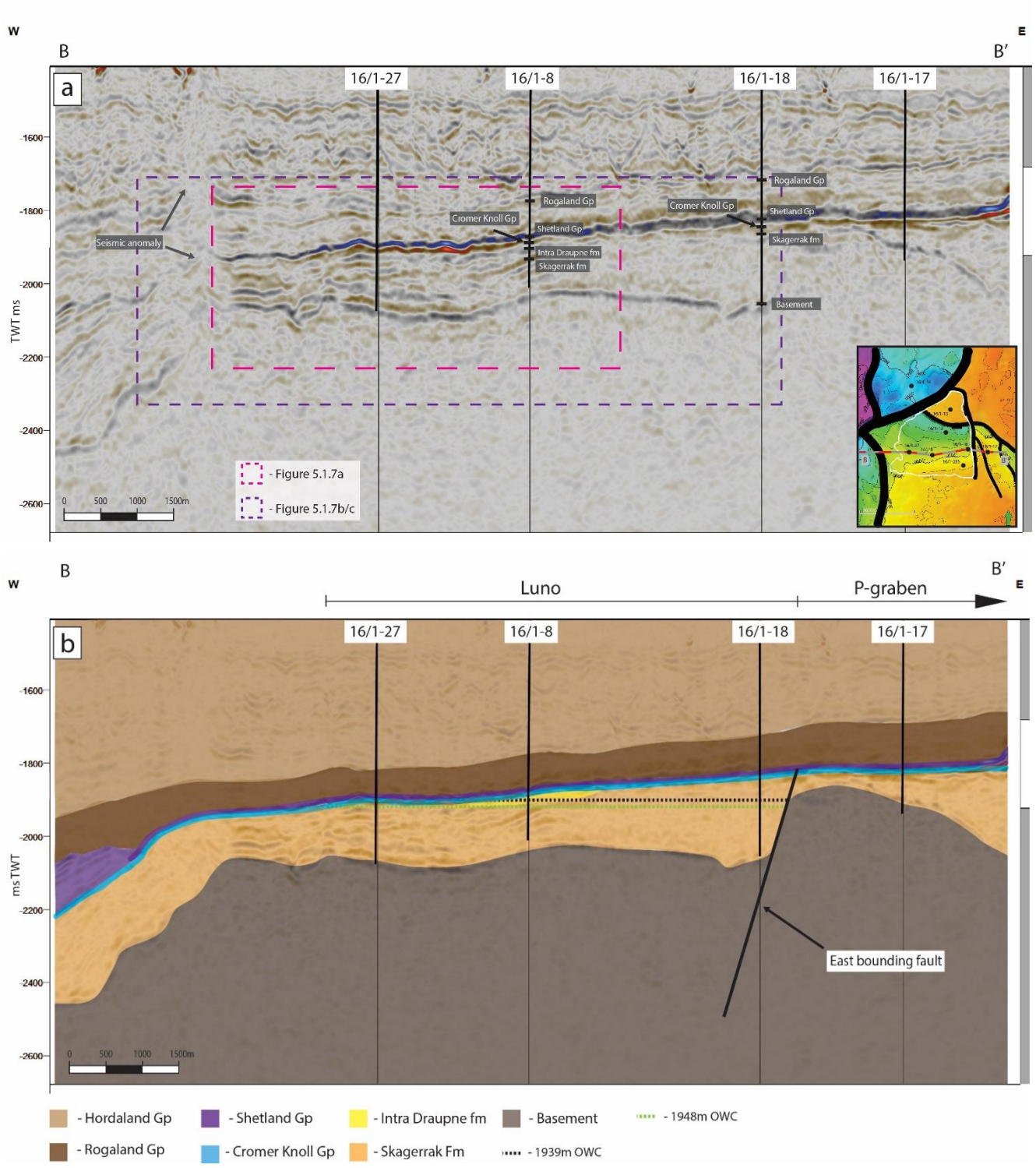

Figure 5.1.5: Uninterpreted (a) and interpreted (b) W-E seismic section of the Luno discovery

Another seismic composite line B-B' (figure 5.1.5) shows (a) an uninterpreted and (b) interpreted seismic section from east to west following the strike direction of the Luno half-

graben. The figure illustrates the fault separating Luno from the P-graben discovery (figure 5.1.3 and 5.1.6) to the east and deepening of the top reservoir to the west. Well 16/1-18 is the eastern most well in Luno and it is near well 16/1-17 (figure 5.1.1). Between these 2 wells there is Luno's east bounding fault. While 16/1-18 has reported movable oil, well 16/1-17 has only reported shows above the OWC calculated for 16/1-18(table 5.1.2). It is important to mention that an ODT situation is observed in 16/1-18 due to impermeable boulder layer with fine matrix underneath, with the top of the layer at 1926m TVD MSL. Despite this the oil pressure gradient in 16/1-18 is like the rest of the Edvard Grieg. Subsequently, only one valid pressure measurement was made in the 16/1-17 at the depth that is under the common contact of the Luno discovery (1939m TVD). This measurement has the pressure value above that of the water level gradient from the Edvard Grieg (figure 5.1.7).

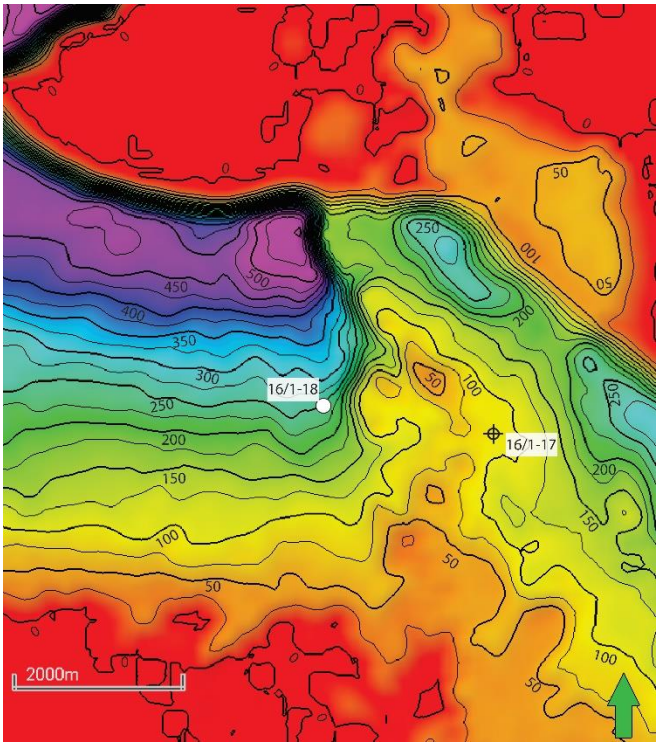

Figure 5.1.6: A thickness map between top basement and BCU reflectors showing wells 16/1-18 and 16/1-17 and graben fill thickness differences up-dip and down-dip of the east bounding fault (located between the wells)

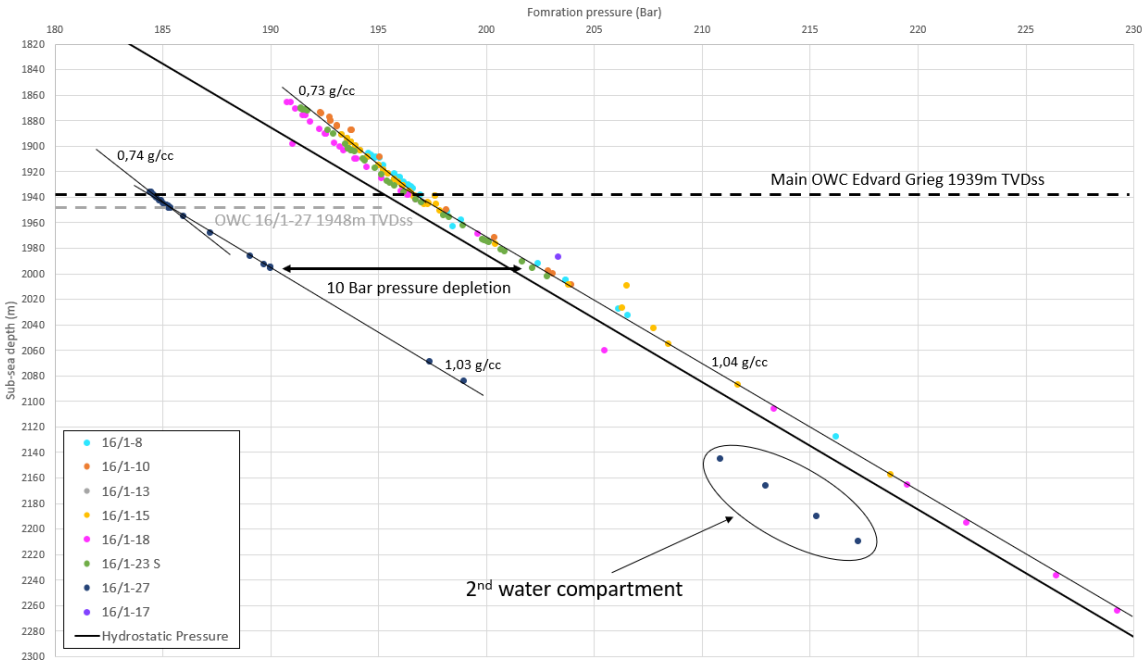

Figure 5.1.7: A combined formation pressure plot of all wells in the Edvard Grieg field

As stated previously there are two wells (table 5.1.2) within the Luno discovery that have different OWC in comparison to the rest of the wells. Figure 5.1.5 and table 5.1.2 shows the top reservoir is deepening to the west. Appraisal well 16/1-27 was drilled to the west from discovery well 16/1-8 to confirm oil in the western part of the Luno. It discovered oil with a slightly deeper OWC then in the rest of the Luno discovery as well as two water filled pressure compartments separated by a shale layer (figure 5.1.8). A 10 bar pressure depletion was also observed, probably due to the start of the production from the Edvard Grieg field two years prior to drilling (figure 5.1.7). Figure 5.1.8 shows the close up on the interval between wells 16/1-27 and 16/1-8 with two interpretations of this interval. Figure 5.1.8a shows the pinch-out of upper Skagerrak fm and the side seal by a shale layer (interpretation nr.1). Uncertainty about the interpretation in this interval mainly comes from chaotic reflections that can be attributed to an unusually high amplitude at the BCU level. Figure 5.1.8b and 5.1.8c shows the reflector discontinuities that were interpreted as a possible fault east of well 16/1-27 that can hinder the connection between the juxtaposed Skagerrak fm reservoir.

Figure 5.1.1c shows the top BCU surface map with two Edvard Grieg outlines. White shows the outline downloaded from NPD's page where 1939m OWC is used. Since well appraisal well 16/1-27 that was drilled outside of the Edvard Grieg includes hydrocarbons with similar oil and water gradients a new western boundary can be drawn using 16/1-27's OWC. This joint field outline is used in all the figures in the thesis.

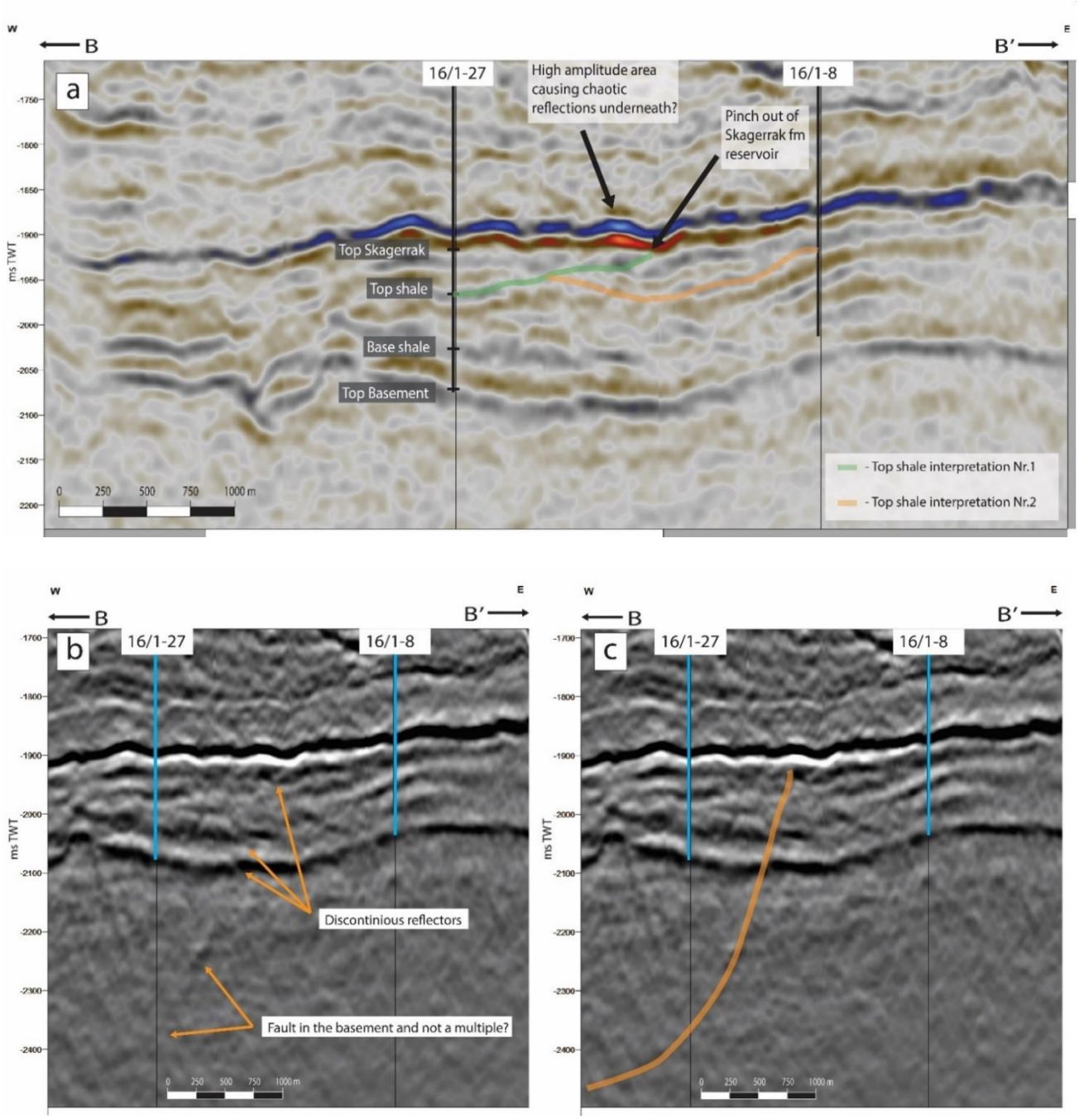

Figure 5.1.8: W-E seismic sections of the Luno discovery showing two interpretations between wells 16/1-27 and 16/1-8. Where (a) shows interpretations of top shale layers in the Skagerrak fm, (b) shows reflector discontinuities and (c) shows fault itself (orange)

The appraisal well 16/1-23S in the south-eastern corner of the Luno discovery (figure 5.1.1). The well has reported oil with a shallower OWC than the rest of the Edvard Grieg field. Pressure measurements showed slightly lower pressure measurements than in the well 16/1-8 (figure 5.1.9), while having similar oil gradient with 16/1-8. The oil column has a larger pressure difference with Edvard Greig than the water column. No faults or other kinds of barriers were observed on seismic.

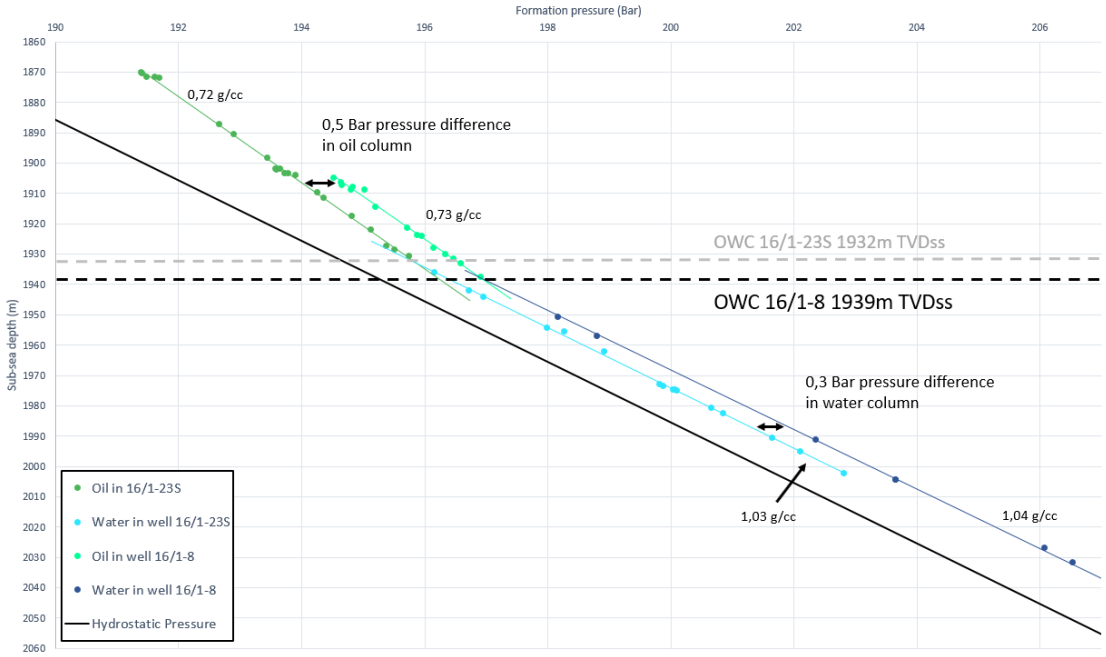

Figure 5.1.9: A combined formation pressure plot from wells 16/1-23S and 16/1-8 (taken as a reference well for main part of Edvard Grieg) showing differences in OWC and pressures between well 16/1-23S and the rest of Edvard Grieg field

Tellus

Tellus is situated to the north of the Luno half-graben on a fault block situated across the Luno bounding fault (figure 5.1.3). Well 16/1-15 was drilled to investigate a potential reservoir in fractured basement. A geological sidetrack 16/1-15 AT2 was drilled to examine changes in the reservoir quality. Well 16/1-15 and its sidetrack penetrated the basement. The basement penetrated by 16/1-15 has good reservoir properties while its sidetrack 16/1-15 AT2 has poor (tight) reservoir properties. They have also shown that the basement is overlain by thin (<2m) Lower Cretaceous Åsgard sandstones which are most likely filling in the paleo topography.

Seismic composite line C-C' (figure 5.1.10) shows (a) an uninterpreted and (b) interpreted seismic section from east to west across the Tellus fault block. The fault block is constrained by three faults to the west, north/east and south (figure 5.1.3). The south bounding fault has

been described in the Luno part. The west bounding fault marks the boundary of the Utsira High towards the Gudrun terrace to the west. The basement reservoir is juxtaposed to the Rogaland gp shales to the west. To the north-east the intra-basement fault can be interpreted as a continuation of the Luno grabens east bounding fault. Figure 5.1.9 shows that both sides of the fault are interpreted to be the basement.

Unfortunately, it is impossible to map Cretaceous sandstones due to their extreme thinness in comparison to the vertical resolution. Fractured basement is the second reservoir that is present in the Tellus. Well 16/1-15 and its sidetrack showed that the quality of the basement reservoir can be greatly different over relatively small distances. Therefore, mapping fracture networks in the Tellus would be preferential. Unfortunately, as it was mentioned in theory chapter, poor data quality is prohibiting from investigating fracture networks in the basement.

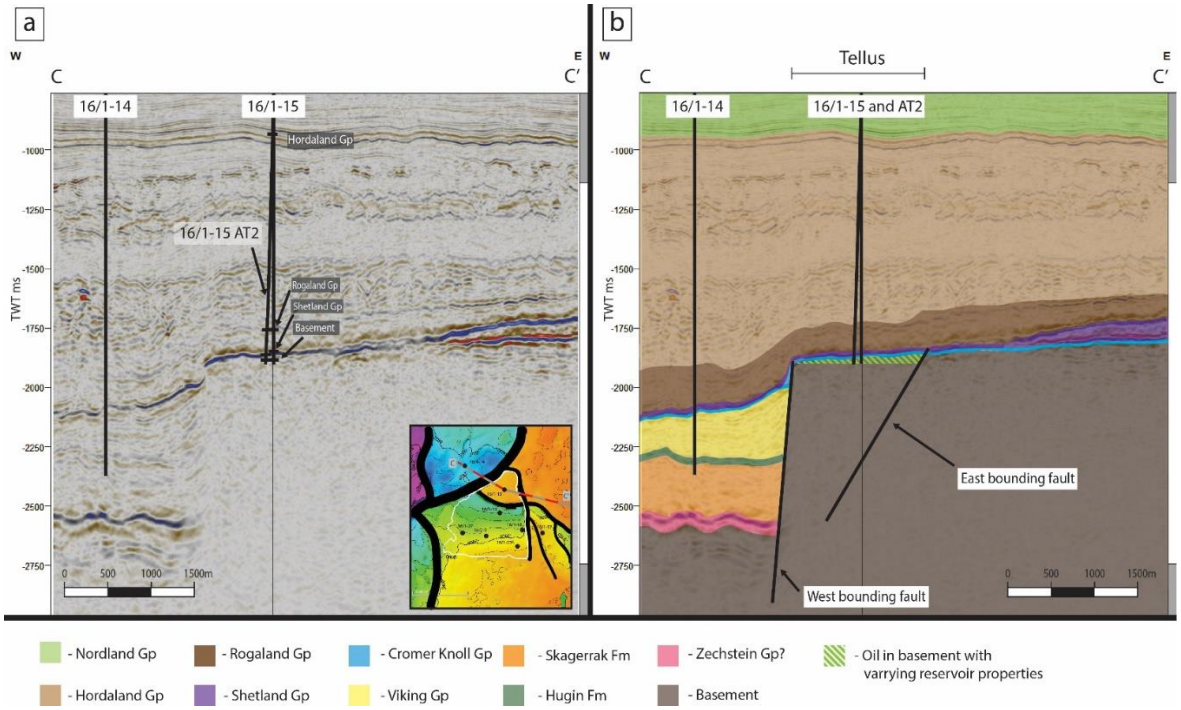

Figure 5.1.10: Uninterpreted (a) and interpreted (b) W-E seismic section of the Tellus discovery

5.2 P-graben and Ragnarrock

The Ragnarrock and P-graben are oil/gas condensate discoveries located in the central part of the Utsira High. The Ragnarrock is on a relatively flat structural basement terrace situated in between Johan Sverdrup and Edvard Grieg fields (figure 5.0.2c and 5.2.1). The discovery has two separate hydrocarbon accumulations in Late- Cretaceous chalk and pre-Devonian basement reservoirs. In this subchapter both accumulations will be described individually. The P-graben is located in a Permo-Triassic half graben south-west of the Ragnarrock discovery.

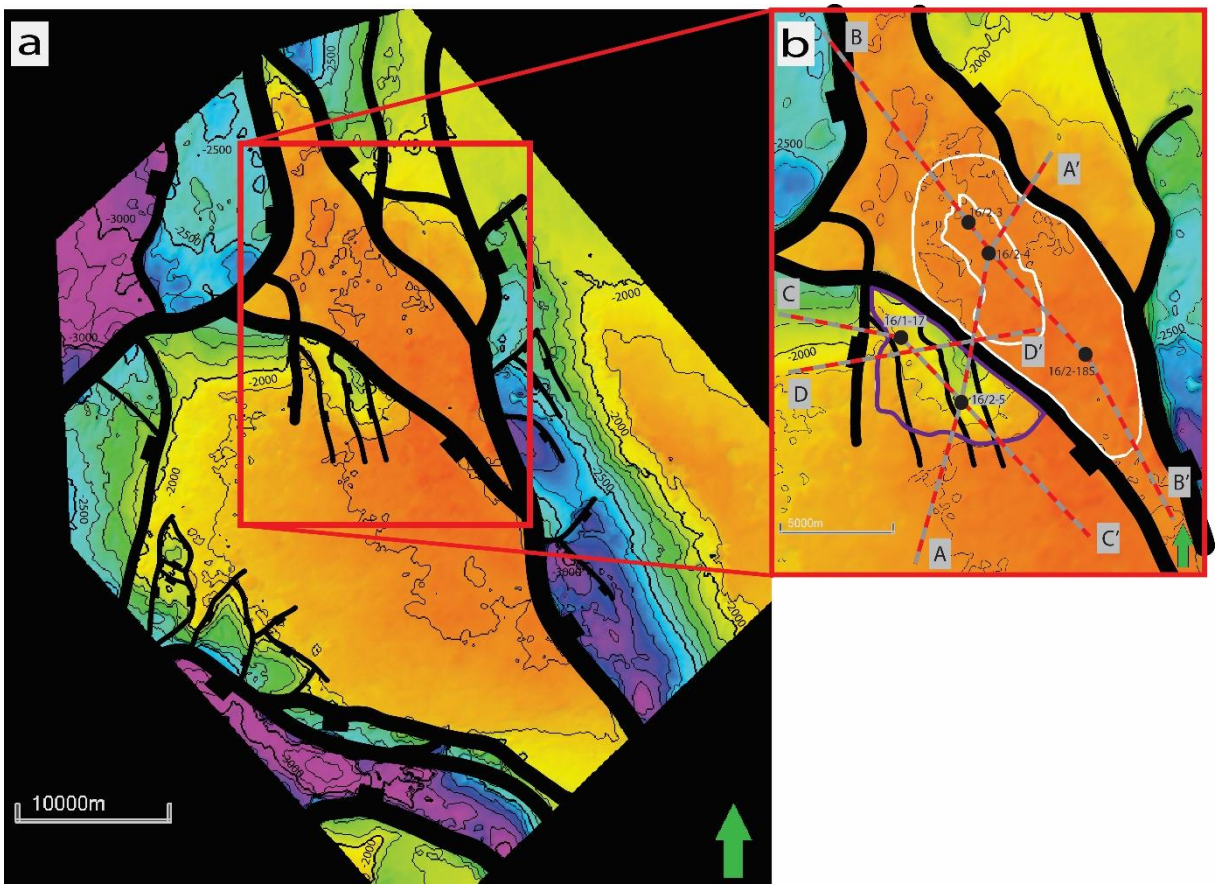

Figure 5.2.1:(a) Top Basement map of the southern Utsira High. (b) close-up on the position of Ragnarrock (white outline) and P-graben (purple outline) discoveries, location of wells, position of seismic composite line A-A' (figure 5.2.3), seismic composite line B-B' (figure 5.2.4), seismic composite line C-C' (figure 5.2.8) and seismic composite line D-D' (figure 5.2.9)

Ragnarrock Basement

The main reservoir is a fractured/weathered basement. The trap can be described as structural-stratigraphic where the top seal is represented by Cromer Knoll marls above the BCU. The base and side seals are defined by the reservoir quality. The reservoir quality is influenced by the extent of weathering and subsequent distribution of the fracture network. The clay mineral precipitation is another factor that affects the reservoir quality. Table 5.2.2 summarizes wells that were drilled in the discovery area. Both wells have proved movable oil with gas

condensate cap. Because of poor formation pressure measurements, it is difficult to determine the fluid contacts by just using the pressure measurements. Subsequently well-logs and mini-DST data were used to determine the contact depth.

Seismic composite line A-A' (figure 5.2.3) shows (a) an uninterpreted and (b) interpreted seismic section from south to north showing the P-graben and Ragnarrock discoveries. The figure illustrates that the Ragnarrock is bounded by the Luno master fault to the south and by the Augvald graben master fault to the north. Seismic composite line B-B' (figure 5.2.4) shows (a) an uninterpreted and (b) interpreted seismic section from N-W to S-E showcasing the Ragnarrock discovery. The figure shows that the dipping top seal (Cromer Knoll gp) will become deeper than the established fluid contacts to both N-W and S-E, thus acting as the top and side seal marking the maximum possible extent of the Ragnarrock discovery with known fluid contact depths. Unlike Tellus or Rolfsnes, no thin Cretaceous sandstone layer was proven overlying the basement. All three wells have reported similar reservoir properties. Primary porosity is represented by fractures that are locally filled by quartz or clay minerals. There is also secondary porosity created after dissolution of the plagioclase or carbonate cements.

Table 5.2.2: Summary of lithologies, fluid contacts, depth of the shows and ODT (oil down to) situations in P-graben and Ragnarrock.

Well	**Discovery**	**Reservoir Group/Formation**	**GOC TVD MSL (m)**	**OWC TVD MSL (m)**	**Top of the reservoir TVD MSL (m)**
16/1-17	P-graben	Skagerrak fm	-	Shows at 1856, 1867 and 1917	1843,4
16/2-5	P-graben	Jurassic/ Triassic unknown	1852	1867	1834,8
16/2-3	Ragnarrock Chalk	Tor fm	1669,5	1747	1667,5
	Ragnarrock Basement	Basement	-	-	1845
16/2-4	Ragnarrock Chalk	Tor fm	-	1721	1660
	Ragnarrock Basement	Åsgard fm, Basement	1840	1887	1831
16/2-18S	Ragnarrock Basement	Basement	-	1887	1841

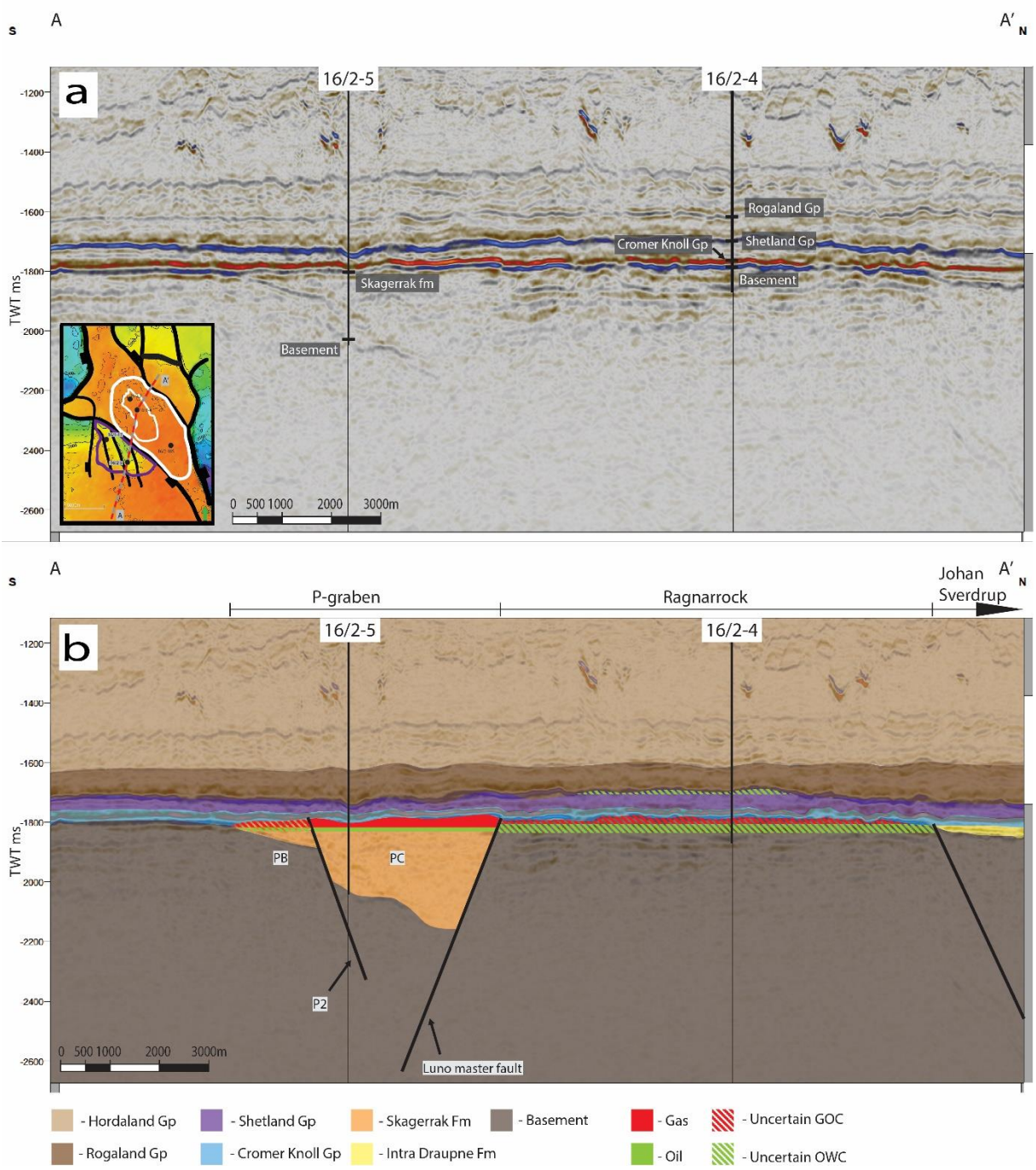

Figure 5.2.3: Uninterpreted (a) and interpreted (b) S-N seismic section of the P-graben and Ragnarrock discoveries

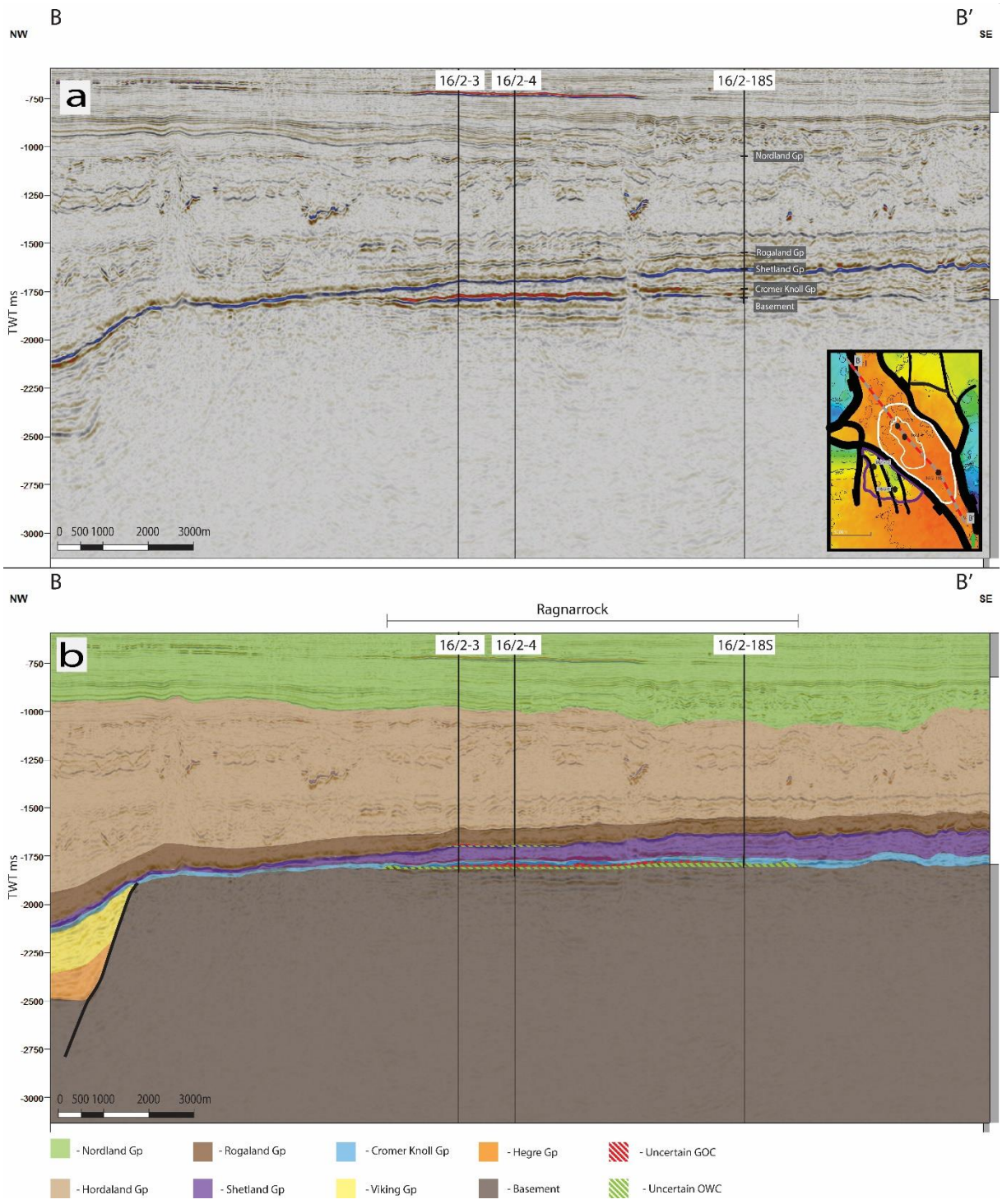

Figure 5.2.4: Uninterpreted (a) and interpreted (b) NW-SE seismic section of the Ragnarrock discovery

Ragnarrock Chalk

Ragnarrock chalk is an oil/gas condensate discovery located above the Ragnarrock basement discovery. As table 5.2.2 shows the discovery was proven by two wells that were drilled in the Ragnarrock discovery. Well 16/2-18S has proven weak shows near the top of the Shetland gp. Out of all wells available for the study only two have proven shows near top of the chalk. Both are located in the just to the east of well 16/2-18S in the Johan Sverdrup field. The reservoir is Late Cretaceous chalk of Ekofisk and Tor fm. The Paleocene Rogaland gp shales are the top seal. Side and bottom seals are determined by reservoir properties that can vary greatly. This is best described by the varying fluid contacts from table 5.2.2. Top of the Shetland gp has a high impedance contrast with the overlying shales. Thus, the effects of the hydrocarbon filling on the impedance contrast along the top Shetland reflection are negligible. Because of these no specific amplitude variations were observed. Figure 5.2.5 shows a top Shetland gp map with outline of the Ragnarrock chalk retrieved from the NPD (2021) and wells where shows were observed as well as some wells for reference.

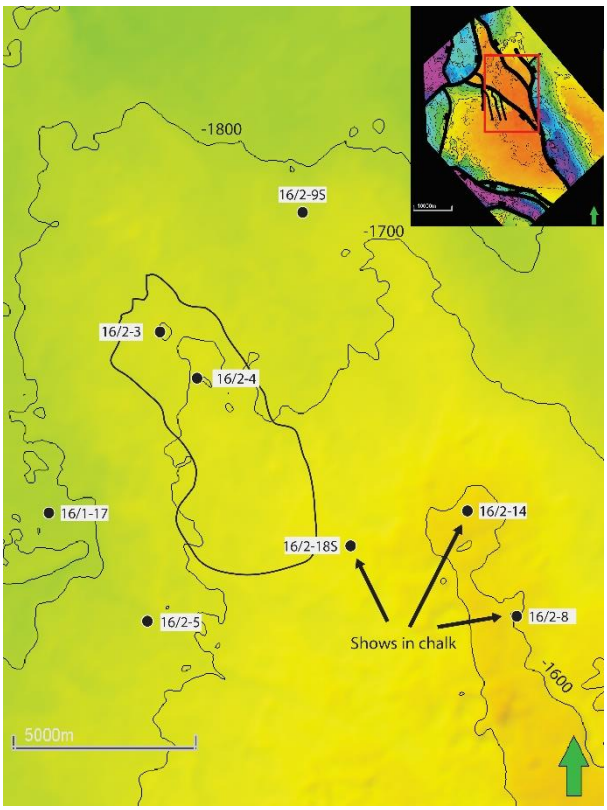

Figure 5.2.5: Top Shetland gp map with black outline of the Ragnarrock chalk discovery, together with some reference wells.

P-graben

The P- graben is an oil/gas condensate discovery located in the central part of the Southern Utsira High. It is located in the same Permo- Triassic half graben as the Edvard Grieg field but is separated from it by a N-S trending fault (figure 5.2.1). The P-graben structure can be described as a structural stratigraphic trap where the top seals are shales/marls of Cromer Knoll gp above the BCU. The side seals are sealing faults or lateral lithological changes in the reservoir. The main reservoir is the Triassic/ Jurassic conglomerates of the Skagerrak fm. The first discovery well (16/2-5) in the structure that was spudded in 2009 yielded no age diagnostic fossils, but well 16/1-17 (spudded in 2013) allowed the graben-fill to be dated and associated to Skagerrak fm. This would also conform with observations from the Edvard Grieg field where most of the graben-fill is dated to be Skagerrak fm conglomerates.

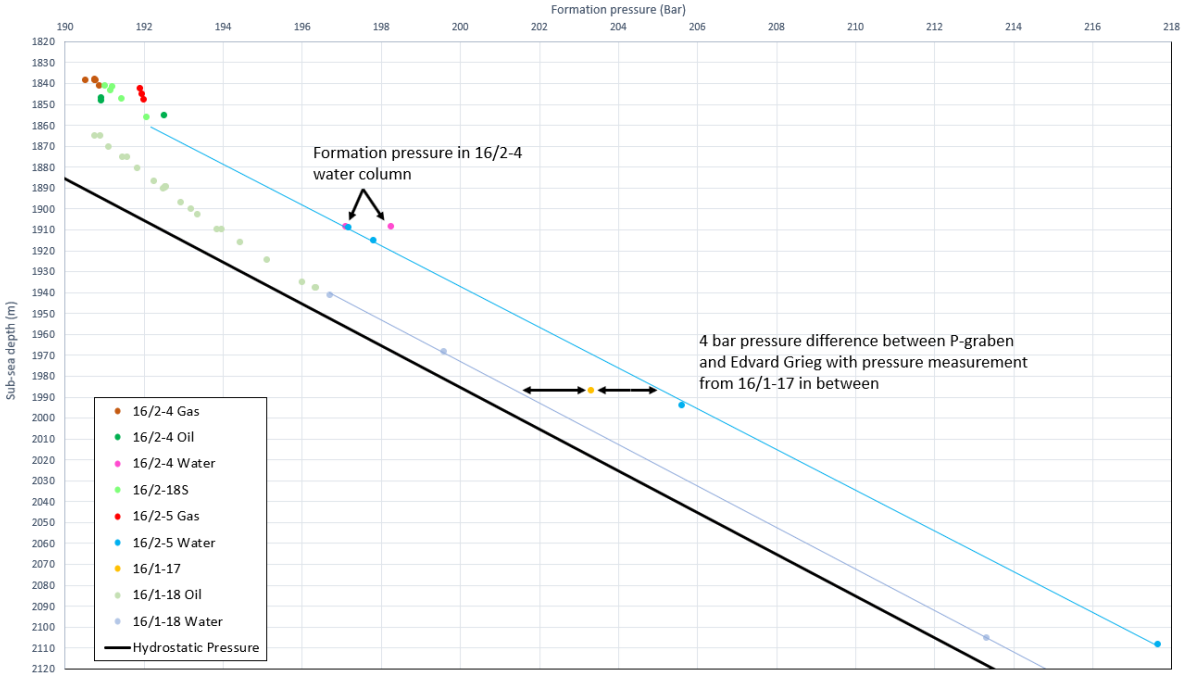

Figure 5.2.6: A combined formation pressure plot of all wells in the Ragnarrock and P-graben discoveries with reference to Edvard Grieg (16/1-18) and hydrostatic pressure

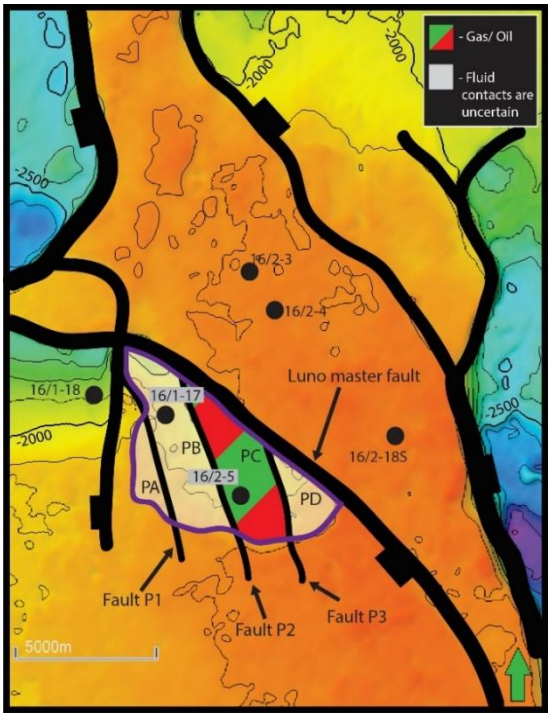

Figure 5.2.7: Top basement surface map showing four pressure compartments (PA, PB etc) and three faults bounding them (P1, P2 and P3)

As it can be seen from table 5.2.2 there were only two wells that were drilled in the P-graben area. Despite proving the oil with gas condensate cap in discovery well 16/2-5, later appraisal well 16/1-17 was tight with oil shows (and thus classified as dry) with 2 out of 3 shows within the 16/2-5's oil leg and beneath the 16/2-5's established OWC.

To the north-east the P-graben is bounded by the Luno master fault. Conglomerates are juxtaposed to the basement. 73m difference in contact depth between the Edvard Grieg and P-graben as well as 4 bar formation pressure difference in the water zone (figure 5.2.6) are suggesting that fault is sealing. Several faults have been observed that are cutting through the P-graben subdividing the half-graben into 4 compartments: PA, PB, PC and PD (figure 5.2.7). None of the wells in the P-graben have cut through the faults so there is no information on the sealing ability of the faults. It is also important to mention that faults were interpreted based on the displacement of the top basement reflector. The chaotic

nature of the graben fill reflectors did not have equally apparent displacement and thus the fault continuity in the graben fill is uncertain. This can be seen in two seismic composite lines. Seismic composite lines C-C' (figure 5.2.8) shows (a) an uninterpreted and (b) interpreted seismic section from north-west to south-east showing the compartments of the P-graben.

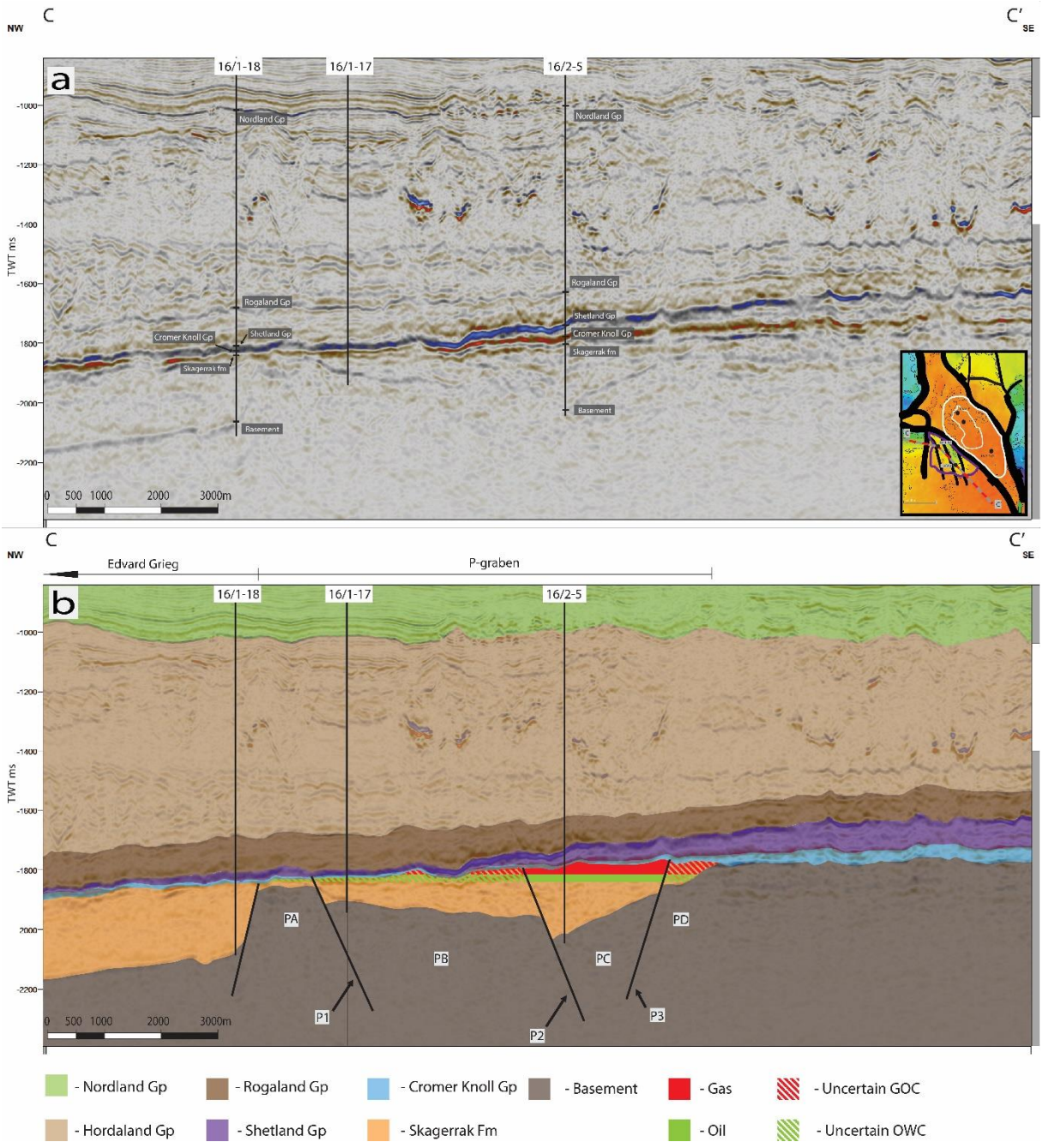

Figure 5.2.8: Uninterpreted (a) and interpreted (b) NW-SE seismic section of the P-graben discovery

Seismic composite lines D-D' (figure 5.2.9) shows (a) an uninterpreted and (b) interpreted seismic section from west to east showing the compartments of the P-graben.

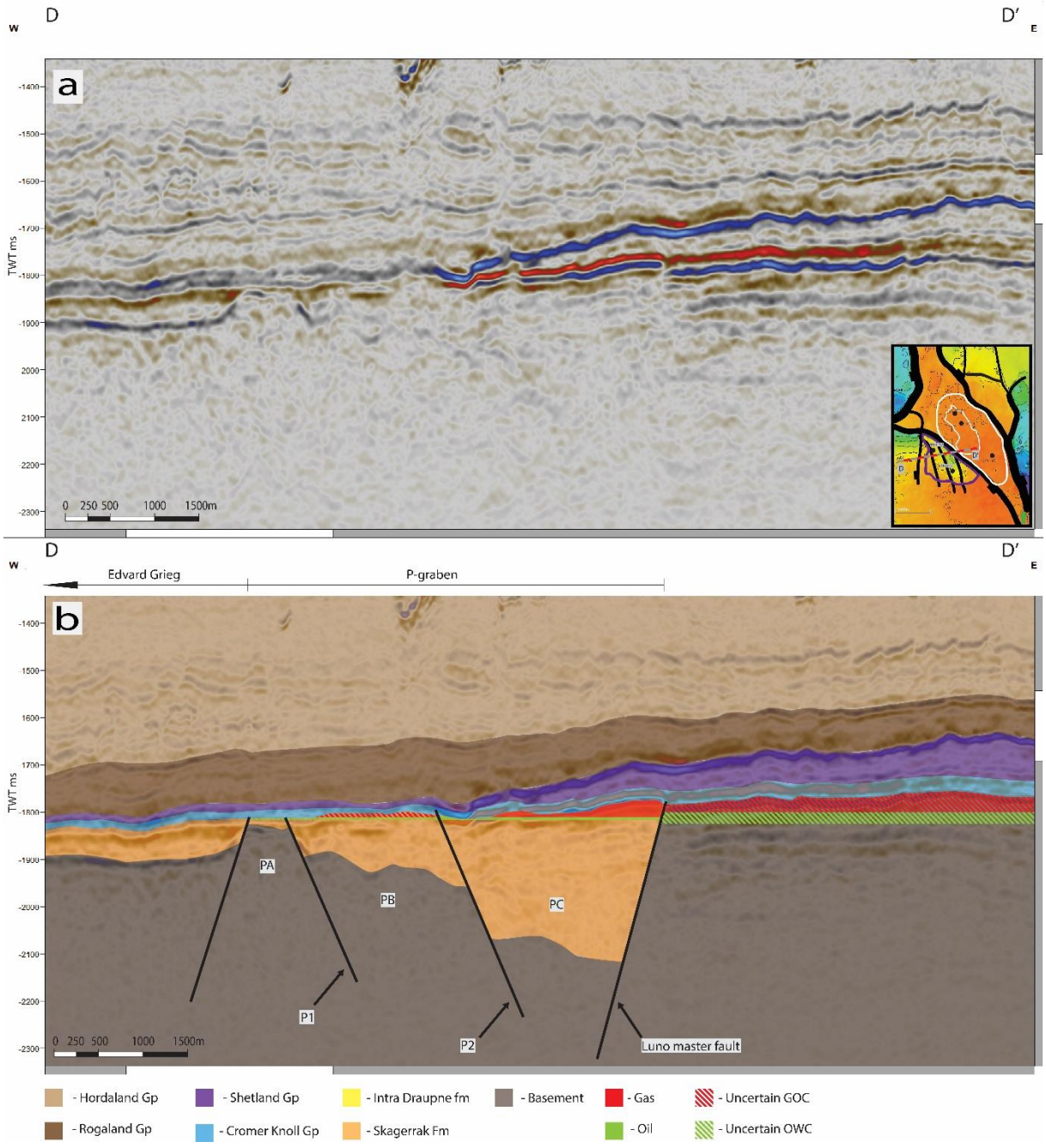

Figure 5.2.9: Uninterpreted (a) and interpreted (b) W-E seismic section of the P-graben and Ragnarrock discoveries

As both the wells shown reservoir conglomerates were mainly made off the breccias and/or the pebbly sandstones with very fine sand/clay as matrix with quartz and hematite cementation. The reservoir unit pinches out towards east, south and south-west with the basement as side seal. Compartment PB is also bounded by Luno discoveries east bounding fault to the north-west (see 5.1).

5.3 Rolfsnes

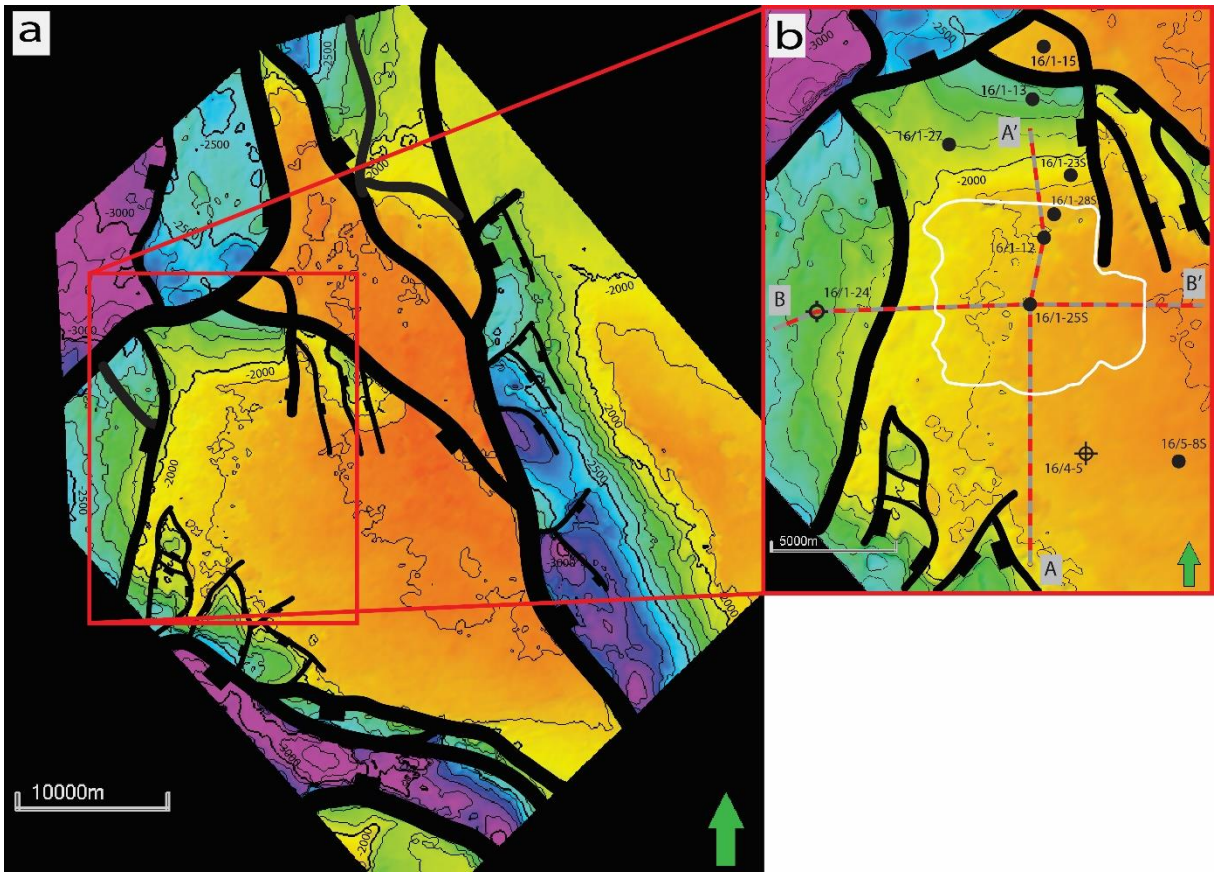

Figure 5.3.1:(a) Top Basement map of the southern Utsira High. (b) close-up on the position of Rolfsnes (white outline) discovery, location of wells, position of seismic composite line A-A' (figure 3) and seismic composite line B-B' (figure 4).

The Rolfsnes is an oil discovery located in the southern part of the Utsira High. The Rolfsnes is on a relatively flat structural basement terrace situated in between the Edvard Grieg and Solveig fields (figure 5.3.1). In the early exploration phase discovery was thought to be a southern extension of the Edvard Grieg field. Later, in the appraisal phase it was discovered that Rolfsnes has shallower contact.

Table 5.3.2: Summary of lithologies, fluid contacts and depths of the top reservoir in the Rolfsnes discovery.

Well	**Discovery**	**Reservoir Group/Formation**	**HC- water contact TVD MSL (m)**	**Top of the reservoir TVD MSL (m)**
16/1-12	Rolfsnes	Åsgard fm, Basement	1929	1886,9
16/1-25S	Rolfsnes	Åsgard fm, Basement	1927,5	1897,6
16/1-28S	Rolfsnes	Åsgard fm, Basement	1928	1890,1
16/4-5	-	Basement	-	1871,8
16/5-8S	Goddo	Basement	-	-

The Rolfsnes structure can be described as a stratigraphic trap where the top seal is represented by Cromer Knoll gp marls overlying the BCU. The main reservoir is fractured/weathered basement. Table 5.3.2 summarizes wells that were drilled in the discovery area.
All of the wells have also proven a thin and permeable Cretaceous sandstone/conglomerate layer above the basement similar to Edvard Griegs's Tellus discovery. This sandstone layer has varying thickness and it is unknown whether the sandstone layer is continuous. In the case of the "patchy" distribution of the individual sand bodies their interconnection would play an important role in the fluid migration mainly due to much higher permeabilities and the ability of sand to communicate permeable basement across impermeable basement. The base sealing is dependent exclusively on the reservoir quality of the basement. The side sealing is dependent on the extent and interconnections of the permeable basement and sandstones.

The maximum possible extent of the discovery can only be determined for the western and northern boundaries (given that the good reservoir quality is present). Seismic composite line A-A' (figure 5.3.3) shows (a) an uninterpreted and (b) interpreted seismic section from south to north showing the Rolfsnes discovery. As this figure shows, to the north the Rolfsnes is bounded by the Luno graben. Well 16/1-28S is a horizontal well that was drilled after the start of the Edvard Greig's production, has proven formation pressure depletion close to the boundary of the Luno graben. Figure 5.3.4 shows that formation pressure increases to the one of wells 16/1-12 and 16/1-25 further away from the Luno graben, although it has to be mentioned that some of the good measurements are looking supercharged. Pressure depletion can be attributed to the start of the production from the Edvard Grieg. This proves at least a partial pressure communication between Edvard Grieg and Rolfsnes.

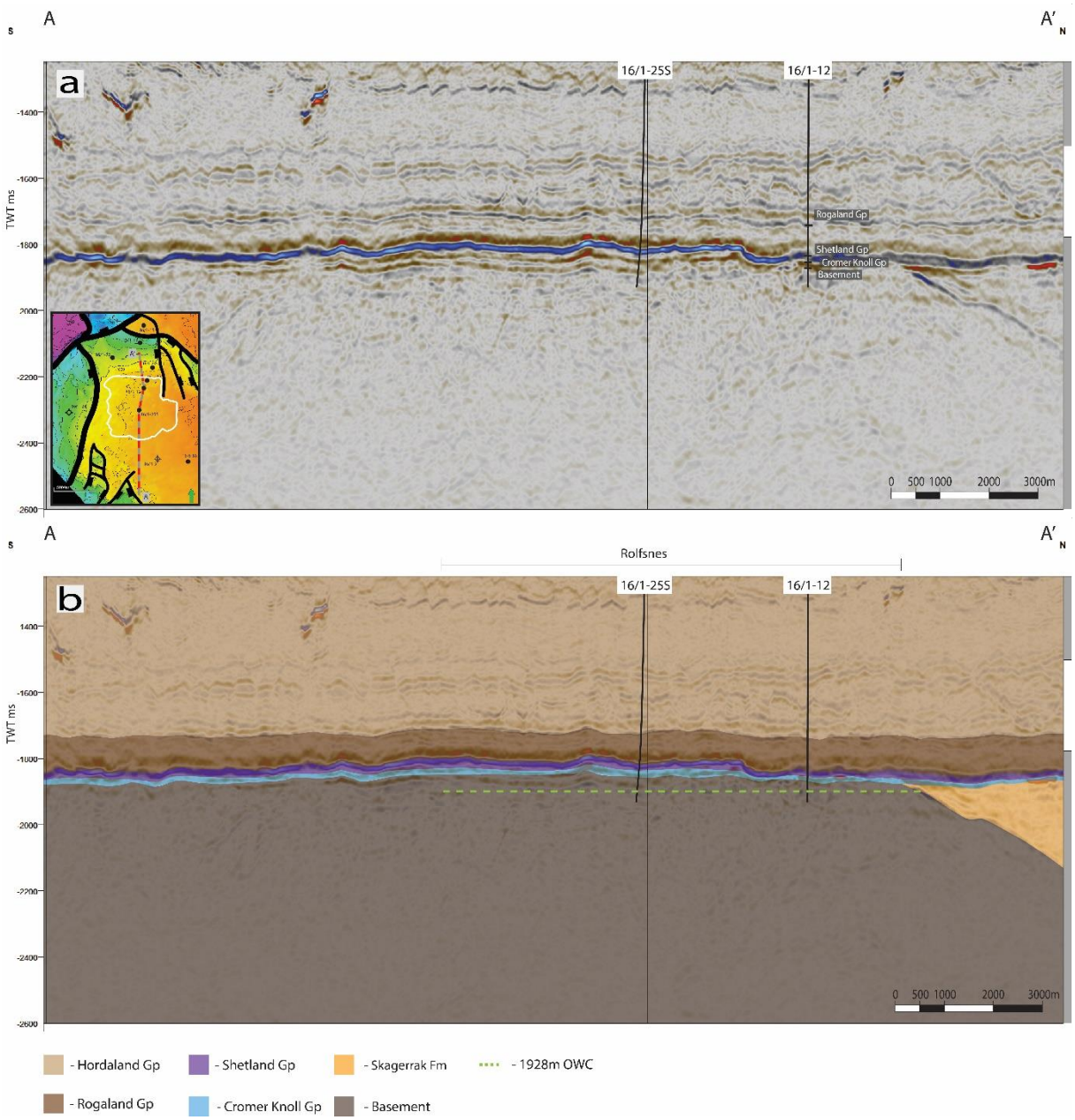

Figure 5.3.3: Uninterpreted (a) and interpreted (b) S-N seismic section of the Rolfsnes discovery

Seismic composite line B-B' (figure 5) shows (a) an uninterpreted and (b) interpreted seismic section from west to east showing the Rolfsnes discovery. This figure shows, that to the west-dipping top seal (Cromer Knoll gp) will become deeper than the established fluid contact, thus acting as the top and side seal the marking maximum possible western extent of the Rolfsnes discovery with known fluid contact depths.

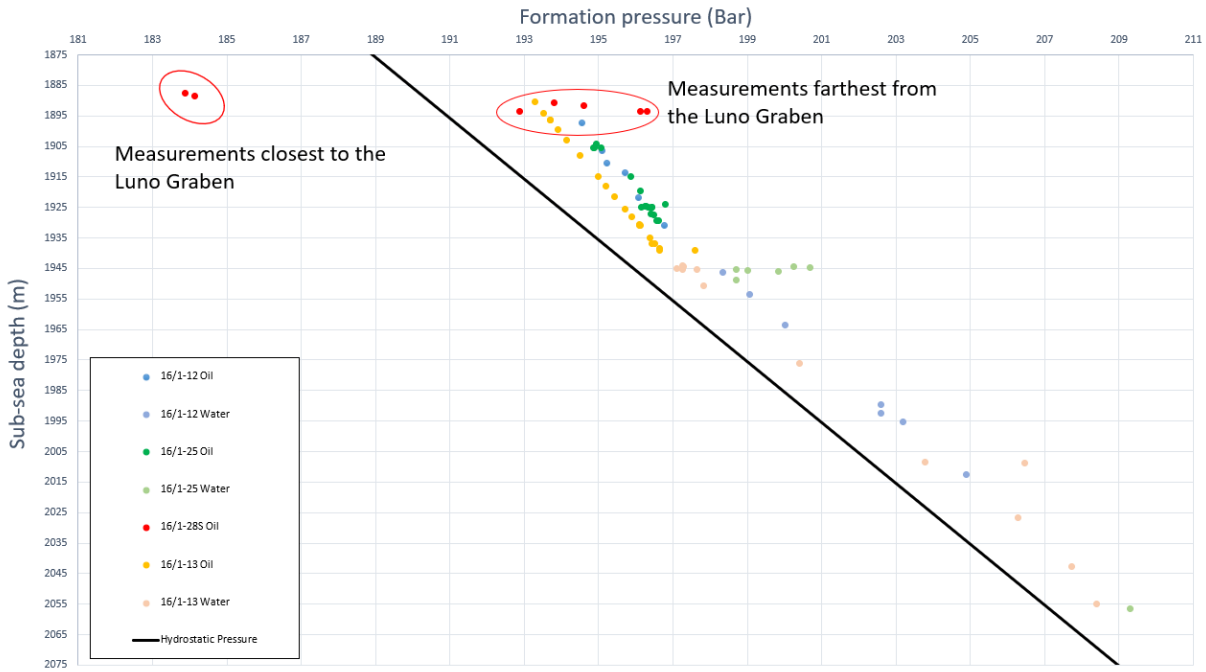

Figure 5.3.4: A combined formation pressure plot of all available wells in the Rolfsnes discovery with well 16/1-13 (Edvard Grieg) for reference.

To the east and south the side seals are defined by the reservoir quality since the top of the reservoir is shallowing or does not change in these directions. Similarly, the Tellus and Ragnarrock reservoir quality is influenced by the extent of weathering, subsequent distribution of fracture networks and possible clay precipitation. The extent of the Cretaceous sandstone layer is also important. Because of data limitations and clearly visible side seals, the discovery outline could not be determined to the south and east and thus the NPD's outline is used for visualization. Two wells have been drilled to the south-east of the Rolfsnes discovery to check for possible extension of the Rolfsnes outline. Available information for both is listed in table 5.2.2. Unfortunately, no formation pressure measurements are available due to the tight formation and the shows in 16/4-5 and that data from 16/5-8S is not publicly available yet. For well 16/5-8S it must be mentioned that according to the press release (NPD, 2019) it is not in pressure communication with Rolfsnes. Also, the Cretaceous sandstone on top of the basement is absent in both wells.

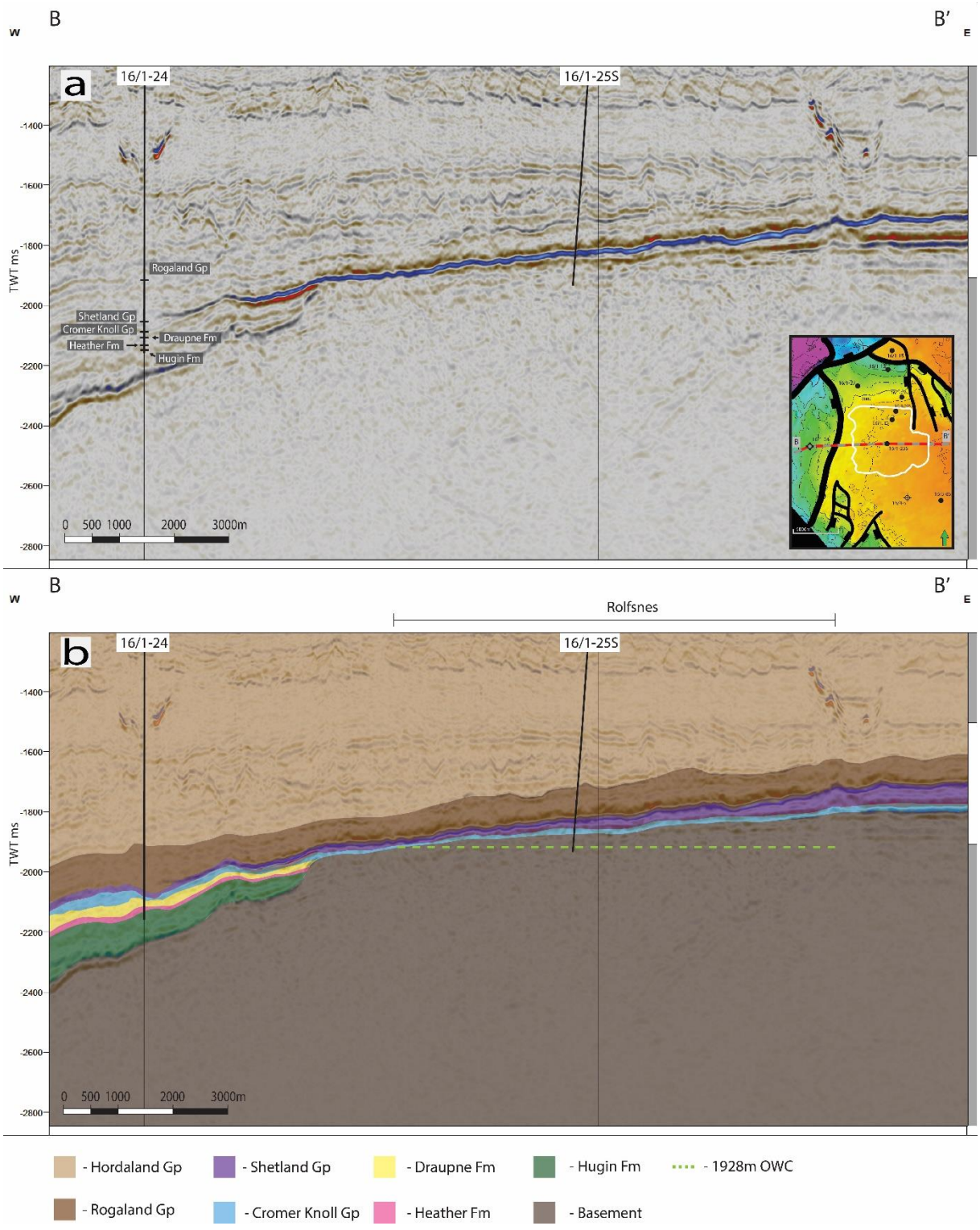

Figure 5.3.5: Uninterpreted (a) and interpreted (b) W-E seismic section of the Rolfsnes discovery.

5.4 Solveig

The Solveig is an oil discovery located in south-eastern part of the Utsira High. The Solveig is on the edge of a flat structural basement terrace situated in several Permo-Triassic grabens (figure 5.4.1). The Solveig structure can be described as a structural-stratigraphic trap. The main reservoir is Triassic Skagerrak fm. Jurassic Vestland gp, Triassic Smith Bank fm in 16/4-6S and Permian Rotliegend gp in 16/4-11 are also mentioned in the biostratigraphic part of the completion reports, but these were determined based on little evidence and are questioned in the reports. Because of that only Skagerrak fm was interpreted. Table 5.4.2 summarizes wells that

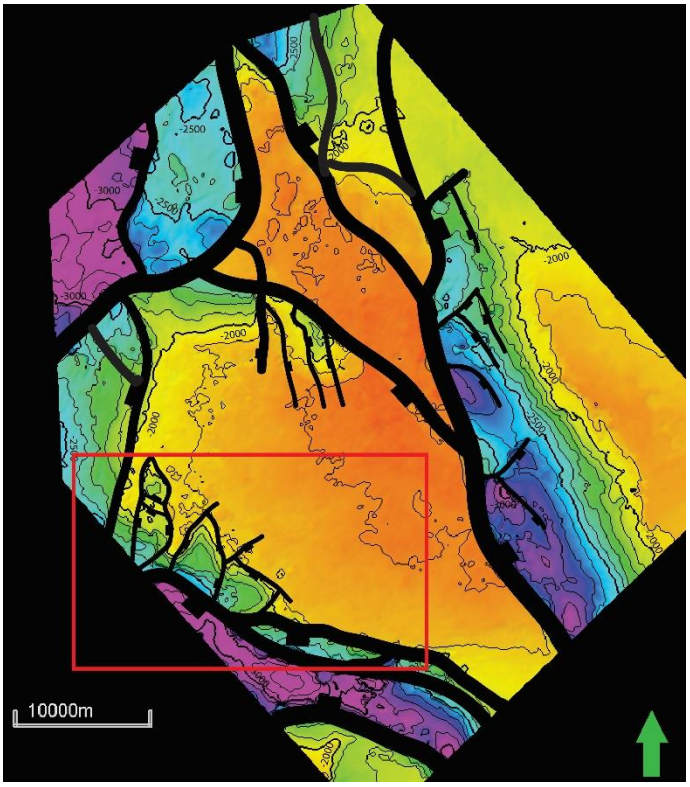

Figure 5.4.1: Top Basement map of the southern Utsira High, red outline shows figure 5.4.3.

Table 5.4.2: Summary of lithologies, fluid contacts, top of reservoir and depth of the shows in Solveig

Well	**Discovery**	**Reservoir Group/Formation**	**HC- water contact TVD MSL (m)**	**Top of the reservoir TVD MSL (m)**	**Shows TVD MSL (m)**	**Oil family**
16/4-6S	Solveig	Vestland gp? Skagerrak fm Smith Bank fm?	1950	1905	1931-1998	1,2
16/4-8S	Solveig	Skagerrak fm	1939	1909	1903-2369	1,2
16/4-9S	Solveig	Skagerrak fm	1956	1931	1935-1992	1,2
16/4-11	Solveig	Skagerrak fm Rotliegend gp?	1946,5	1925	1927-1979	1,2
16/5-5	Solveig	Skagerrak fm	Shows	1914	1912-1957	2

were drilled in the discovery area. All the drilled wells have proven two oil families in the reservoir, well 16/5-5 has proven only one as shows. Of these, family one is heavily bioturbated oil from marine bioturbated oil from marine Draupne fm similarly to the rest of the Utsira high (marked as family 1 in table 5.4.2). Family two is non-bioturbated and stems

from terrestrial source rock (marked as family 2 in table 5.4.2). This indicates at least two periods of charge into the Solveig.

The reservoir temperature is 75-80°C. Several pressure compartments have been identified, these align well with the individual grabens as seen from figure 5.4.3. Drilled grabens have

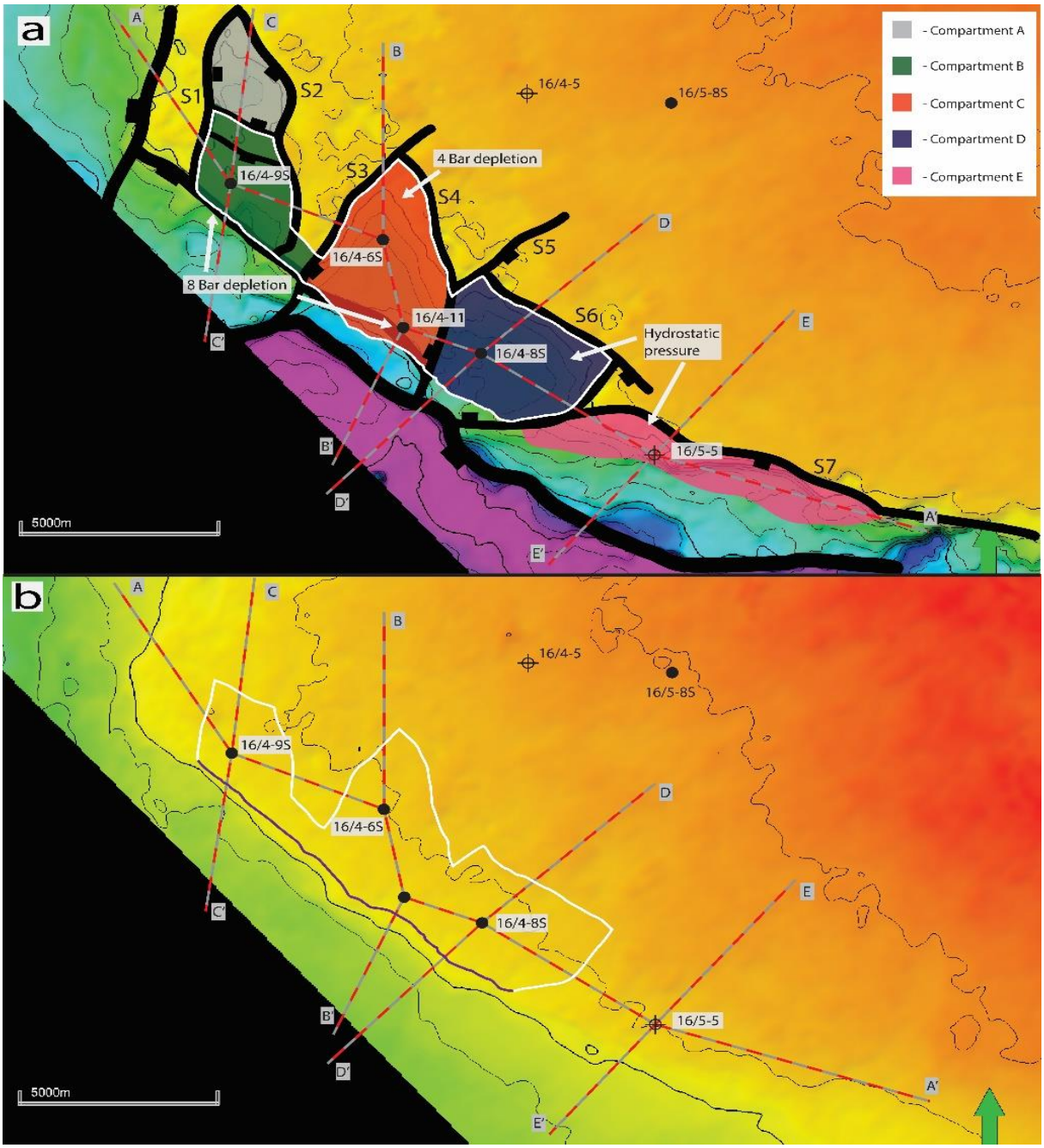

Figure 5.4.3: (a) Top basement surface map showing Solveig grabens in color, faults bounding them (S1, S2 etc), position of the Solveig field (white outline), location of wells, position of seismic composite line A-A' (figure 5.4.4), seismic composite line B-B' (figure 5.4.6), seismic composite line C-C' (figure 5.4.7), seismic composite line D-D' (figure 5.4.8) and seismic composite line E-E' (figure 5.4.9). (b) Top BCU surface map showing Solveig outline with seismic composite lines and wells for reference. Purple line shows outline where side sealing is represented by the marls above the BCU and white line shows outline of the field where top reservoir pinches-out

different contact depths and formation pressures. Compartment E was proven to be dry and compartment A is undrilled as for late 2020. Oil legs in the compartments are of the first oil

family, but some asphaltene was observed within the oil leg in well 16/4-6S. Shows are made of bioturbated second oil family in oil bearing wells. Shows in well 16/5-5 is made of the second oil family.

The top seal is represented by Cromer Knoll gp and Shetland gp marls overlying the BCU. The side sealing is represented by the stratigraphic pinch-out of the reservoir against the basement towards Utsira high generally to the north and east. To the south and west side sealing are made by dipping marls above the BCU. Each of the compartments will be discussed individually in this subchapter. No base seal has been observed in any of the wells, but in areas where the reservoir pinches-out the basement can potentially act as base seal. Seismic composite line A-A' (figure 5.4.4) shows (a) an uninterpreted and (b) interpreted seismic section from north-west to south-east showing overview of all drilled compartments in the Solveig.

All of the described compartments and faults are shown in figure 5.4.3, where compartments are assigned with letters A-E and faults are assigned with numbers 1-6 counting from northernmost to southernmost compartments/faults.

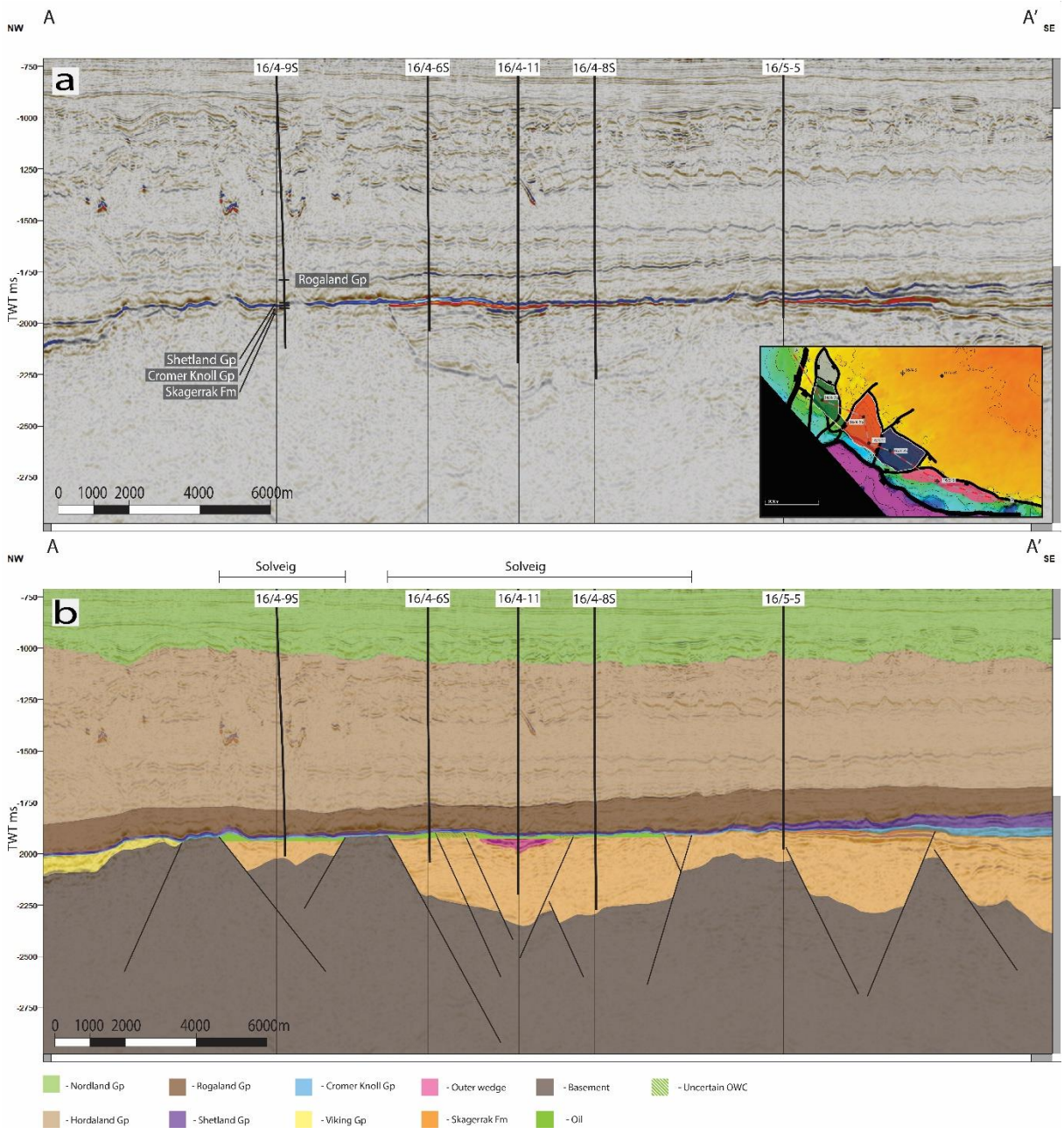

Figure 5.4.4: Uninterpreted (a) and interpreted (b) NW-SE seismic section of the Solveig field.

Compartment C is in the central part of the Solveig discovery, located in the Permo-Triassic graben that is bounded by NE-SW trending fault 3 and NNW- SSE trending fault 4. This compartment was drilled by two wells 16/4-6S and 16/4-11. Both have proven oil and thin gas cap in 16/4-6S, with similar OWC contacts (table 5.4.2) but 4 bar difference in formation pressure (figure 5.4.5). The reservoir quality is moderate to good in both wells. Seismic

composite line B-B' (figure 5.4.6) shows (a) an uninterpreted and (b) interpreted seismic section from south to north showing compartment C. The lateral sealing to the north, the east and most of the west is represented by the pinch-out of the reservoir against the basement towards the faults and by the dipping marls above the BCU to the south. Several minor faults were identified between the wells. Well 16/4-11 has also penetrated a well distinguishable outer wedge situated at the edge of the high. This wedge is laterally continuous into the compartment B just to the south of the basement high that separates these compartments.

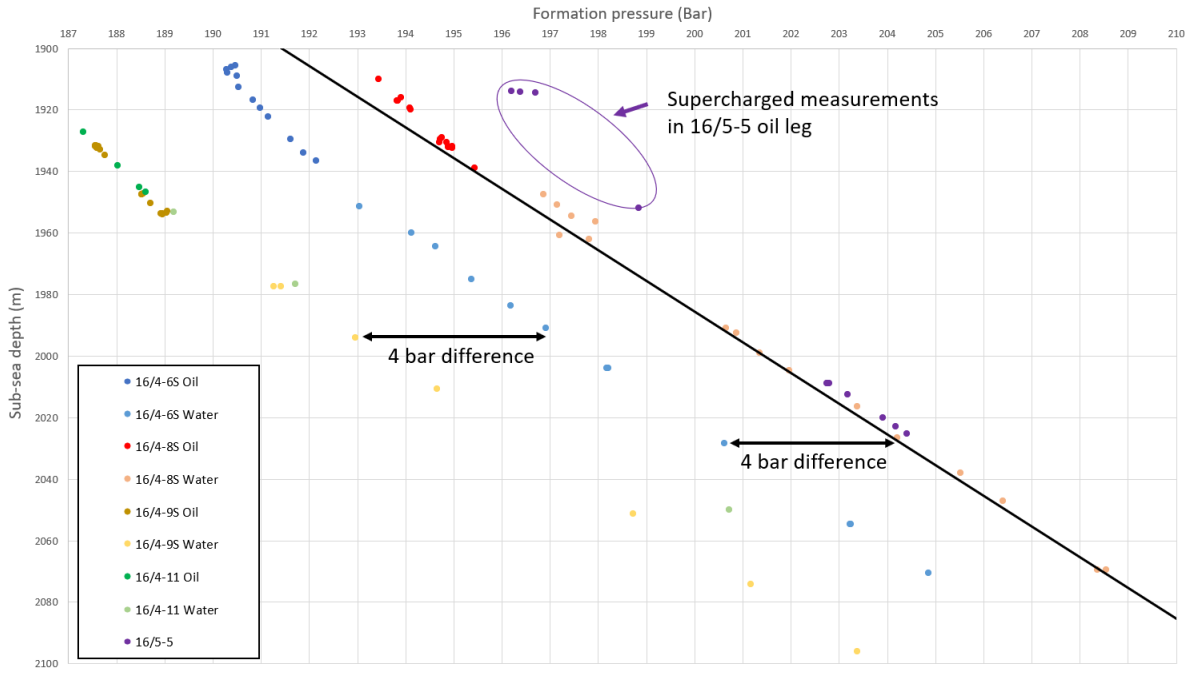

Figure 5.4.5: A combined formation pressure plot of all wells in the Solveig field and hydrostatic pressure gradient (black line), showing pressure differences between the different compartments.

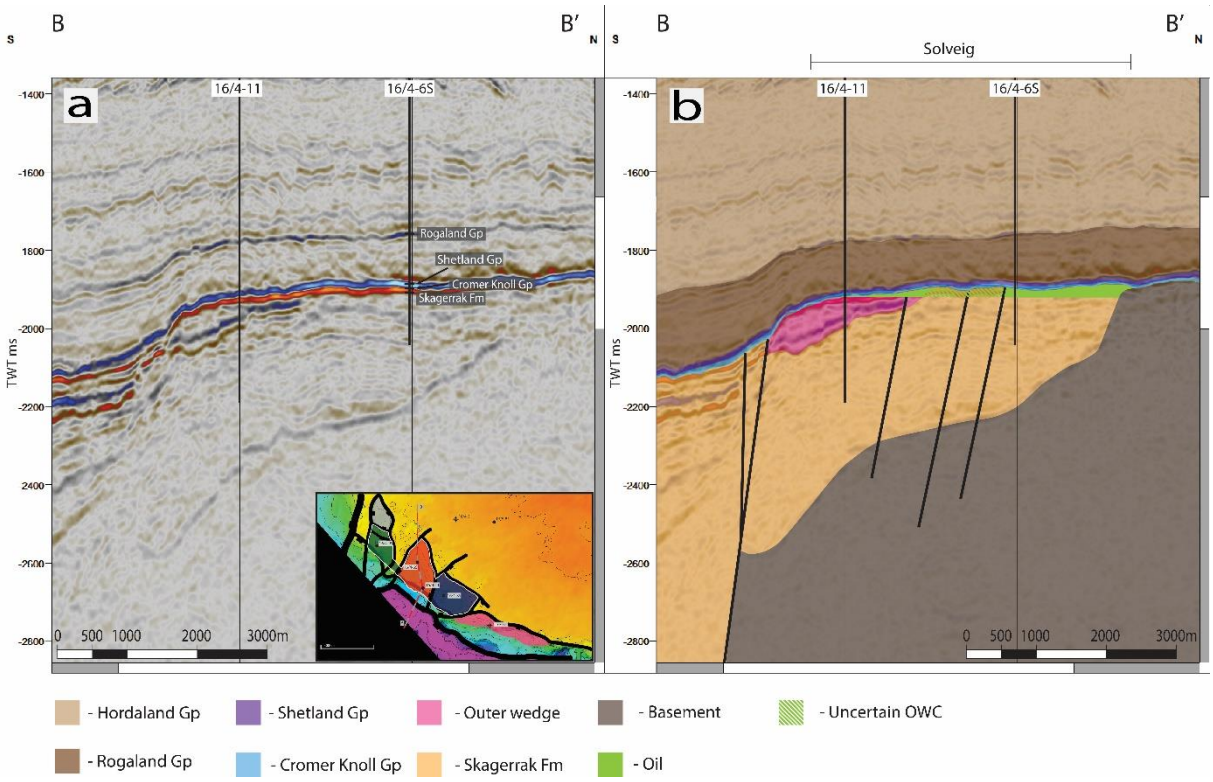

Figure 5.4.6: Uninterpreted (a) and interpreted (b) S-N seismic section of the compartment C of the Solveig field.

Compartment B was drilled by the well 16/4-9S and it proved 45m oil column with thin gas column (<1m) at the top. It lies in the Permo-Triassic graben that is bounded by N-S trending fault 1 and NNW- SSE trending fault 2. Seismic composite line C-C' (figure 5.4.7) shows (a) an uninterpreted and (b) interpreted seismic section from south to north showing compartments A and B. The sealing towards the N (compartment A) is described in the next paragraph. Compartment B is sealed by the pinch-out against the basement to the NW and NE. To the SE the dipping BCU and the marls above it create a dip seal. Well 16/4-9S similarly to 16/4-11 penetrated the outer wedge that is continuous between both wells. Figure 5.4.5 shows that this compartment is 8 bars depleted in comparison to hydrostatic pressure. It has similar pressure with well 16/4-11 in compartment C while being 4 bars depleted in comparison to well 16/4-6S from the same compartment. Table 5.4.2 shows that there is a 10m OWC difference between both outer wedge wells. No internal barriers such as faults were observed in the wedge leaving the possibility for communication with compartment C.

-

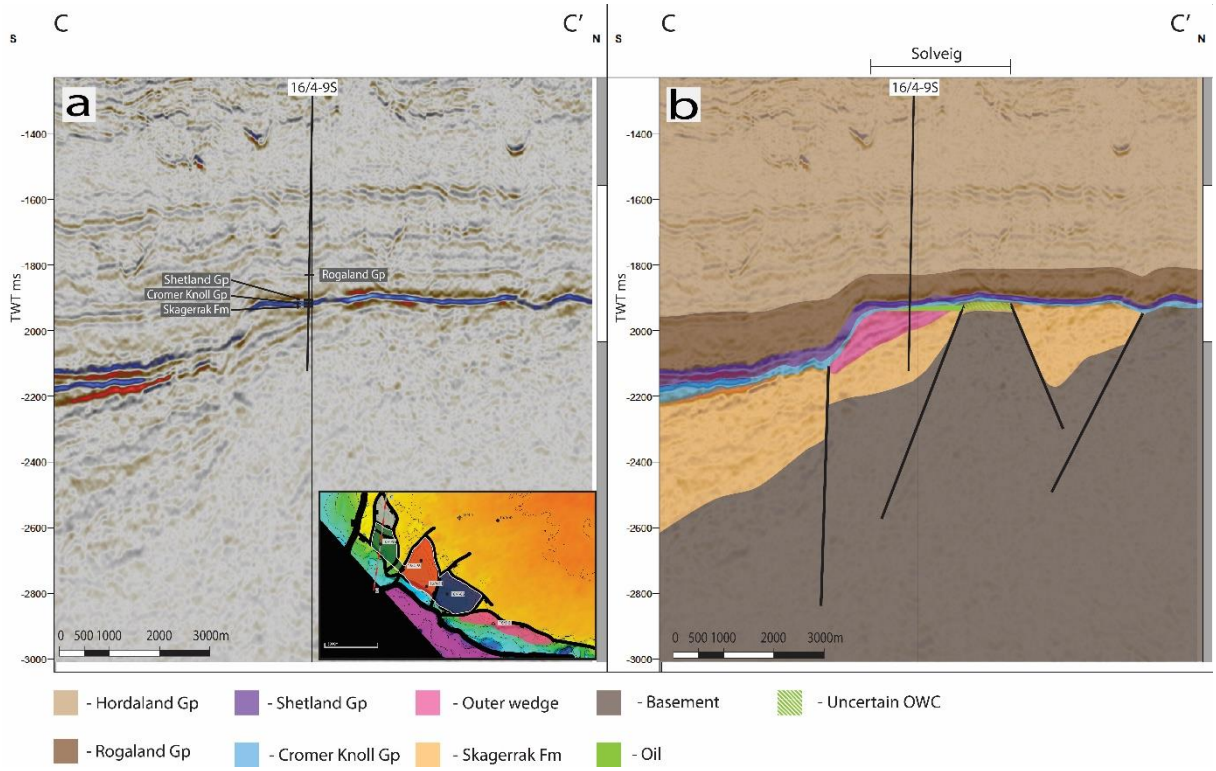

Figure 5.4.7: Uninterpreted (a) and interpreted (b) S-N seismic section of the compartments A and B of the Solveig field.

Compartment A is in the north-western part of the Solveig discovery. It lies in the same Permo-Triassic graben as compartment B. NW-SE trending fault zone that creates a horst like structure (figure 5.4.7) is dividing the half-graben in two compartments, A and B. A is the only compartment in the Solveig that is undrilled to the time of writing of this thesis. Thus, infilling, fluids and formation pressure of this compartment is unknown. Figure 5.4.7 shows that the NW-SE fault zone leaves room for a possible reservoir connection between the A and B compartments. Sealing between A and B compartments is dependent on the quality of the reservoir and sealing properties of the faults in the fault zone. In all other directions compartment A is sealed by the pinch-out of the reservoir against the basement. Reflectors within the compartment A exhibit similar features such as dip and relative continuity to the reflectors in other compartments in the Solveig. This may suggest a similar depositional environment to the other compartments and thus the infill is interpreted to be of the Triassic Skagerrak fm.

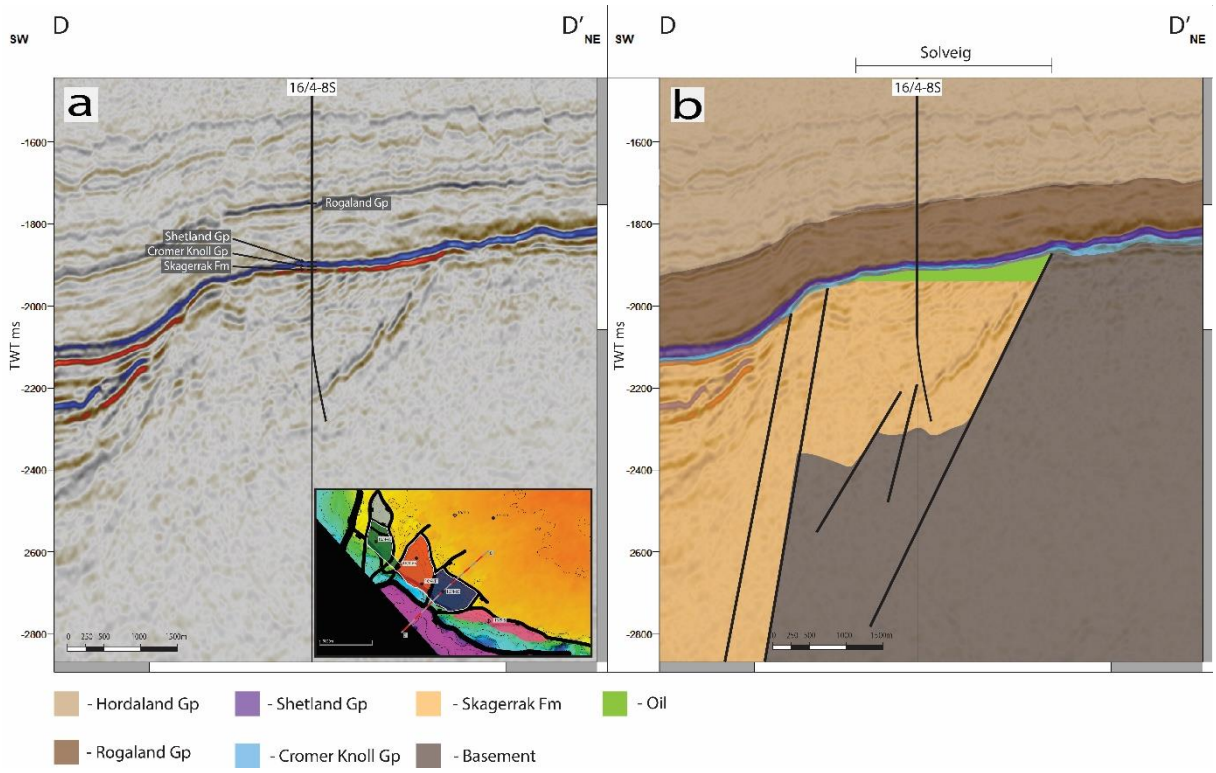

Figure 5.4.8: Uninterpreted (a) and interpreted (b) S-N seismic section of the compartment D of the Solveig field.

Compartment D was drilled by the well 16/4-8S and it proved around a 30m oil column with thin gas cap (<1m). It lies in the Permo-Triassic graben that is bounded by three faults: NNW-SSE trending fault 4, NNW- SSE trending fault 5 and W-E trending fault 6. Formation pressure in the compartment is slightly above the hydrostatic (figure 5.4.5) and is 4-8 bars higher than in compartments B and C. Seismic composite line D-D' (figure 5.4.8) shows (a) an uninterpreted and (b) interpreted seismic section from south-west to north-east showing the compartment D. Outer wedge has not been observed in this compartment. Compartment is sealed by the faults on all the sides besides SE where dipping BCU and marls above it create a dip seal. To the NE the reservoir pinches-out against the basement. To the NW fault 4 is the biggest candidate for side seal especially considering 8 bar pressure difference between wells. Fault 6 is separating compartment D from E.

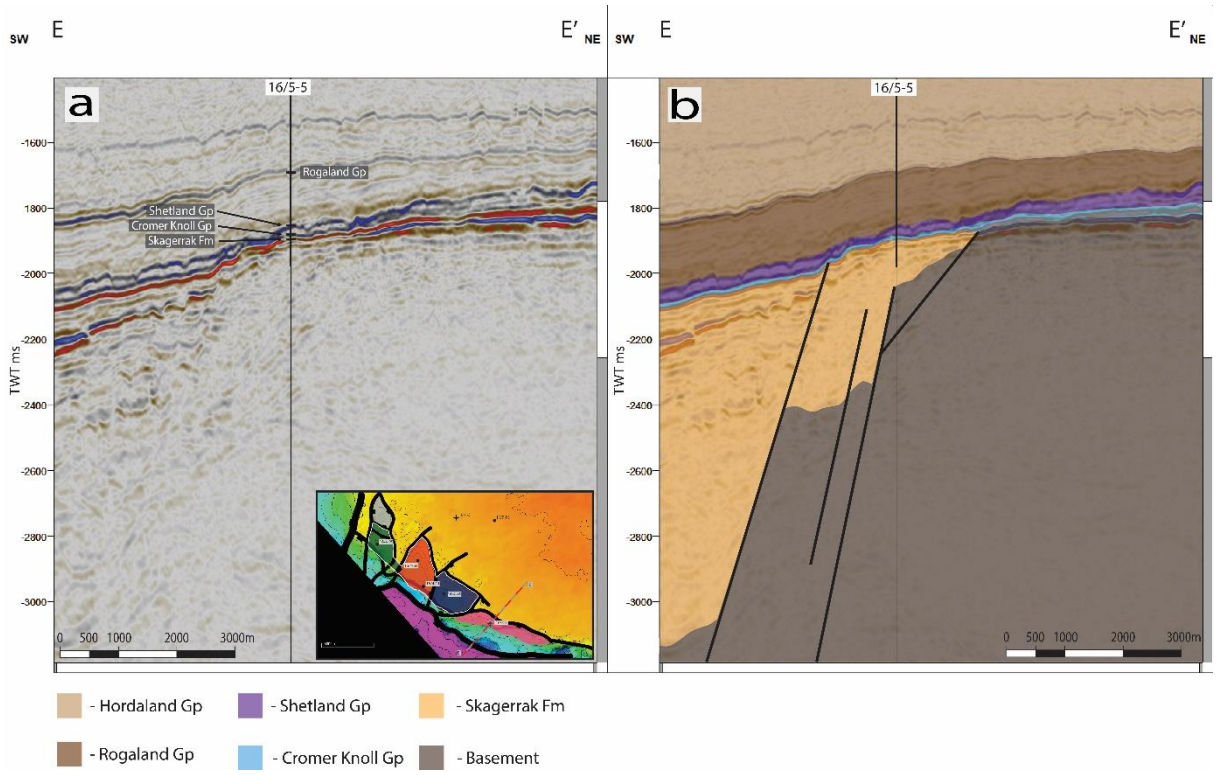

Figure 5.4.9: Uninterpreted (a) and interpreted (b) S-N seismic section of the compartment E of the Solveig field.

Compartment E is in the south-eastern part of the Solveig discovery. Seismic composite line E-E' (figure 5.4.9) shows (a) an uninterpreted and (b) interpreted seismic section from south-west to north-east showing compartment E. It was drilled by the well 16/5-5. The well was dry with the shows of heavily bioturbated oil. The formation had generally poor reservoir quality in the upper part, resulting in mostly supercharged formation pressure measurements (figure 5.4.5). The reservoir quality improved with the depth and water gradient similar to compartment D could be established. Thus, it was interpreted that fault 7 is not sealing, mostly tight upper part of the reservoir can explain why the 2nd charge of the hydrocarbons in the Solveig has not reached compartment E. The compartment outline in the figure with all compartments is based on the OWC from compartment D adjusted for check shots from well 16/5-5. This outline would fit if the well penetrated a locally tight reservoir. To the SE compartment is sealed by the dipping marls above the BCU. To the north and east it is sealed by the pinch-out of the reservoir.

5.5 Johan Sverdrup:

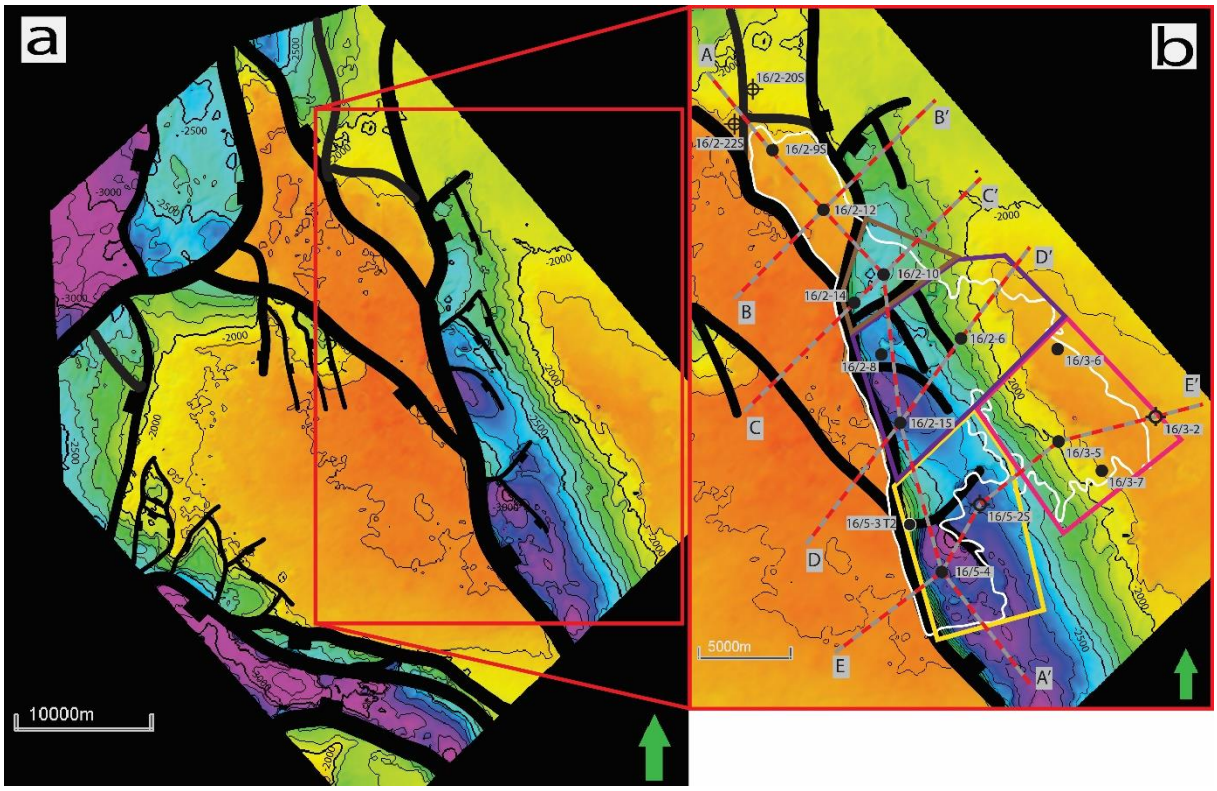

Figure 5.5.1:(a) Top Basement map of the southern Utsira High. (b) close-up on the position of Johan Sverdrup field (white outline), location of wells, position of seismic composite line A-A' (figure 3), seismic composite line B-B' (figure 4), seismic composite line C-C' (figure 5), seismic composite line D-D' (figure 6) and seismic composite line E-E' (figure 4). Field within the Augvald graben is subdivided into four parts: northern (brown outline), central (purple outline), eastern (pink outline) and southern (yellow outline).

The Johan Sverdrup is an oil field located in the north-eastern part of the Utsira High. The Johan Sverdrup field is in a Permo-Triassic Augvald graben with the bounding NW-SE trending normal fault to the south-west and on the terrace to the north-west (figure 5.5.1). It was first drilled by well 16/2-6 which encountered oil in Intra Draupne fm sandstones. Subsequently, 31 appraisal wells were drilled to delineate the discovery, appraisal wells have discovered a regional contact of 1922 TVDSS. The results from wells used in this work are shown in table 5.5.2. The main reservoir is the Jurassic Intra Draupne fm sandstone, but in some wells hydrocarbons are also found in some deeper lying Jurassic, Triassic and Permian sediment. The Johan Sverdrup structure can be described as a structural stratigraphic trap where the top seal is represented by Cromer Knoll and Vestland gp shales overlying the BCU. The base seal is present only in the southern extension of the field, wells 16/5-3 and 16/5-4. The side seal description will be separated into two parts: the Augvald graben and the north-western terrace (figure 5.5.1).

Table 5.5.2: Summary of lithologies, fluid contacts, depth of the top reservoir and shows in the Johan Sverdrup. All depths are given in TVD MSL.

Well	Part of the Johan Sverdrup	Reservoir Group/Formation	HC- water contact	Top of the reservoir	Depth of shows
16/2-6	Augvald graben	Intra Draupne fm, Hugin fm, Sleipner fm	1922	1904,9	-
16/2-8	Augvald graben	Intra Draupne fm, Hugin fm, Sleipner fm	1920,7	1853,2	-
16/2-9S	NW Terrace	Intra Draupne fm	1906,6	1898,9	-
16/2-10	Augvald graben	Intra Draupne fm, Hugin fm, Sleipner fm	1934,2	1868,2	-
16/2-12	NW Terrace	Intra Draupne fm, Hugin fm, Basement	-	1871,3	-
16/2-14	Augvald graben	Intra Draupne fm	-	1834,6	-
16/2-15	Augvald graben	Intra Draupne fm, Statfjord gp	1923	1890,5	1929
16/2-20S	NW Terrace	Draupne fm, Statfjord gp	Shows	1945	1950
16/2-22S	NW Terrace	Intra Draupne fm	Shows	1895	1923
16/3-2	Augvald graben	Intra Draupne fm	Dry	1948	-
16/3-5	Augvald graben	Intra Draupne fm, Zechstein gp	1923	1892,7	-
16/3-6	Augvald graben	Intra Draupne fm	1926	1914,6	1930
16/3-7	Augvald graben	Intra Draupne fm	1925	1922,7	1984
16/5-2S	Augvald graben	Intra Draupne fm	Dry	1928,4	1937
16/5-3 T2	Augvald graben	Intra Draupne fm	ODT 1889	1876	-
16/5-4	Augvald graben	Intra Draupne fm	ODT 1911,4	1905,7	-

North-western terrace

The north-western terrace is located to the north-west from the Augvald graben. The terrace has been drilled by five wells, information from four of these and their sidetracks has been used (table 5.5.2). Seismic composite line A-A' (figure 5.5.3) shows (a) an uninterpreted and (b) interpreted seismic section from the north-west to the south-east showcasing the NW terrace and the Augvald half-graben. This figure shows that the NW-terrace is separated from the Augvald half-graben by a N-S trending fault. The top of the Jurassic reservoir sequence is continuous across the fault. As figure 5.5.4 shows that the formation pressure in the oil-filled wells in the terrace is similar to the rest of the Johan Sverdrup field. Measurements in the other two wells are 1-3 Bars lower, so it was interpreted that these wells are not in communication with the Johan Sverdrup field. At the same time the reservoir quality decreases to the north-west towards dry wells, the reservoir becomes finer grained with a spiculite matrix in the wells 16/2-9S, 16/2-20S and 16/2-22S. This type of matrix is characterized by high capillary entry pressure which can explain shallower OWC due to a longer transition zone in well 16/2-9S while having similar pressures with the rest of Johan Sverdrup. The shows below 16/2-9S and common Johan Sverdrups (1922m TVDSS) OWC's

have been recorded in the 16/2-20S and 16/2-22S. OWC for well 16/2-12 was not encountered. Deepening of the top of the reservoir to the north-west acts as a side seal.

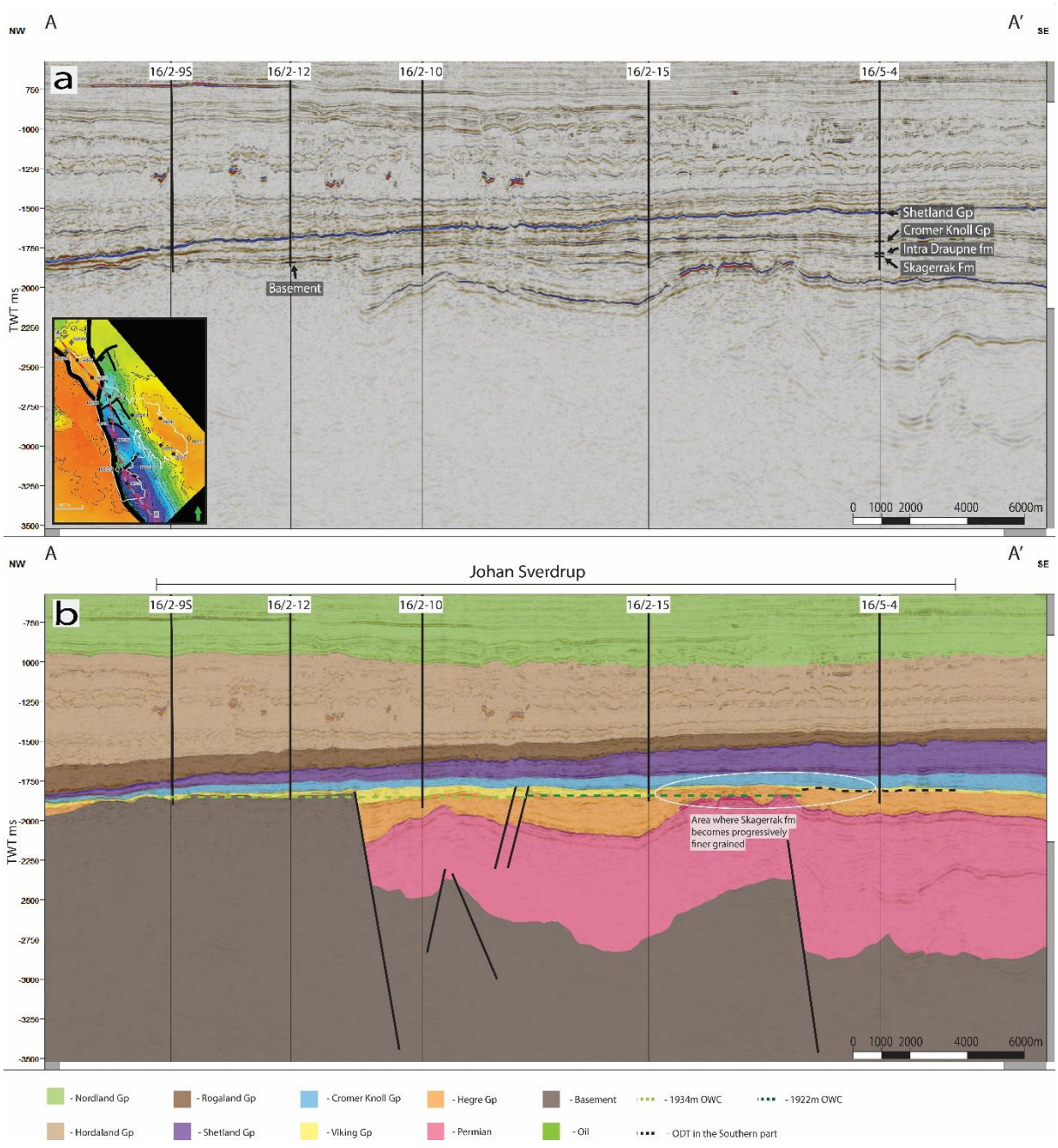

Figure 5.5.3: Uninterpreted (a) and interpreted (b) NW-SE seismic section of the Johan Sverdrup field

Seismic composite line B-B' (figure 5.5.5) shows (a) an uninterpreted and (b) interpreted seismic section from south-west to north-east showcasing the NW terrace. This figure shows that the south-west and north-east terrace is bounded by two faults. The to the south-west reservoir is juxtaposed against a basement of unknown reservoir quality. The north-east reservoir unit is juxtaposed with Cretaceous marls/shales.

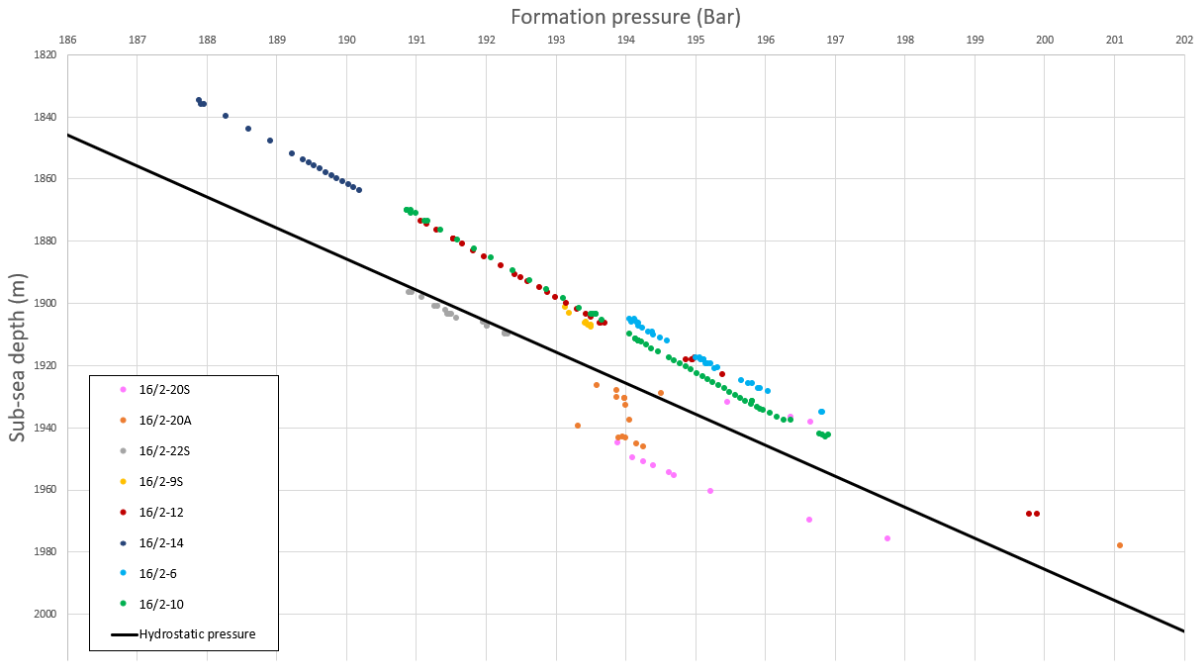

Figure 5.5.4: A combined formation pressure plot of all wells, sidetracks in the north-western terrace and three closest wells from the Augvald graben.

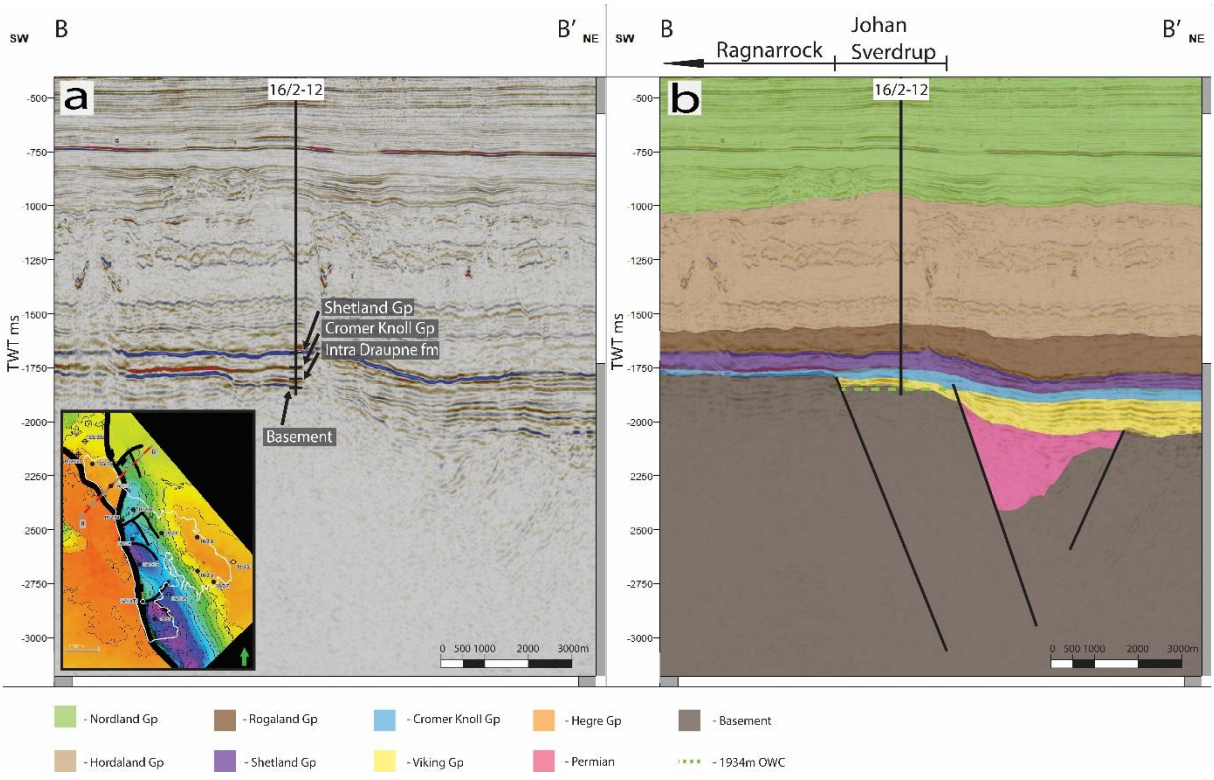

Figure 5.5.5: Uninterpreted (a) and interpreted (b) SW-NE seismic section of the Johan Sverdrup field, showing north-western terrace.

Augvald graben

The Permo-Triassic Augvald graben is bounded by the NW-SE trending normal fault to the south-west and by the Avaldsnes high to the north-east. The side sealing to the south-west is provided by the Augvald graben master fault. To the north west the Augvald graben is in

connection with the NW terrace. To all other sides, side seals are represented by dipping top seal. Observations within the Augvald Graben will be divided into 4 parts: northern, central, southern and eastern (figure 5.5.1). The regional OWC of around 1922m is present in most of the Augvald graben besides the northern part (16/2-10 and possibly 16/2-14).

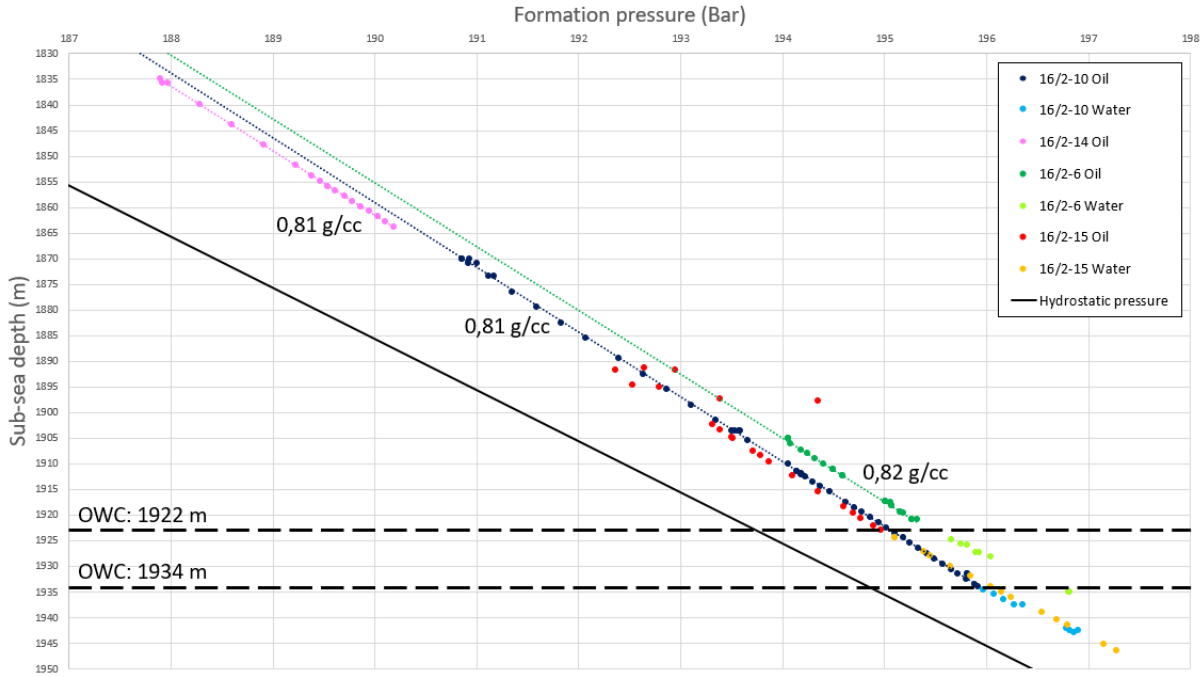

Figure 5.5.6: A combined formation pressure plot of all wells, sidetracks in the northern and central parts of the Augvald Graben.

The northern part has been separated from the central part based on the deeper contact found in the 16/2-10. 16/2-14's formation pressure has been measured in the oil column only. The oil gradient is similar to 16/2-10 and thus it can be assumed that OWC is possibly similar (figure 5.5.6). Seismic composite line C-C' (figure 5.5.7) shows (a) an uninterpreted and (b) interpreted seismic section from south-west to north-east showcasing northern most part of the Augvald graben. As this figure shows no barriers such as fault were observed between wells 16/2-10 and 16/2-14, reservoir properties are similar in both of the wells. Several minor faults were identified between the northern and central part (figure 5.5.3). Although throw along them should not be sufficient for sealing. The reservoir is similar in both northern and central parts. The completion report has

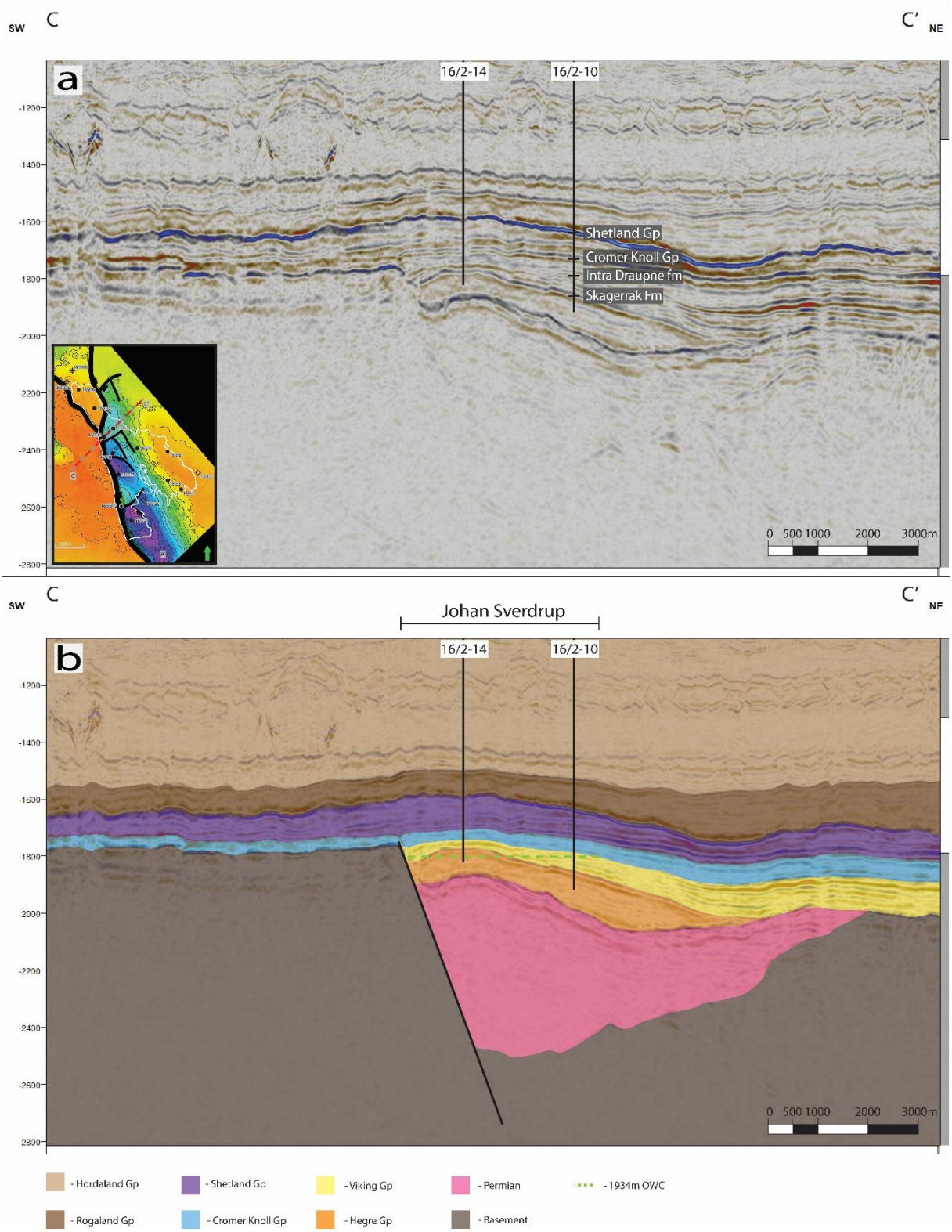

Figure 5.5.7: Uninterpreted (a) and interpreted (b) SW-NE seismic section of the Johan Sverdrup field, showing Augvald grabens northern part

Seismic composite line D-D' (figure 5.5.8) shows (a) an uninterpreted and (b) interpreted seismic section from south-west to north-east showcasing the central part of the Augvald graben. In the central part several faults were observed that are parallel with the Augvald

graben's master fault. Due to similar formation pressures and contact depths in the central parts wells these faults are not sealing.

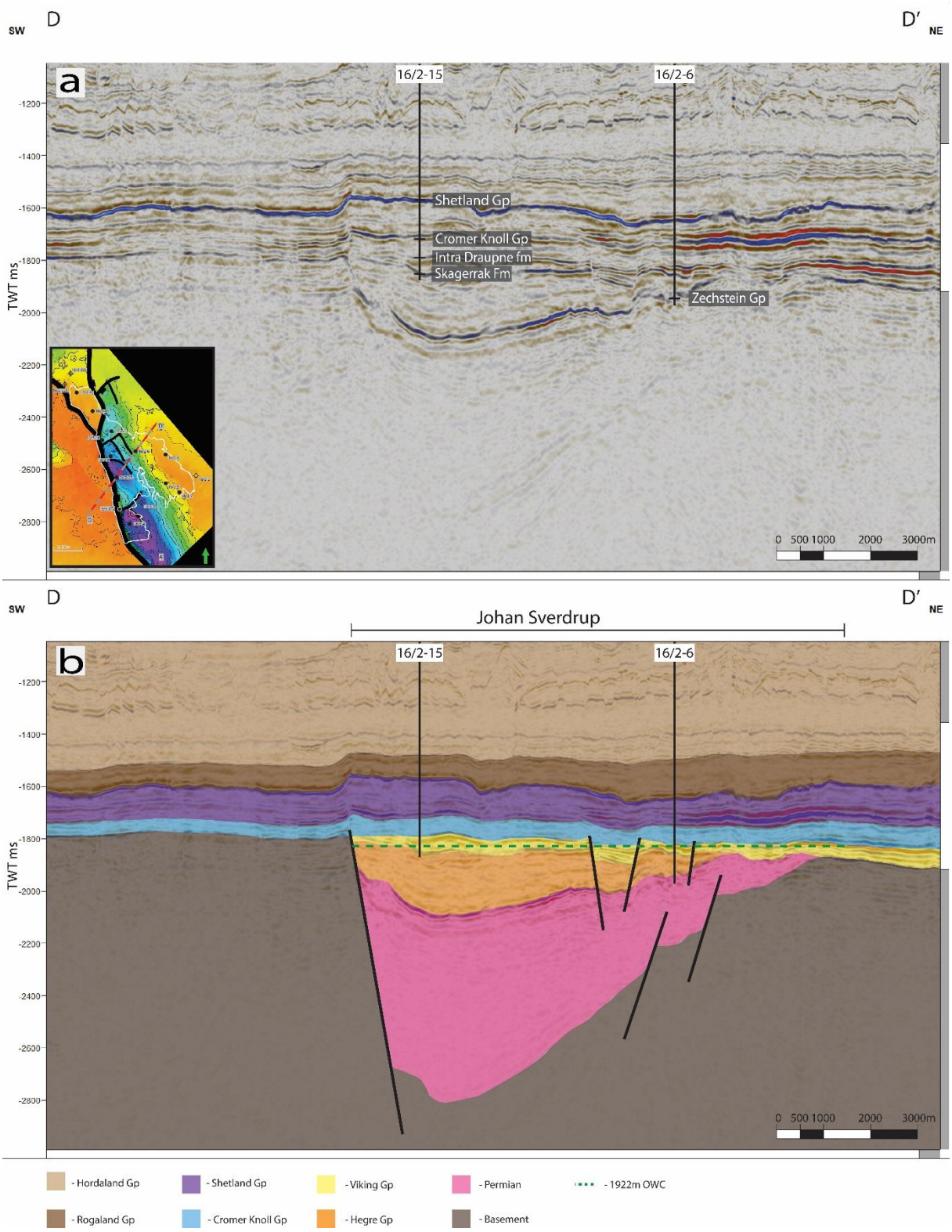

Figure 5.5.8: Uninterpreted (a) and interpreted (b) SW-NE seismic section of the Johan Sverdrup field, showing Augvald grabens central part

The seismic composite line E-E’ (figure 5.5.9) shows (a) an uninterpreted and (b) interpreted seismic section from south-west to north-east showcasing southern and eastern parts of the Augvald graben. Southern and eastern parts are differentiated based on a top reservoir deepening in between. This deepening was proven by the well 16/5-2S that drilled in this deeper part proving top of the reservoir beneath the common OWC of 1922m TVDSS (table 5.5.2). Unfortunately, this deepening is not observable on the BCU reflector in the time domain dataset that was used for this thesis. Thus, the field outline from the NPD was used. In the southern part, two wells have encountered ODT situations (table 5.5.2). In both cases Intra Draupne fm sandstones had similar reservoir properties and formation pressures to the rest of the Johan Sverdrup field, while underlying Skagerrak fm was proven to be tight unlike Skagerrak fm in other parts of the Johan Sverdrup. In the eastern part Intra Draupne is unconformably overlaying different Permian or Triassic sediments. Wells drilled in this part show that Intra Draupne fm is in pressure communication with the underlying sediments. No major faults were observed in both of these parts. Wells in the eastern part have proven shows beneath the oil column. Shows, especially, in well 16/3-7 are the deepest in whole field (table 5.5.2)

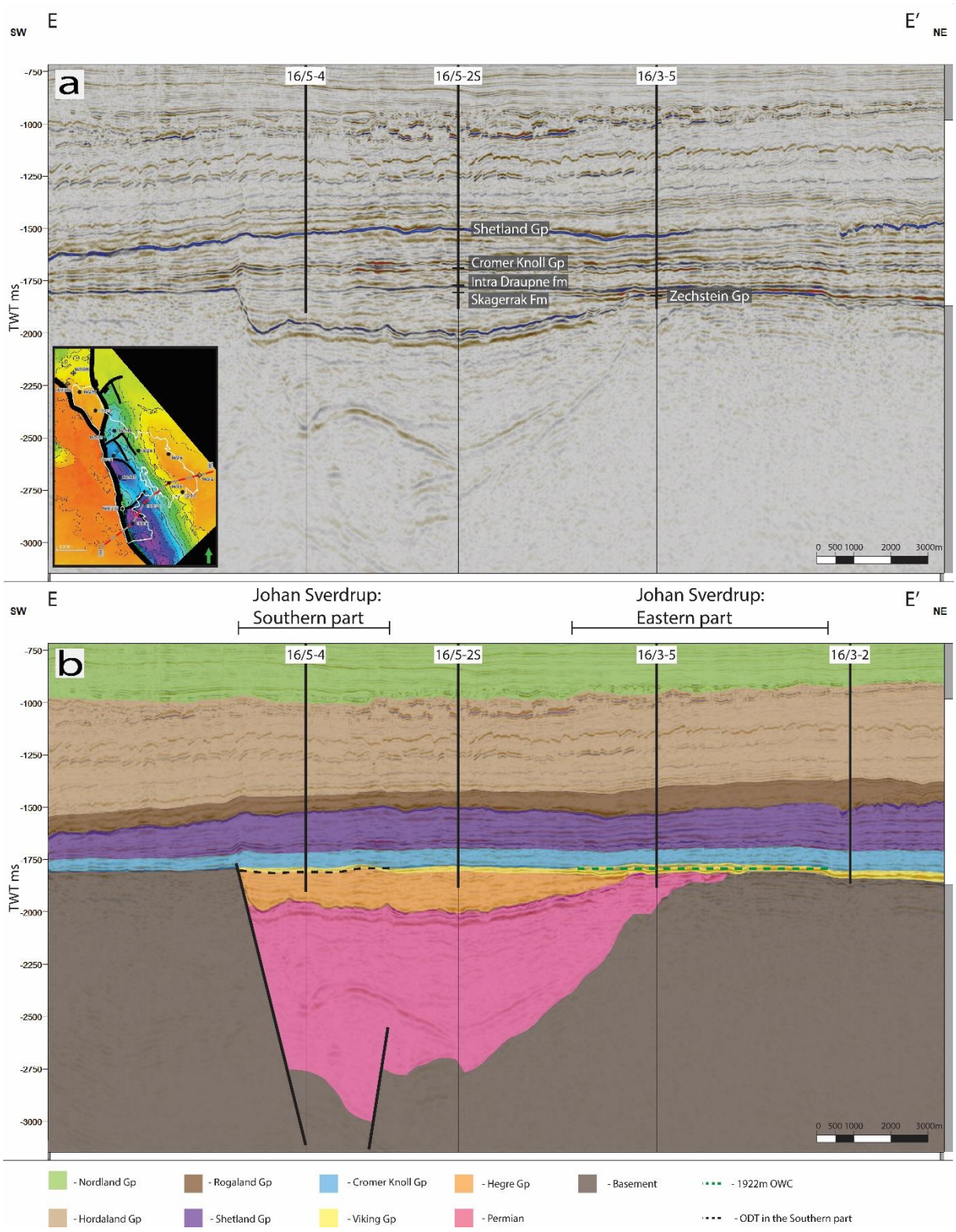

Figure 5.5.9: Uninterpreted (a) and interpreted (b) SW-NE seismic section of the Johan Sverdrup field, showing Augvald grabens southern and eastern part

6. Discussion

The purpose of this study was to investigate the geological constraints on the hydrocarbon contacts and the migration pathways in the Utsira High. A large variety of the fluid contacts, pressure regimes and structures have been identified within the six discoveries/fields located in the study area. Geochemical data has been used to identify the complicated migration history of the Utsira High. The chapter is divided into three sub-chapters. The first subchapter is describing the paleo-migration routes onto the Utsira High. The second sub-chapter proposes and explains the trapping mechanisms as well as models for migration. Finally, the third subchapter proposes and explains several migration pathways for filling the structures in the Utsira High, based on the results from the second subchapter.

6.1 Migration routes onto the Utsira High

The high-quality Jurassic source rocks are mostly absent on the Utsira High, but they are present in the numerous basins like the Stord Basin, the Ling Depression and the South Viking Graben surrounding the High. Several studies and exploration history highlight that the source rocks in the Ling Depression and the Stord Basin are mostly immature (Sørensen and Tangen, 1995, Kubala et al., 2003, Olsen et al., 2017, Hansen et al., 2020). Thus, the South Viking Graben is expected to be the primary source area for the hydrocarbons found on the Utsira High. This can be further proven by the vitrinite reflectance map (figure 6.1.1) of the top Draupne formation (age equivalent to the Kimmeridge clay). Considering that the type 2 kerogen enters the oil-window with a vitrinite reflectance of >0.7, the charge would need to happen directly from the west, south-west and/or north west. The Upper and Middle Jurassic Draupne and Heather formations are the main source rocks in the South Viking Graben. The older and deeper lying Heather formation is mainly gas-prone but has a good oil potential in some small sub-basins (Justwan et al., 2006). The

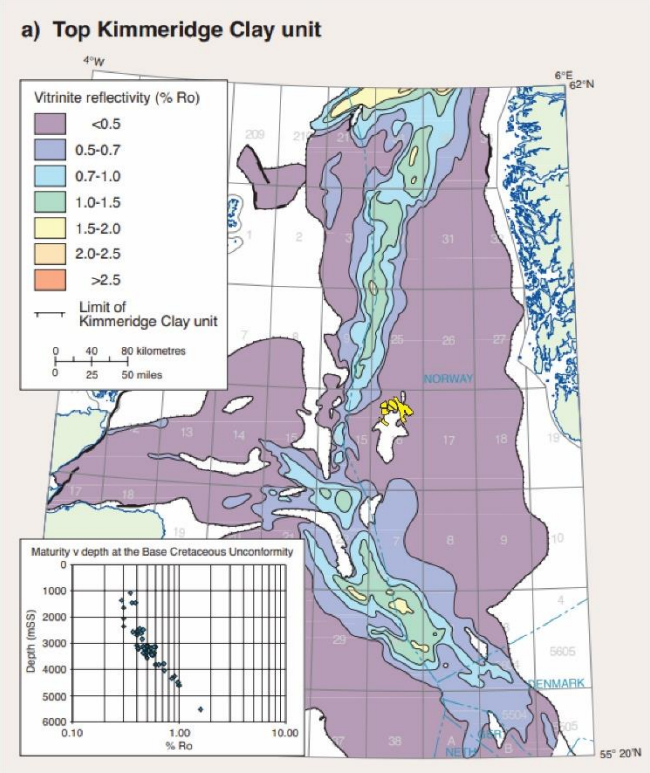

Figure 6.1.1: Top Draupne formation vitrinite reflectivity with fields from the study area (yellow). Modified from: Kubala et al., (2003)

overlying and younger Draupne formation is mainly oil-prone (Isaksen et al., 2002, Justwan et al., 2006). Geochemical data suggests that all hydrocarbons in all the fields/discoveries in the study area have been produced by the slightly different facies of the Draupne formation with kerogen type 2. The heather formation was suggested as a possible source rock for at least one of the biodegraded oil families in the Solveig field. Justwan et al., (2006) calculated the vitrinite reflectance for both formations, suggesting that the oil-window for both starts after 3500m for the Draupne shales and 3800m for the Heather shales.

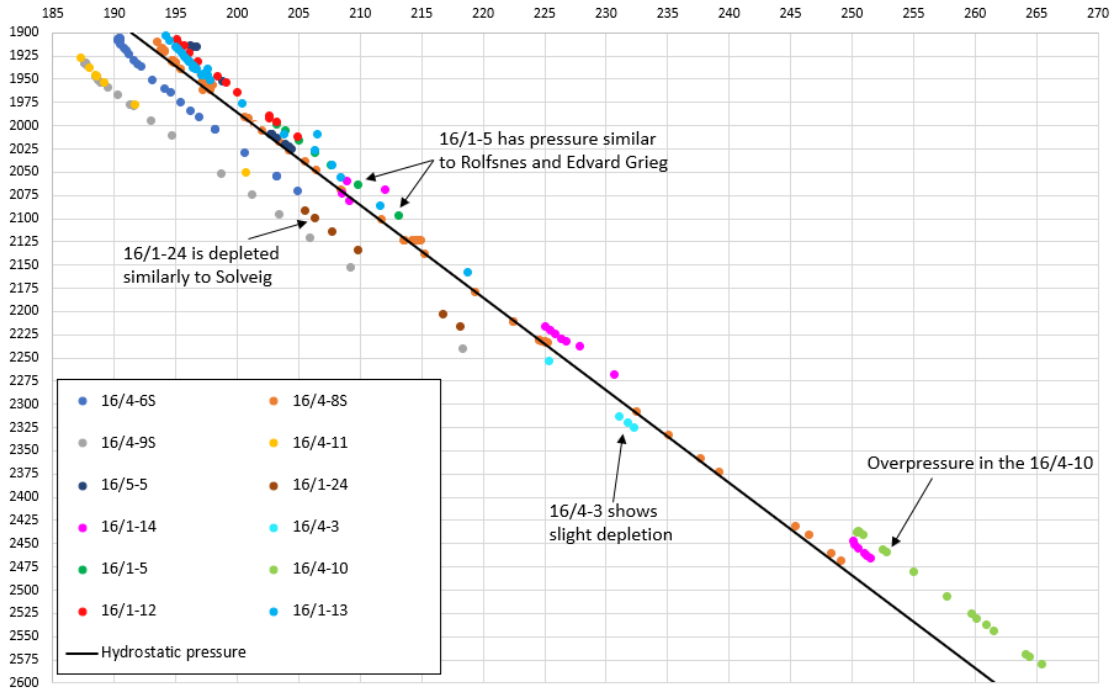

Figure 6.1.2: A combined formation pressure plot of all wells used for the analysis of the south-western migration routes (as shown in the figure 6.1.2) with reference to Edvard Grieg (16/1-13), Rolfsnes (16/1-12), Apollo (16/1-14), Solveig (16/4-6S, 16/4-8S, 16/4-9S and 16/4-11) and the hydrostatic pressure.

Several authors have written that the Utsira High has been the focal point for the hydrocarbon migration east of the Viking Graben (set sources). At least two periods of charge into the high have been identified. Early charge into the high has been observed in the compartments of the Solveig field as heavily bioturbated oil. The late charge is the one responsible for the filling of all the structures where non-biodegraded oil is found. There is a noticeable formation pressure difference between the Solveig field and the other fields to the north. Two compartments in the Solveig are pressure depleted while the rest of the Utsira High has the hydrostatic pressure (figure 6.1.2). There is a pressure boundary across the terrace right to the west from the Rolfsnes. As figure 6.1.2 shows wells 16/1-24 and 16/1-5 have 6 bar pressure difference, most likely due to depletion in well 16/1-24. A series of NW-SE trending faults are expected to be sealing considering that the reservoir in both

wells is of excellent quality (figure 6.1.3). Observed geochemical data also suggests that late charge potentially has been sourced from different source rocks within the South Viking Graben and thus must have had different migration pathways.

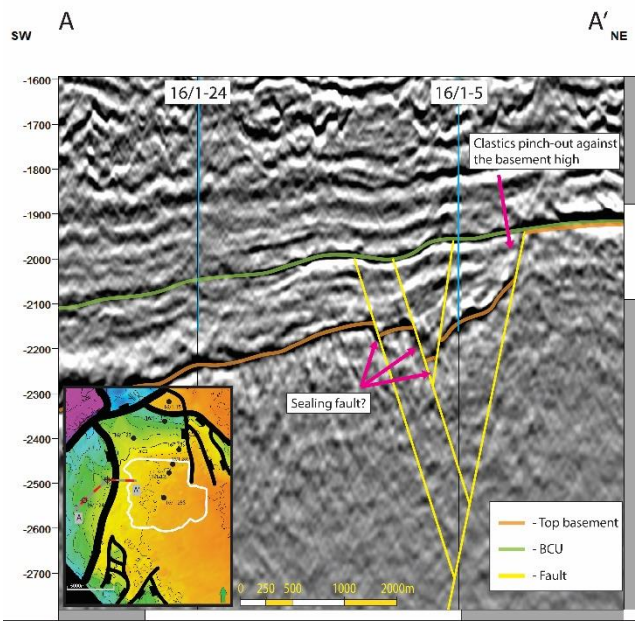

Figure 6.1.3: An interpreted SW-NE seismic section of the terrace west of the Rolfsnes field with several sealing faults between two wells 16/1-24 (depleted) and 16/1-5 (hydrostatic pressure)

South-western migration route

This migration route is located outside of the study area and it has been responsible for the filling of the Solveig field (figure 6.1.4). Solveig is the only field in the study area that has depleted formation pressure. The biggest pressure depletion is at around 8 bars, which most likely is caused by the regional pressure depletion caused by the production of the hydrocarbons. In addition to this the observed geochemical signature of the oil suggests a close affinity with the oil found in the Mesozoic reservoir in the Sleipner East field.

A total of 3 possible migration routes are proposed from the Sleipner East to the Solveig areas (figure 6.1.5a). The area between the Utsira High and the Sleipner Terrace is mainly characterized by the numerous minibasins that have been developed due to the salt movement in the Triassic (Jackson et al., 2010). The area has a complicated sub-BCU distribution of the sediments from both the Triassic and the Jurassic. The Triassic sequence in the wells usually consists of the Hegre group sandstones (Skagerrak and Smith bank formations) interbedded with shales (NPD, 2021). The Jurassic sequence consists of the Early-Middle Jurassic Vestland

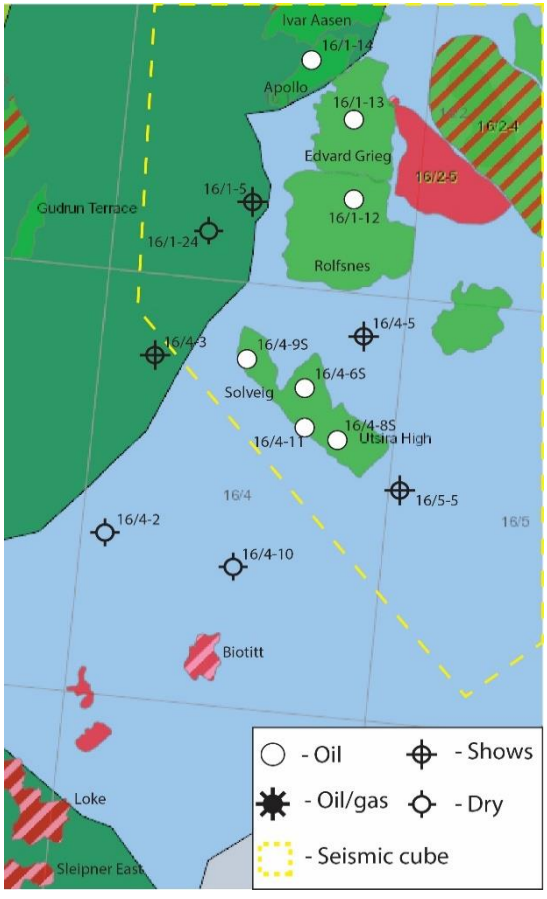

Figure 6.1.4: The map of the south-western margin of the study area (yellow stippled outline) showing location of the main discoveries/fields, location of the main structural elements (Utsira high=blue and Gudrun Terrace=green) and location of the wells that are used for the analysis of the south-western migration route. Modified from NPD (2021)

group sandstones (Hugin and Sleipner formations) overlain by the Middle-Late Jurassic shales of the Viking group (Heather and Draupne formations) (Jackson et al., 2010). Figure 6.1.2b shows the top Triassic time-structure map with possible migration routes. It is also important to note that the Jurassic sediments are filling in the minibasins with the BCU being fairly flat with a gentle dip towards the south west.

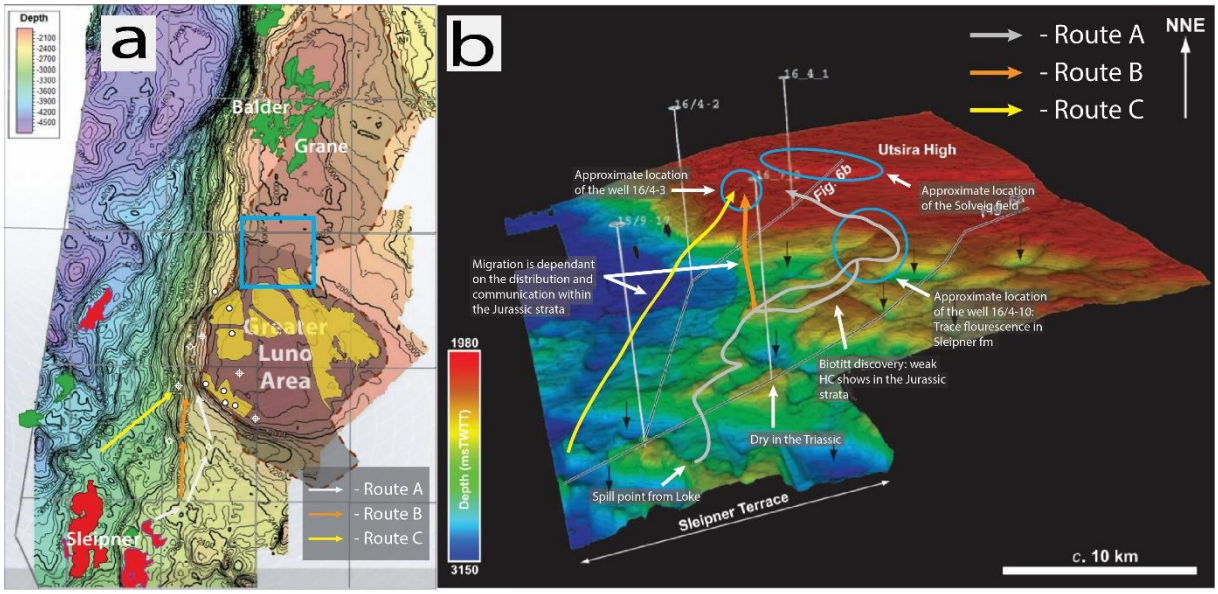

Figure 6.1.5: (a) Top BCU map of the South Viking Graben and the Utsira High with superimposed field outlines, wells used for this analysis as well as migration routes from the Sleipner area towards the high. The blue outline shows a flat area to the north-west of the study area. Modified from Rønnevik and Jørstad (2014). (b) Top Triassic map of the area south from the Utsira High with superimposed observations as well as migration routes (that are following the top BCU in figure 6.1.5a and thus are drawn just for representation). Modified from Jackson et al. (2010).

Route A is reflecting the migration along the top Triassic, since a map of the top Jurassic sandstones is not available. This route is the result of the spilling from the Sleipner East and the Loke fields towards the north-west. The route follows the structural highs. Available well information shows that there are hydrocarbon shows in the Jurassic or Triassic sediments at the highs along the route. Figure 6.1.5b shows the approximate positions of the observations made along the route. The route starts with a Loke discovery spilling towards the north-east, bypassing the 16/7-2 Paleocene discovery due to no recorded hydrocarbons in the Triassic. The route continues into the Biotitt discovery, where weak hydrocarbon shows were recorded in the Jurassic and spill towards the well 16/4-10 where weak fluorescence was recorded in the Jurassic. Northwards from the well 16/4-10 the top Triassic and the top BCU are fairly flat and thus the migration would be dependent on the reservoir quality as well as local barriers such as faults. It is important to note that formation pressures along the migration route would need to be depleted if the well was drilled after the production start in the Sleipner area. Unfortunately, not all well data was available from this area, but the formation pressure of the

well 16/4-10 was. As figure 6.1.2 shows there is an overpressure situation in the well 16/4-10 instead of an expected depletion.

Due to the overpressure situation along the route A, route B and C are considered to be more likely. With route B diverging from route A before the well 16/4-10 and tracking up-dip from the fault along the western margin of the minibasins. Following the BCU contours and the shallow top Triassic area to the east from route A as seen from figure 6.1.5 route C is tracking over the southern-western of the Utsira High in the area with the deep top Triassic. The margin of the Utsira High has been drilled by the well 16/4-3, proving hydrocarbon shows. The well has also proven a slight pressure depletion. This depletion, although smaller than in the Solveig, can be explained by the short time between the production start in the Sleipner area in 1993 and the drilling of the well in 1998 (NPD, 2021). Both route B and C would require migration through the Jurassic Vestland group since the top Triassic is too deep in the proposed migration routes. Figure 6.1.6 shows a geoseismic section of the seismic line 6b from the Jackson et al. (2010) paper, the location for this line can be seen in figure 6.1.5b. This figure shows that the SU1 unit comprised of the Hugin, Sleipner and Heather formations is continuous in the areas where the top Triassic is deepest and that it pinches-out to the north against the Utsira High thus making routes B and C viable options.

Overall, it is unknown what causes the elevated formation pressures along parts of the route A. It can be proposed that an early charge into the Solveig could have happened via this route with a later sealing of faults or changes in the reservoir. As for the late charge, it is certain that migration could not have taken place through the route A and the late charge would need to migrate through route B or C. There is also a possibility for other late charge routes to be open due to glacial tilting and subsequent rebound. This possibility is recognized by the author but has not been examined in detail.

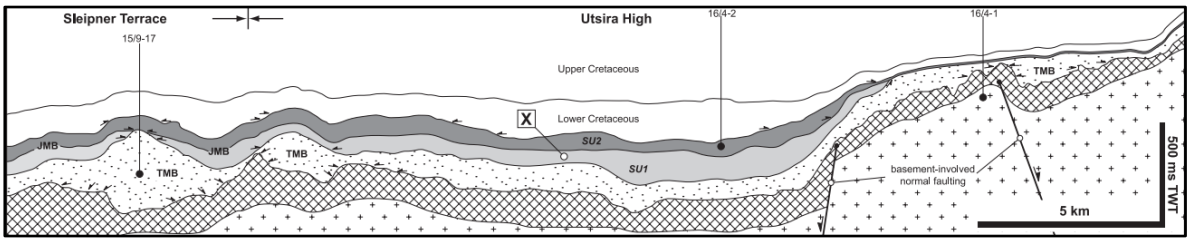

Figure 6.1.6: NE–SW trending geoseismic sections across the SW margin of the Utsira High. Modified from Jackson et al. (2010).

Western migration route

The possibility of the hydrocarbon migration from the South Viking Graben towards the Gudrun Terrace and the subsequent spill to the Utsira High from the west has been known before the first major discoveries in these areas were made (Kubala et al., 2003; Justwan, 2006).

Figure 6.1.7 shows the petroleum system map of the South Viking Graben with the blue arrows indicating Draupne formation drainage based on the top-Middle Jurassic geometry (Justwan, 2006). Two of the arrows marked in the figure are pointing directly towards the Gudrun Terrace and thus are assumed to be responsible for filling the Ivar Aasen field and the Apollo discovery downdip from the Edvard Grieg field on the westernmost point of the Utsira High (figure 6.1.4). Both fields/discoveries have deeper contacts below the BCU than the Edvard Grieg, 2406m TVD MSL in the Ivar Aasen and 2155m in the Apollo respectively (NPD, 2021).

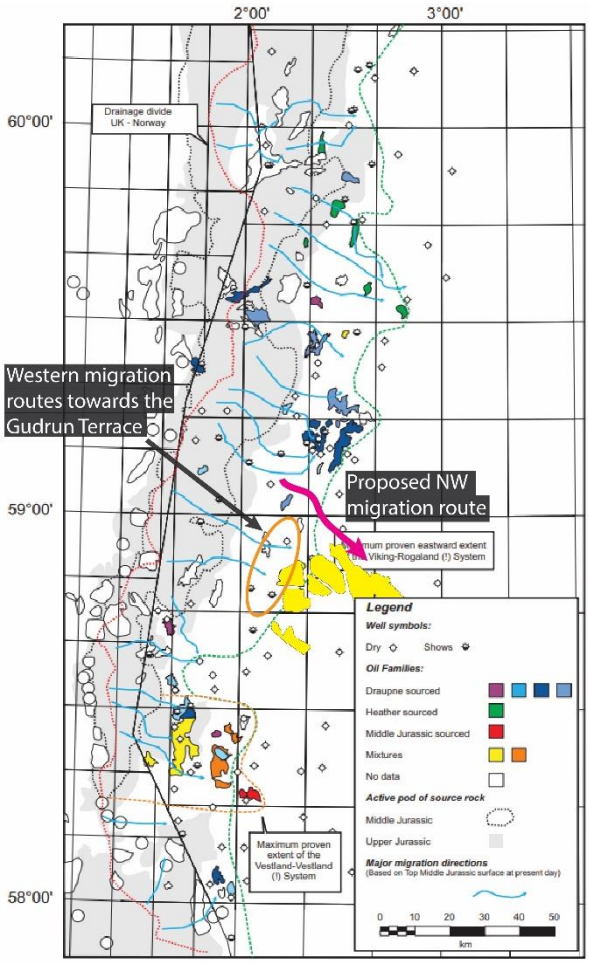

Figure 6.1.7: Petroleum systems map of the South Viking Graben showing major migration directions along the top-Middle Jurassic geometry showing western migration routes towards the Gudrun Terrace and the proposed north-western migration route. Modified from Justwan (2006).

North-western migration route

The migration into the Johan Sverdrup field has been one of the main questions since the start of the exploration of the Utsira High. This proposed migration route is part of the description of the migration route 2 from the "migration within the Utsira High" subchapter (figure 6.3.1). Since available regional migration maps such as figure 6.1.7 have been mostly made before the first discovery at the Utsira High in 2007, it can be speculated that some of the earlier interpretations could have been wrong. To the north-west from the Utsira High the migration directions are generally coming towards the Balder/Grane area. As figure 6.1.5a shows the BCU/top of the reservoir is flat between the Balder/Grane and the study areas. This area is outside of the available seismic cube and nothing has been written about it in the

literature. What is available, however, is information from the three wells that were drilled in the area: 25/11-17, 25/11-28 and 25/11-29S. All three have proven to be dry. Considering that as it is a general practice within the industry to drill the structural highs, it may suggest a conclusion that the hydrocarbons have not migrated through that area. At the same time there is no available map evidence to conclude that with certainty.

6.2 Utsira High migration models

The Utsira High is a unique area in the Norwegian part of the North Sea. The most prominent feature of the area is the permeable Caledonian basement. Before the discovery of the Rolfsnes, any granitic rocks observed in the North Sea were assumed to be impermeable and thus sealing. After the Rolfsnes discovery proved viability of the basement play, the combination of the basement and the clastic reservoir was considered to be an effective reservoir and/or fluid conduit. The clastic reservoir in the area is mainly represented by sandstones and conglomerates with little to no barriers for the fluid communication. Base seals are mostly absent and side seals are mainly represented by faults or pinch-outs against the basement. While the sealing faults have been explained in the background theory chapter, this subchapter will address the influence of the clastic reservoir pinch outs against the basement. But first, the migration through the fractured basement must be conceptualized.

The crystalline basement in the area is mainly represented by the gabbro, granodiorite, granite and metasediments and they have very low to non-existent primary porosities (Lie et al., 2016). Because of that the migration of the fluids through the basement is mainly dependent on the fractures. The basement in this area is highly fractured and weathered (Riber et al. 2015). Well-developed weathering profiles can be observed in some wells across the high, while in other wells the weathering profile is absent. The fractured basement is believed to have its highest significance as the migration paths, while the areas where the deep-weathered rocks are preserved can contribute as reservoirs (Riber et al. 2015).

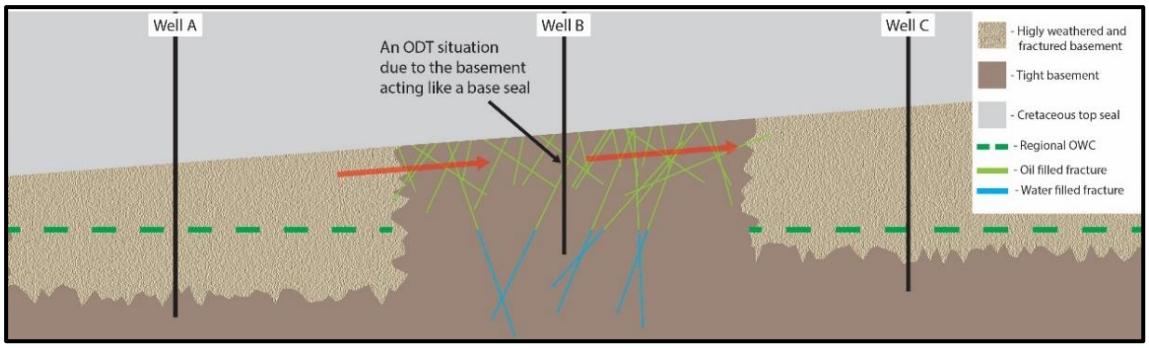

Figure 6.2.1: Simplified cross-section of the basement overlain by the sealing shales showing three wells (A, B and C) and migration between two areas with deeply weathered rocks through an area with interconnected fractures.

Figure 6.2.1 shows a simplified cross-section of the basement showing two deeply weathered areas being interconnected by the area with just fracturing. Each of the areas has been penetrated by a well as seen from the picture. The area penetrated by the well B is permeable in this case as all the fractures are interconnected. And while the OWC in both wells A and C will be similar, the situation in well B will be resembling an ODT situation since the fractures that this well is penetrating are not permeable to the depth of the local OWC. This makes the basement act as a base seal.

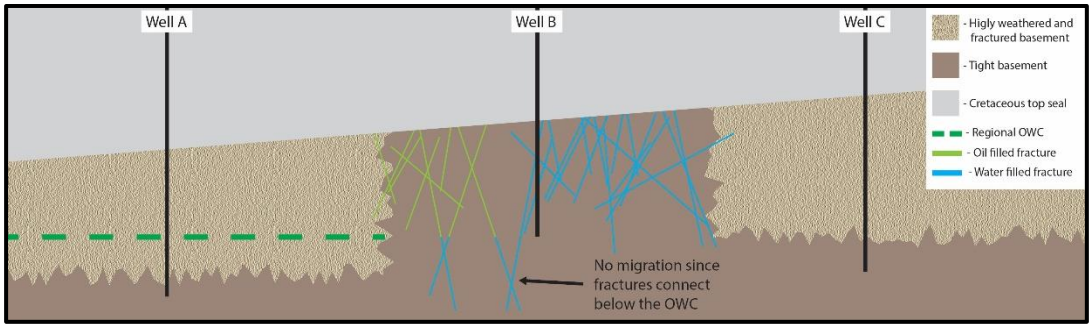

Figure 6.2.2: Simplified cross-section of the basement overlain by the sealing shales showing three wells (A, B and C) and no possible migration between two areas with deeply weathered rocks through an area with interconnected fractures.

Figure 6.2.2 shows a similar cross-section to figure 6.2.1, but in this case the fractures are not interconnected above the OWC in the well A area. Because of this the migration through the fractured area is not possible. This concept has to be also viewed in three dimensions. The Well C area must be surrounded by impermeable fractured areas to obstruct it from the hydrocarbon migration. The fracture connectivity can also be blocked because of the weathering by, for example, clay precipitation and poor permeability of the matrix between the fractured rock (Riber et al. 2015).

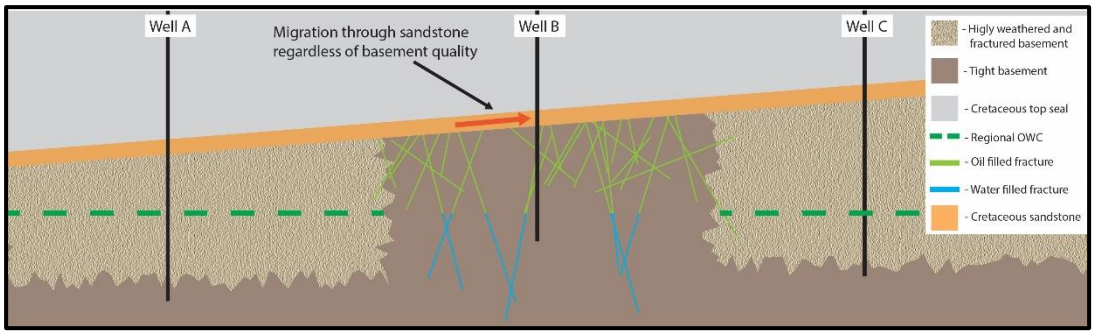

Figure 6.2.3: Simplified cross-section of the basement overlain by the Cretaceous sandstone showing three wells (A, B and C) and migration between two areas with deeply weathered rocks through an area with interconnected fractures.

Lastly, several wells in the Utsira High have reported the thin, transgressive Cretaceous sandstone to be overlying the basement. Figure 6.2.3 shows that areas where sandstones do overlie the basement they can act as conduits between the basement with reservoir properties, regardless of the interconnections between the fracture networks. Figure 6.2.4 shows sandstones are found in the western part of Haugaland High in the Rolfsnes and the Tellus discoveries and are completely absent in the central parts. Because of this, the model from figure 6.2.1 is seen to be most important for the migration across most of the high, while in the Rolfsnes and the Edvard Grieg sandstones are more important as fluid conduits. Unfortunately, it is not possible to map fracture networks with the available data. Despite that there are methods that can be utilized to effectively predict and map fracture networks on the Utsira High. The use of these has led to the discovery of, for example, Rolfsnes and Tellus (Lie et al., 2016).

Figure 6.2.4: Thickness map between the top reservoir (BCU) and the top basement showing thickness of the clastic sediments. Deep red represents areas where thickness of the clastic sediments is below the seismic resolution. White and blue circles represent wells penetrating the basement reservoir.

The hydrocarbons can enter the crystalline basement at the places where clastic reservoirs are juxtaposed against the basement. Figures 6.2.5a and 6.2.5b show the cross-section where the clastic sediments are directly pinching out against the permeable basement. In this case the charge would just continue freely onto the high and use fracture networks or overlying sandstones to migrate further. When the sediments are juxtaposed to the tight basement with no overlying sandstones the charge will have to continue laterally along the pinch out line (figure 6.2.5c). The lateral migration will continue until a barrier or a permeable area is reached. In that case the fluids would move into the basement until it is filled to spill and continue migrating along the pinch out line (figure 6.2.5d).

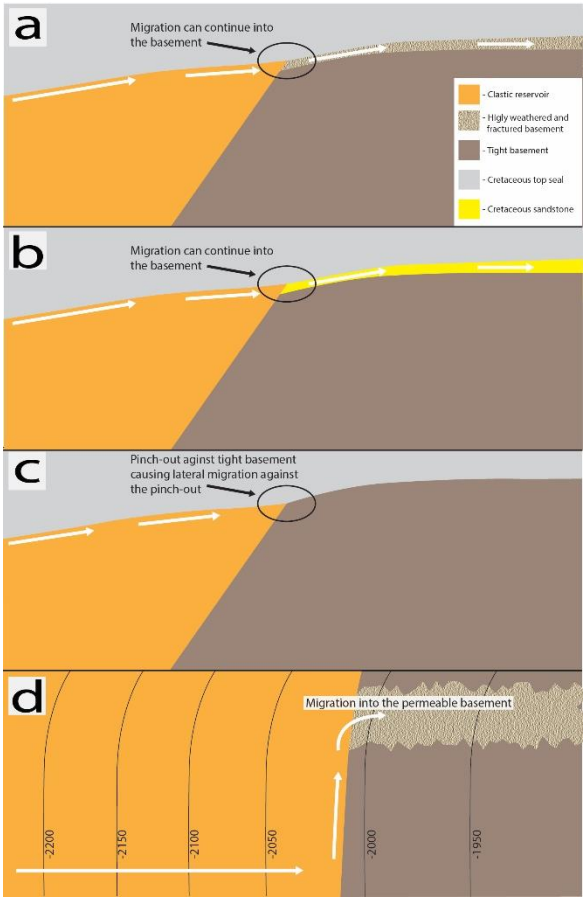

Figure 6.2.5: (a) A cross-section of reservoir pinch-out against the permeable basement. (b) A cross-section of reservoir pinch-out against the basement overlain by the Cretaceous sandstone. (c) A cross-section of reservoir pinch-out against the tight basement. (d) A map showing later migration along the reservoir pinch out.

6.3 Migration routes around the Utsira High

As concluded in subchapter 6.1 there are three possible migration routes onto the Utsira High. Taking into consideration the proposed points of the hydrocarbon entrance into the system, a map with potential migration routes between the fields and the discoveries around the Utsira High was made. Figure 6.3.1a shows the top reservoir (BCU) map with field outlines and five proposed migration routes between the fields. The Migration routes for each field will be explained together with likely spill directions based on the observation and other available data. Figure 6.3.1b shows the top reservoir map with field outlines and the location of five cross-sections that will be used in this sub-chapter.

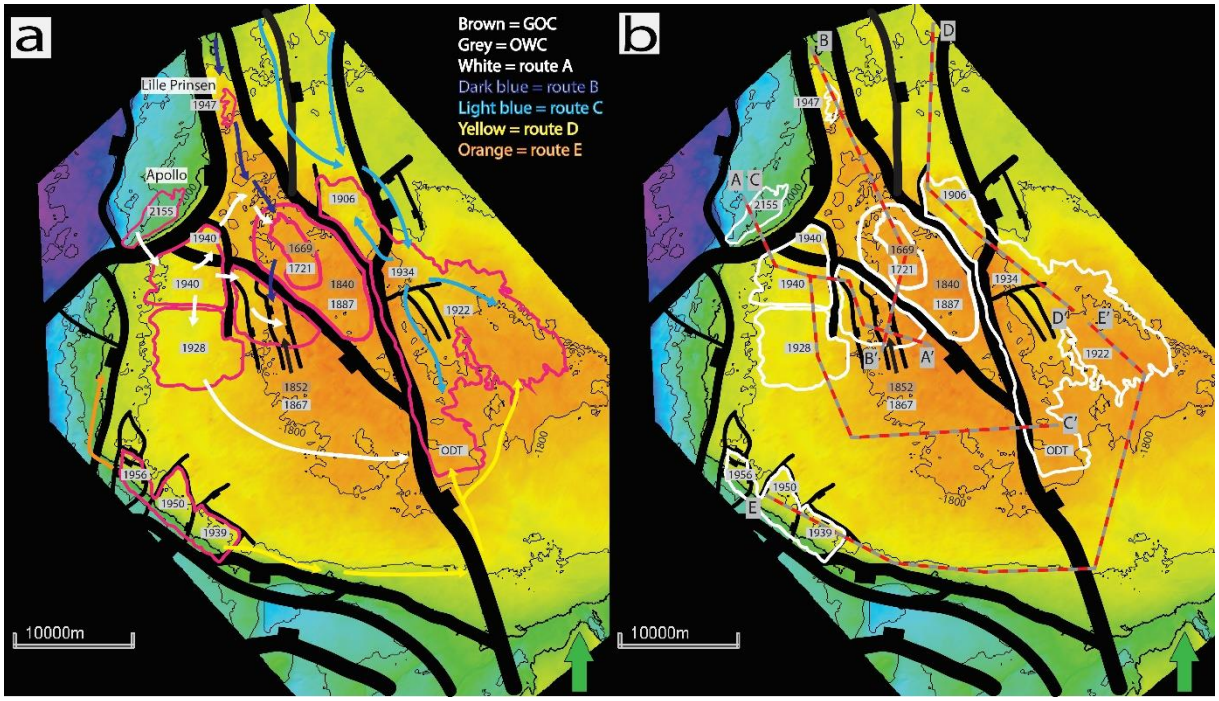

Figure 6.3.1: (a) Top reservoir (BCU) map with the field outlines (including the Apollo and the Lille Prinsen acquired from the NPD (2021)), the fluid contacts and the migration routes between the fields. (b) Top reservoir (BCU) map with the field outlines, the fluid contacts and location of the cross-section line A-A' (figure 6.3.3), cross-section line B-B' (figure 6.3.5), cross-section line C-C' (figure 6.3.7), cross-section line D-D' (figure 6.3.9) and the cross-section line E-E' (figure 6.3.10).

Route A part 1

The Edvard Grieg field has the deepest contact and is believed to be filled by the spill from one of the fields in the Gudrun Terrace. The closest field on the Gudrun Terrace is the Apollo, located down-dip from the west bounding fault that has two hydrocarbon columns, in the Paleocene and the Cretaceous. The water gradients of both fields are similar, suggesting a pressure communication as it can be seen from the figure 6.3.2. The Edvard Grieg has three potential spill points, northern, eastern and the southern (figure 6.3.1a)

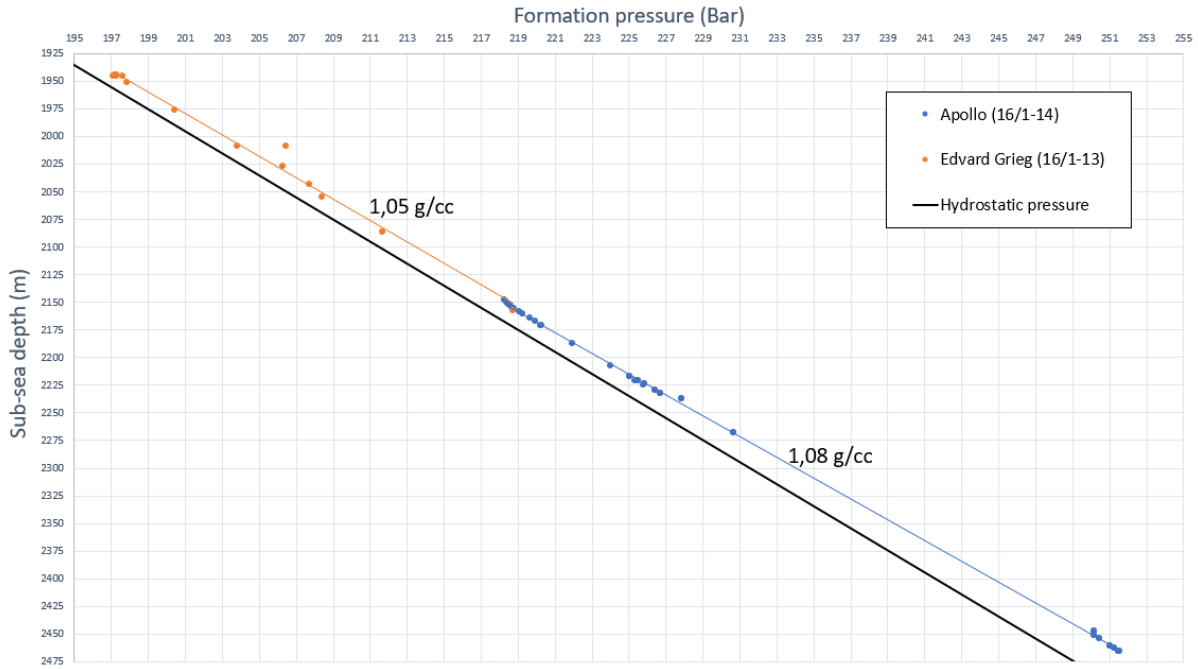

Figure 6.3.2: A combined formation pressure plot of water gradients in the Edvard Grieg and the Apollo fields.

The northern and the eastern spill points would spill the hydrocarbons towards the P-graben and the Ragnarrock basement discoveries. Both are around 4 bars over pressured in comparison to the Edvard Grieg field, suggesting a seal between the fields. The northern spill point requires connectivity with the fracture networks in the Ragnarrock. As per now the pressure differences suggest that the fracture networks are not in communication and it is unknown whether they have been in communication before. It is possible that stresses induced by the glacial rebound could have affected the connectivity.

The eastern spill point is controlled by the eastern bounding fault that is separating the Edvard Grieg field from the PB compartment in the P-graben penetrated by the well 16/1-17 (figure 6.3.3). There is a 2-bar pressure difference between the PB compartment and the Edvard Grieg

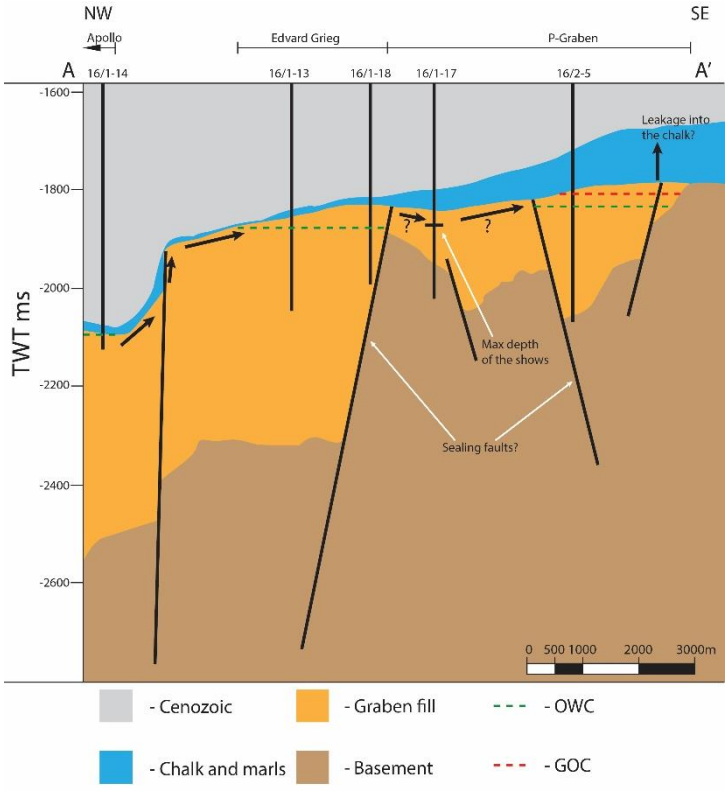

Figure 6.3.3: Simplified NW-SE cross-section A-A' showing migration from the Gudrun Terrace to the Utsira High.

(figure 5.2.6). Although there is evidence in form of oil shows in the well 16/1-17 that prove that the fault was not always sealing, and hydrocarbons could at some point migrate into the P-graben. The change in the sealing capacity can be attributed to the stresses caused by the glacial rebound that may have caused a fault reactivation. There is also no evidence of spill from the Johan Sverdrup field due to similar pressure difference as with the Edvard Grieg as well as absence of the sulphate in the formation water or the oil in the Ragnarrock or P-graben.

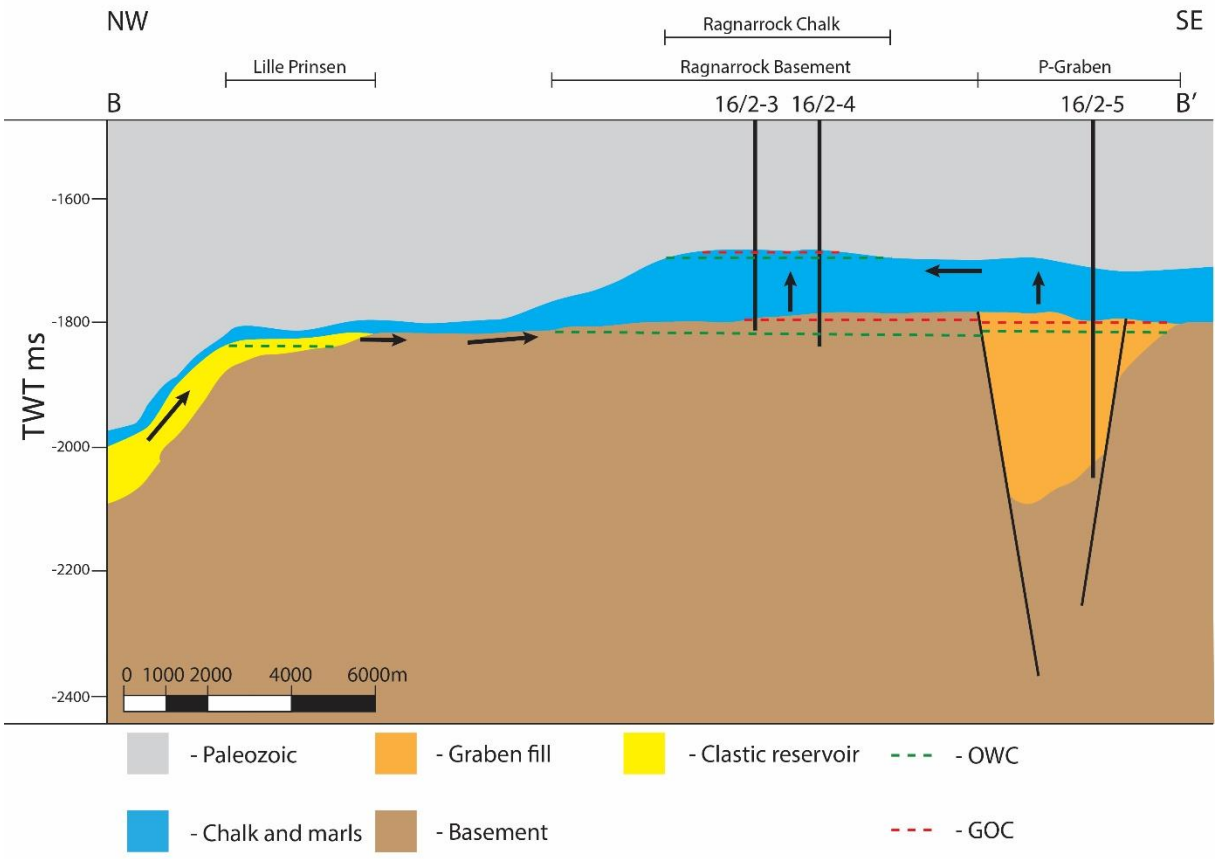

Figure 6.3.4: Simplified NW-SE cross-section B-B' showing migration from the Lille Prinsen discovery towards the Ragnarrock basement with subsequent spilling into the P-graben

Route B

To the north-west from the Ragnarrock basement there is the Lille Prinsen discovery located in the Permian sediments that are wedging down from a stretched basement high (figure 3.3.1a., NPD, 2021). Route B from the Lille Prinsen towards the Ragnarrock is shown in figure 3.3.4 and 3.3.1a. This route would require a permeable basement to be present between the discoveries. Figure 3.3.5 shows a formation pressure plot comparing the pressure between the Lille Prinsen's discovery well 16/1-29S (drilled in 2018) and the pressures from the Ragnarrock basement, P-graben and the Edvard Grieg. The figure shows that the reservoir in the Lille Prinsen is depleted either because of regional depletion or depletion due to the

production start in the Edvard Grieg. In any case it proves that Lille Prinsen and the Ragnarrock basement are not in communication. If the depletion in the Lille Prinsen is caused by the regional pressure depletion it would have been logical to expect some sort of depletion in the Ragnarrock. And if Lille Prinsen is depleted due to the production start in the Edvard Grieg it cannot be in communication, since the Ragnarrock and the Edvard Grieg are not in communication.

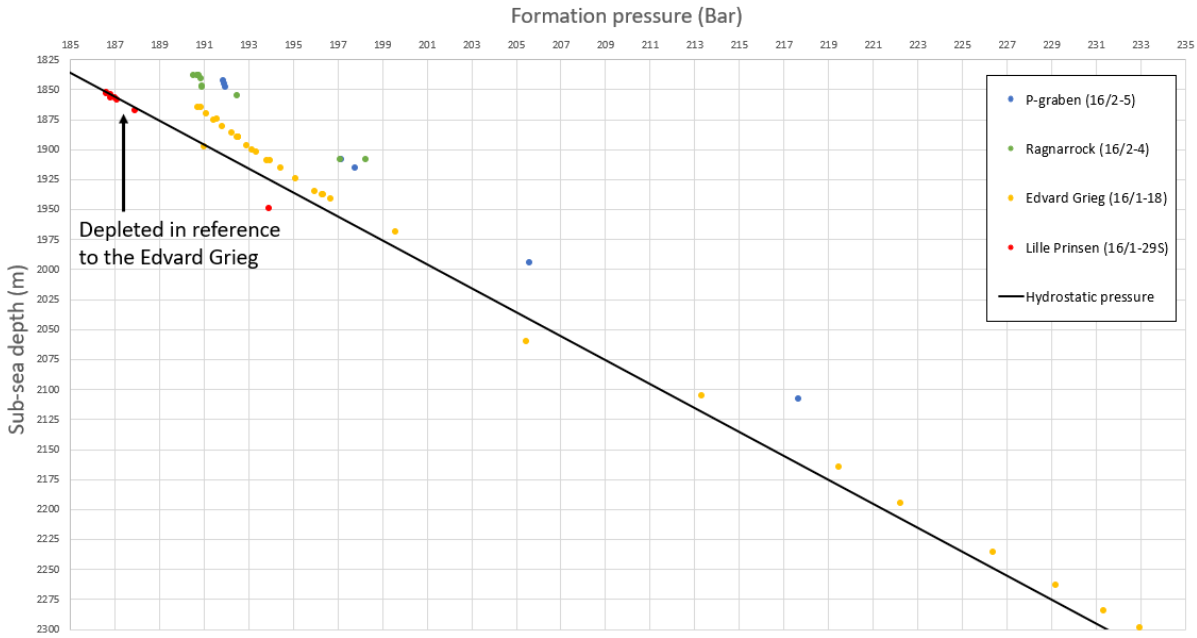

Figure 6.3.5: A combined formation pressure plot used for the comparison of the Lille Prinsen (16/1-29S) to the Edvard Grieg (16/1-18), Ragnarrock (16/2-4), P-graben (16/2-5) and the hydrostatic pressure.

The P-graben and the Ragnarrock basement are in pressure communication between each other but can be separated from the other fields due to an appeared pressure barrier forming its own pressure compartment. The overpressure within this compartment can be explained by the precipitation of the clay that is present between the pores in the conglomerate and in the basement fractures. There can be some smaller contributions to the overpressure, such as a temperature increase due to a steady subsidence since the Cretaceous. Overlying shales and marls are not mature to generate any hydrocarbons. At the same time regardless of the cause for the overpressure it is evident that both fields are laterally sealed from the other hydrocarbon accumulations. Differences in the contact depths can be attributed to the generally poor reservoir quality (especially in the P-graben) and thus there are big uncertainties regarding the contact depths.

Both discoveries are located at the apex of the Utsira High while also having the shallowest contacts. Due to an apparent lateral sealing, the leakage from the compartment could only

happen vertically. The top seal above the compartment is represented by a 20-30m of thick shale unit that is most likely sealing because of its thickness. Within the shale there are occasional marl and sandstone layers, which can in theory act as fluid pathways. There is no observable seismic evidence of the fault reactivation into the top seal allowing a potential leakage along the fault plane. It has to be mentioned that the Ragnarrock chalk oil exhibits similar properties to the oils observed along the migration route A, leaving the possibility for vertical leakage from the Ragnarrock basement and the P-graben (figures 6.3.3 and 6.3.4).

The main focus of this study was on the fields located in the Mesozoic and the basement reservoirs. Because of that the Ragnarrock chalk was not studied in much detail. Although the migration pathway as well as the history of the Ragnarrock chalk is uncertain, the possible spill route has been identified. Figure 6.3.6 shows a top Shetland Group map with wells where the hydrocarbon shows were observed in the chalk. The arrows show that there is a potential leakage towards the south-east from the Ragnarrock chalk. Shows in the wells 16/2-18S, 16/2-14 and 16/2-8 can confirm this pathway.

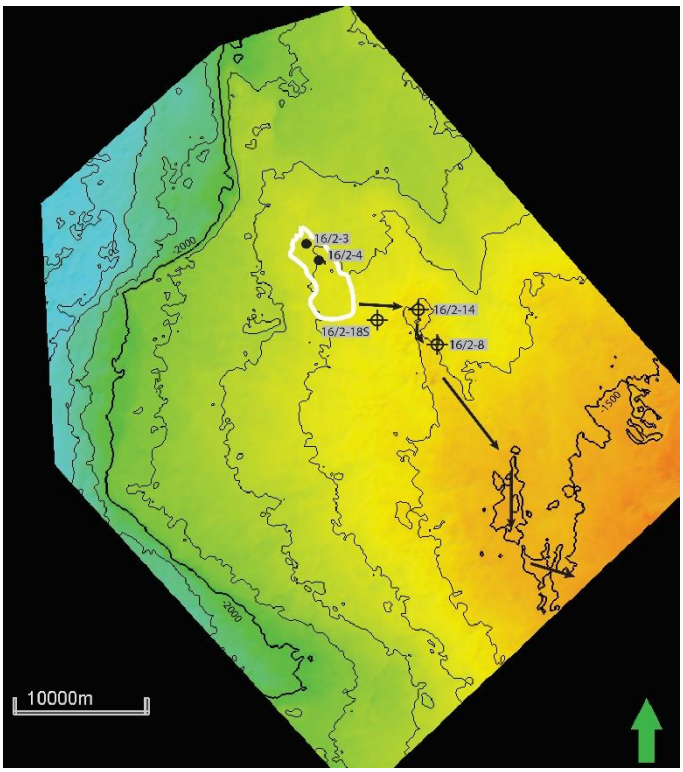

Figure 6.3.6: Top Shetland Group map with the outline of the Ragnarrock chalk (NPD, 2021), all the wells in the study area that have proven shows within the chalk reservoir and black arrows showing a proposed spill route out of the Ragnarrock chalk.

Route A part 2

Once the migration towards the Ragnarrock and the P-graben was not possible the hydrocarbons could spill to the south towards the Rolfsnes discovery. The Rolfsnes is separated from the Edvard Grieg by the pinch out of the Luno grabens sediments towards the basement high. As discussed in 6.2, for this pinch out to be permeable, a highly weathered and fractured basement or an overlying sandstone bed must be present. Luckily, both are present in the Rolfsnes as all of the wells have proven Cretaceous sandstone of varying thickness above the highly weathered and fractured basement. The pre- Edvard Grieg production pressure measurements in the Solveig have shown slight overpressure of around

0,5 bars compared to Edvard Grieg (figure 5.3.4). Variations of similar magnitudes are present between wells within the Edvard Greig field. Subsequent drilling of well 16/1-28S, that was drilled post the production start, has proven depletion in the Rolfsnes. Due to this it can be safely concluded that the Rolfsnes and the Edvard Grieg are in the pressure communication (figure 5.3.4). As it was mentioned in 5.3 the southern and the eastern boundaries of the Rolfsnes could not have been identified since the lateral sealing is dependent on the properties of the basement fracture networks. This is especially important since none of the basement wells east or south of the Rolfsnes have proven Cretaceous sandstone. Migration route A shows that if the basement is permeable there could be a potential pathway all the way across the Haugland High towards the Johan Sverdrup (figure 6.3.7). The Johan Sverdrup has a similar pressure regime as the Edvard Grieg and the Rolfsnes. In summer 2019, Lundin has made a discovery in the middle of the Haugland High. Unfortunately, the information from this well was not available for this study. But the discovery itself proves that the hydrocarbons can migrate into the central parts of the high, making migration across it possible.

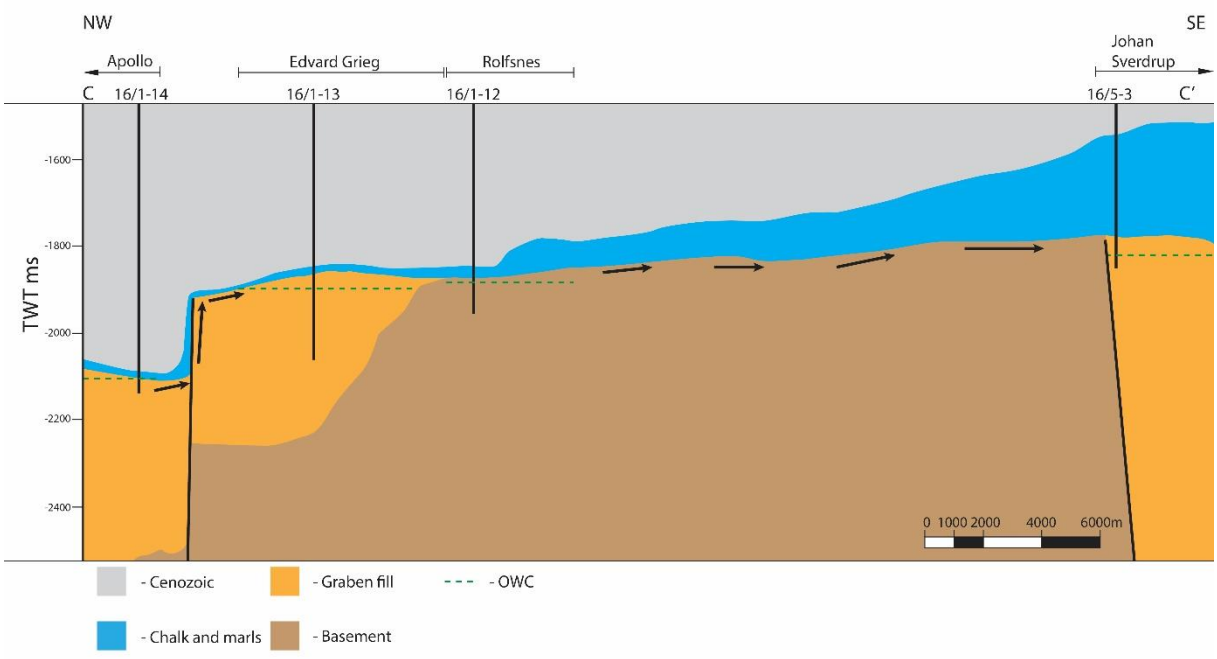

Figure 6.3.7: Simplified NW-SE cross-section C-C' showing migration from the Gudrun Terrace discovery towards the Johan Sverdrup field across the Utsira High.

Route C

Geochemical observations imply similar oil families in all the fields besides the Johan Sverdrup and the Solveig. As mentioned in the geochemistry subchapter, the slightly lower Pr/Ph ratios suggest different oil family from one in the Edvard Grieg field. At the same time

variations within the Johan Sverdrup are of similar magnitudes as the difference between the Edvard Grieg and the Johan Sverdrup. Because of this it cannot be concluded that oil in the Johan Sverdrup is different to the Edvard Grieg. In addition to the GOR and API are not reliable sources for the determination of the source rock. The unusually high sulphate content in the oil and the formation water across the Johan Sverdrup field can be attributed as a possible indicator for a different oil family. Ramstad et al. (2016) have speculated that the increased sulphate content in the Johan Sverdrup's formation water can be a result of (a) mixing of the formation water across the field over the geological time as well as (b) interactions with the underlying anhydrites of the Zechstein Group that were proven by several wells in the eastern part of the Johan Sverdrup. Both principals can explain the increased overall sulphate levels compared to the other fields, as well as a relatively lower sulphate concentration in the NW terrace of the Johan Sverdrup field because of the absence of the Permian evaporites and low velocities for fluid mixture. Because of these observations the Johan Sverdrup's oil family cannot be determined with certainty and thus migration from other migration pathways must be discussed in addition to the migration route A.

The route C is the continuation of the north-western migration route onto the Utsira High discussed in 6.1. In that part it was concluded that there is little evidence to suggest that hydrocarbons could enter the Utsira High from that side. This is mainly assumed due to several dry wells that have been drilled to the north-west of the study area. Within the study area there are several observations that are proving this. The deepest contact in the Johan Sverdrup field is in the northern part of the Augvald graben south from the NW terrace requiring migrating hydrocarbons to move downdip the fault that is bordering the NW terrace to the north-east (figures 3.6.1a and 5.5.1b). If the charge would move up dip it would need to enter the field through the northern boundary of the NW-terrace. The NW-terrace has the shallowest contacts in the whole field which can be explained by an

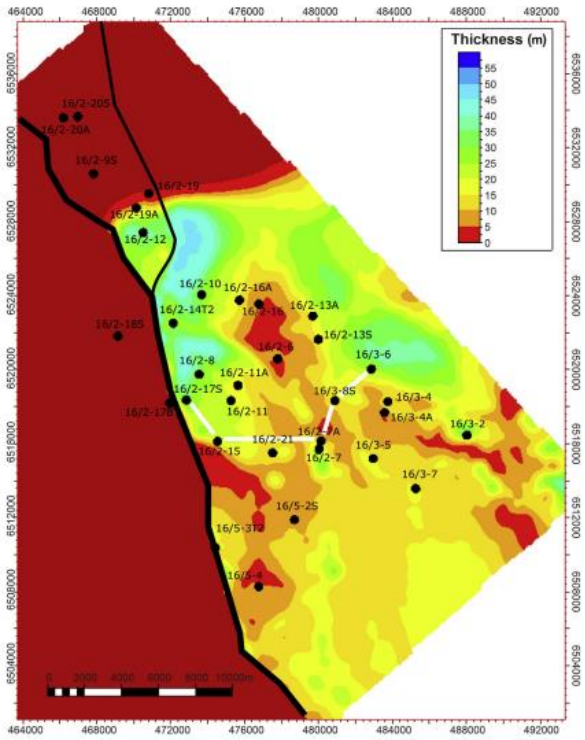

Figure 6.3.8: Intra Draupne fm isochore map. Adopted from Olsen et al., 2017.

unusual reservoir. The spiculitic sandstones have relatively high porosity while having low permeabilities with high capillary entry pressure (Olsen et al., 2017). This can result in a thick oil-water transition zone that is not reflecting the actual OWC. Figure 6.3.8 shows that there is a sudden decrease in thickness of the permeable sandstone in the NW-terrace between the wells 16/2-12 and 16/2-9S (figure 6.3.9). Even considering that the shallower OWC is not certain it still has to be mentioned that two wells, 16/2-20S and 16/2-22S, that have been drilled north of the NW-terrace are pressure depleted, meaning that there is a pressure barrier to the north of the NW-terrace. These facts combined make it unlikely for the route C to be responsible for filling of the Johan Sverdrup. Thus, route A is believed to be a more likely route to be responsible for filling of the Johan Sverdrup.

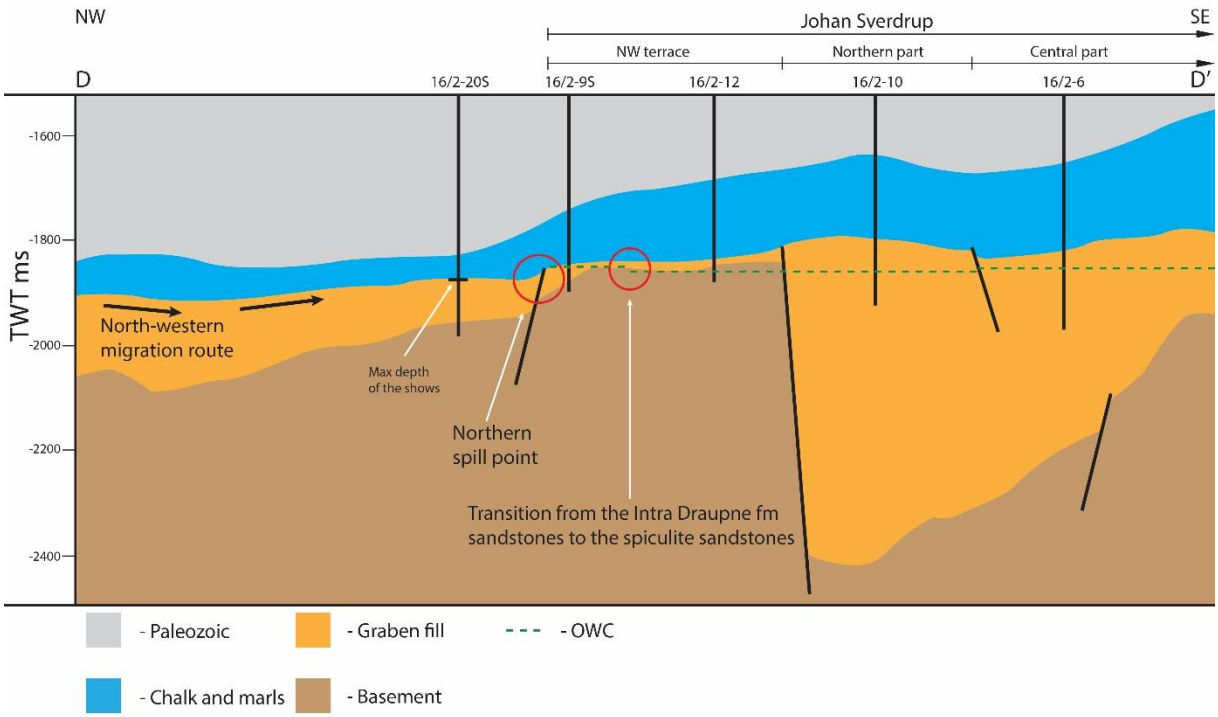

Figure 6.3.9: Simplified NW-SE cross-section D-D' showing migration pathway from the north-west towards the Johan Sverdrup field.

Route D

According to the geochemical observations from the Solveig field, it has a different migration history in comparison to the rest of the Utsira High. The Solveig unlike other fields has experienced an early charge that has biodegraded and later mixed with the newer charge that is of similar age with the charge that is responsible for the filling of the Edvard Greig field (Georgiev et al., 2021). Higher Pr/Ph ratios and other data in the Solveig suggest Draupne formation source rock with some influence from the terrestrial source rocks (Pfeiffer et al., 2016). Because of these marked differences the migration out of the Solveig must be viewed

on its own. Two possible spill points out of the Solveig have been identified, to the south-east (route D) and to the north-west (route E).

The Solveig field is divided into several pressure compartments that have different contact depths. A relationship between the pressure depletion and the contact depth can be observed, the pressure is lowest in the north-west where the OWC is deeper. Compartments with higher pressure have shallower OWC. Georgiev et al. (2021) writes that the mixing between the older and younger oil in the compartment D is in its earliest stages while the mixing in the compartment C is at a much later stage. Considering that the pressure depletion is regional and can be caused by the production from the other fields, it can be postulated that several pressure barriers are present in the area. Since the reservoir has generally a good quality, the faults are the obvious choice for the barriers. Fault seal properties in the field are not known but it can be speculated that they are partially sealing since the least depleted compartment has youngest oil. The charge into the field happened through the compartment B since it has the deepest contact. It has been depleted the most and it subsequently spilled into the compartment C, D and possibly E. Compartment A has not yet been drilled as per 2021 so it is unknown whether it contains any hydrocarbons (figure 5.4.3).

Route D shows a spill from the compartments D and E, which are in pressure communication, further to the south-east. The migration is to continue along the pinch out of the sediments package against the basement. The top of the basement as well as the BCU are dipping towards the south effectively dip-sealing the route. The hydrocarbons will start accumulating along this line as shown by the red circle in figure 6.3.10. In case the hydrocarbons can migrate into or across the basement there is a possibility for spilling into the Augvald Graben with migration towards the eastern part of the Johan Sverdrup, since the reservoir in the southern part is pinching out against shaly Triassic conglomerates. Despite the possibility the migration from Solveig into the Johan Sverdrup is seen as unlikely mainly due to different oil families and lack of biodegraded oil column in the Johan Sverdrup.

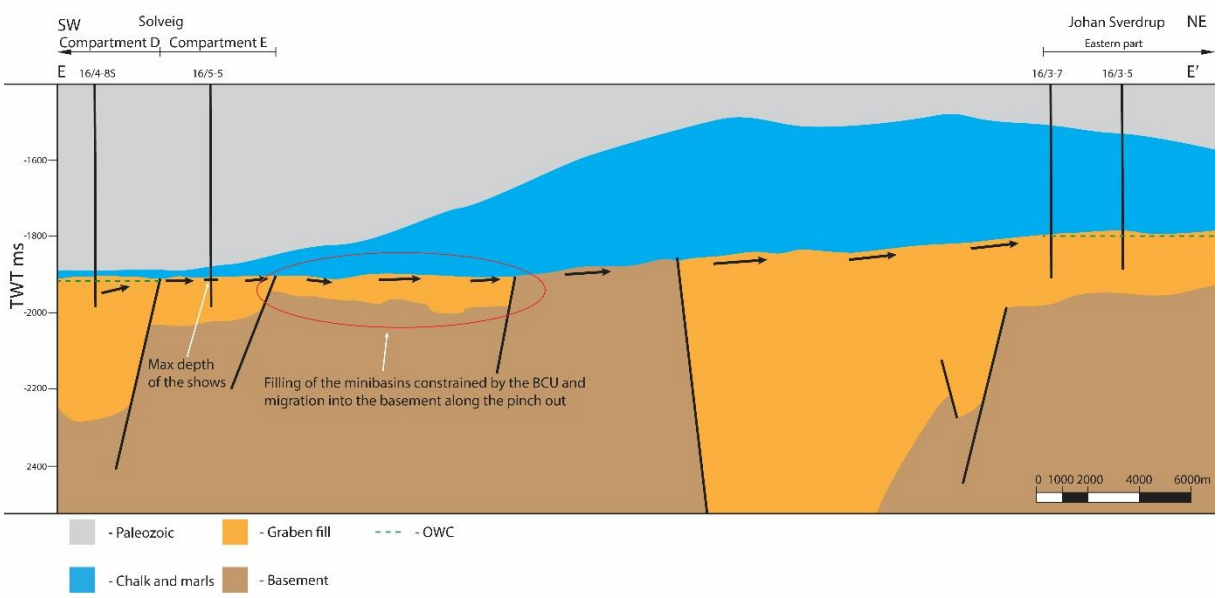

Figure 6.3.10: Simplified SW-NE cross-section E-E' showing migration pathway from the Solveig towards the basement high with a possible continuation over to the Johan Sverdrup.

Route E

Route E shows a spill point of the compartment B from the Solveig field towards the smaller terrace to the north-west (figure 3.6.1a). This terrace has been drilled by the well 16/1-24 which despite being dry has proven a depletion of around 6 bars. This observation makes it likely that the fault S1 from the Solveig field (figure 5.4.3a) is not sealing completely and partial pressure communication exist between compartment B and the terrace. As discussed in chapter 6.1, this terrace is divided by a fault into two parts with two distinctive pressure regimes (figure 6.1.3). Migration would subsequently happen along the pinch out with possible accumulation on the terrace or migration into the basement.

Spilling from the Johan Sverdrup

The Johan Sverdrup field has the shallowest OWC out of all fields that have close to hydrostatic pressure. Because of this a potential spill point from the Johan Sverdrup must be identified. Currently the Johan Sverdrup is not filled to the spill point. To the south-west the field is sealed by the Augvald graben master fault. The top of the reservoir is shallowest in the northern part of the Augvald graben forming a three-way dip closure, meaning that to all the sides besides the south-west the top of the reservoir will dip below the OWC. Vertical leakage through the cap-rock is most likely not possible due to considerable thickness of the shale (> 50m). To the south the top of the reservoir continuously dips all the way until the Ling Depression.

Two potential spill points are proposed, one in the eastern part of the field and one in the norther part of the field. The closest dry wells in each of these directions have proven top of the reservoir to be at 1948m TVD MSL to the east in well 16/3-2 (table 5.5.2). To the north wells 16/2-20S and 16/2-22S proved top reservoir to be 1945m and 1895m TVD MSL immediately down-dip from the faults that that bound the northern boundary of the NW-terrace (table 5.5.2). Figure 6.3.12 shows both potential spill points together with location of their closest dry wells. From the same figure it can be seen that the top BCU in the east is flattening out. Unfortunately, the top BCU in this location doesn't represent the top of the reservoir. Here the top BCU is represented by the Draupne fm shales that are overlying the top of the reservoir. The top of the reservoir in this location is not mappable due to sub seismic thickness of the overlying shales (around 25 meters) and according to data from the well 16/3-2 the top of the reservoir is deeper than in the north.

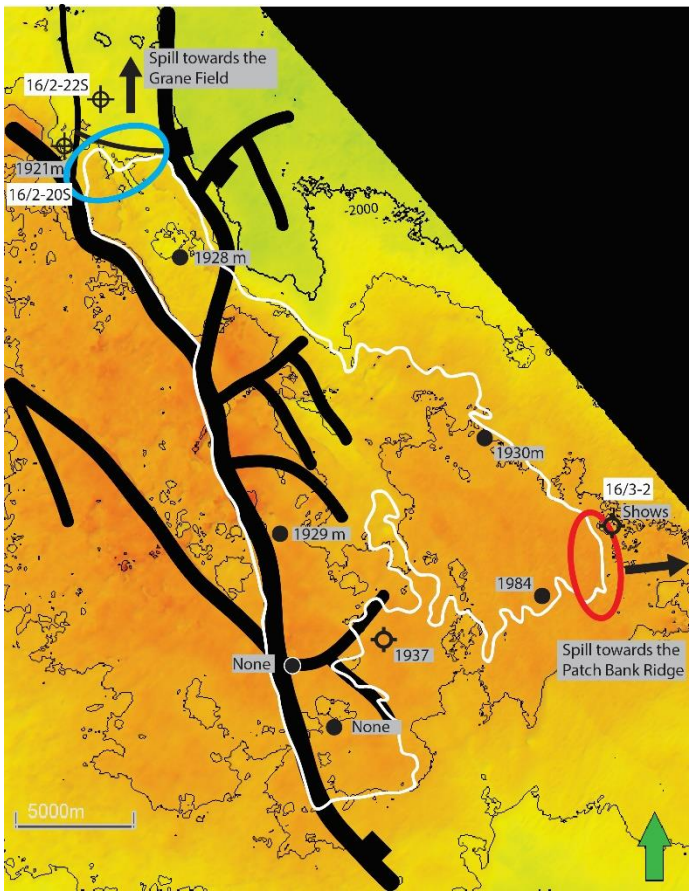

Figure 6.3.12: Top BCU map of the Johan Sverdrup field with faults, depths of the shows (grey) in TVD MSL and spill points. Blue circle is northern spill point and red circle is eastern spill point.

The northern spill point (blue circle in figure 16.3.12) represents a possible spill point towards the Grane field located in the northern Utsira High. In its essence the northern spill route is the inverted north-western migration route and route C described earlier in this chapter. The top of the reservoir is relatively flat all the way until the Grane field. The top of the Jurassic reservoir in the Grane's discovery well (25/11-15) is at 1959 TVD MSL (NPD, 2021). The top of the reservoir is deeper in the Grane field than it is along the eastern spill point. Relatively flat top reservoir makes the spill towards the north-west reasonably predictable. It also has to be mentioned that both wells drilled are pressure depleted in relation to the rest of the Johan Sverdrup field. Because of that it is likely that the faults bounding the field to the

north are sealing. The properties of the sealing faults are not known. This together with a deeper top reservoir along the spill route require the eastern route to be reviewed

The eastern spill point is marked by red circle in figure 6.3.12. This spill point is located deeper than the northern spill point. The top BCU in the area is flat but thickness of the Draupne fm shales are not known and cannot be mapped. In addition, the spill point is located close to the edge of the seismic data prohibiting the interpretation. Because of that a further spill towards the Patch Bank ridge cannot be evaluated with much confidence, due to lack of information from the area. There is very little information published on the Patch Bank ridge. The area is mostly undrilled and underexplored. Because of that there is a lack of publicly available maps that can aid with the interpretation of top of the reservoir outside of the available seismic data. Also, a possibility of previous spills towards the east must be reviewed in relation to the glacial tilting. The deepest shows have been recorded in the eastern side of the Johan Sverdrup. Deepest shows were recorded at depth of 1980m below the sea level. If interpreted to be a result of the glacial tilting, these shows can potentially indicate that some of the oil could have leaked through the eastern spill point. Stoddart et al., (2015) writes that the cores and fluids from the well 16/3-2 were reanalyzed by Fluid Inclusion Stratigraphy (FIS) and subsequent molecular geochemical analyses that proved trace oil shows close to the top of the reservoir. Overall interpretation of spilling towards the east is highly uncertain, due to lack of a map of the structures east of the Johan Sverdrup and public glacial tilting models.

The potential of a spill point to the south was not reviewed due to continuous dip of the top reservoir towards the Ling Depression. Wells that have been drilled within the Ling Depression have proven that the top of the reservoir is situated at around 2300m below the sea-surface (NPD, 2021). This makes spill towards the south highly unlikely.

Summary of the migration routes

The hydrocarbons are entering the Utsira High from the west and south-west in the Edvard Grieg and the Solveig fields, respectively. Solveig is not in communication with any other field in the area and has completely different migration history. The migration from the Solveig is most likely to occur to the north-west or to the south-east. The faults are controlling the migration of the hydrocarbons in the Solveig. Since the fault seal parameters are not know both migration routes are likely.

The Edvard Grieg has the deepest contact out of the fields located north of the Solveig. Migration from the Edvard Grieg towards the P-graben and Ragnarrock likely occurred in the

past. Currently fields are not in pressure communication, but their hydrocarbons show similar properties. Migration into the Ragnarrock from the Lille Prinsen discovery is unlikely due to formation pressure differences. The oil for the Edvard Grieg also migrates to the Rolfsnes discovery. Both accumulations have been interpreted to be in pressure communication. The Rolfsnes is also believed to be spilling towards the central parts of the Haugaland High and possibly all the way across to the Johan Sverdrup field. The Johan Sverdrup is believed to be sourced by the migration through the permeable basement since other proposed migration routes are not possible due to pressure barriers. Two spill points from the Johan Sverdrup were proposed, both have a lot of uncertainties attached. The eastern spill route seems to be most promising mainly due to good quality of the reservoir and likely absence of pressure barriers due to area being located over the Avaldsnes high.

7 Conclusion

The aim of this study was to investigate the migration routes in the Utsira High area in the northern North Sea. Detailed geological mapping has been conducted. The pore pressure measurements, fluid contacts and geochemical data from 57 wells has been collected and analyzed.

The main conclusions are:

- Three different migration routes into the Utsira High have been proposed based on the information from outside the study area. Two of the three migration routes have been interpreted to be responsible for filling of the different fields in the Utsira High area. The south-western migration route is responsible for filling the Solveig field with two individual oil charges, one late and one early. The western migration route is responsible for filling of the Edvard Grieg field and subsequent migration into the other fields around the area. The north-western migration route was concluded to not to be a likely charge route into the high, mainly due to absence of the hydrocarbons along the route as well as obvious pressure barriers.
- Several models were proposed describing the possible fluid migration mechanisms through the permeable basement. The migration in the permeable basement is mainly dependent on the interconnectivity between the fracture networks. Fluid migration along the pinch outs against the basement was explained. The migration is dependent on the ability of fluids to enter the basement high. Fluid accumulations can be expected in areas where the basement acts as side seal along the pinch out line.
- Five different migration routes have been proposed in the Utsira High area based on the seismic interpretation and the well data. The route A explains the filling of the Ragnarrock, P-graben, Rolfsnes and the Johan Sverdrup fields as a result of migration from the Edvard Grieg field. The route B provides an alternative for the migration into the Ragnarrock and the P-graben discoveries. This route is thought to be less likely responsible for the filling of these two discoveries, mainly due to pressure barriers along the migration route. The route C provides an alternative for the migration into the Johan Sverdrup field. This route is a continuation of the north-western migration route into the Utsira High. Because of that it is also thought to be an unlikely route for the migration into the Johan Sverdrup field. Routes D and E provide possible migration routes out of the Solveig field. Both routes are dependent on the fault seal properties as well as on continuity of the good reservoir.

8 Proposal for future work

There is a relatively high level of uncertainty regarding the charge history and the migration routes around the high. Possible future work is proposed to reduce the uncertainties encountered in this study.

- Analysis of the basement reservoir using different kinds of data, such as gravitational, magnetic, and reprocessed seismic, in order to successfully predict the basement reservoir properties.
- Development of better models for the migration through the basement reservoir.
- Modelling the tilting and the stress levels as a result of the Quaternary glaciations in order to predict possible migration routes towards the traps where the main risks are associated with the charge.
- Identification of the pressure barriers and processes responsible for their creation between the Edvard Grieg field, P-graben and the Ragnarrock.
- Investigation into possible long-distance migration into the Ragnarrock chalk from outside the area.
- Investigation of the charge history of the Solveig field and membrane seal faults that are separating the compartments creating pressure variations and slowing the hydrocarbon migration.

9 References

- Barnard, P., and Bastow, M., 1991. *Hydrocarbon generation, migration, alteration, entrapment and mixing in the Central and Northern North Sea*: Geological Society of London, Special Publications, v. 59, p. 167-190.
- Barton, C. A., Hickmanz, S., Morin, R., Zoback, M. D., and Benoit, D., 1998 *Reservoir-scale fracture permeability in the Dixie Valley, Nevada, geothermal field*, in Proceedings Society of Petroleum Engineers, Trondheim,p. 315-322.
- Berg, R. R., 1975, Capillary pressures in stratigraphic traps: AAPG Bulletin, v. 59, p. 939-956
- Buhrig, C. 1989. *Geopressured Jurassic reservoirs in the Viking Graben: modelling and geological significance.* Marine and Petroleum Geology, 6, 31-48.
- Chapman, R. E., 1972. Primary migration of petroleum from clay source rocks: AAPG Bulletin, v. 56, p. 2185-2191.
- Connan, J.,1984. *Biodegradation of crude oils in reservoirs*. In Advances in Petroleum Geochemistry. J Brooks, DH Welte (eds.). London: Academic Press, pp. 299–330
- Copestake, P, Sims, A P, Crittenden, S, Hamar, G P, Ineson, J R, Rose, P T and Tringham, M E. 2003. *Lower Cretaceous*. 191-211 In: Evans, D., Graham, C., Armour, A. & Bathurst, P. (eds) The Millennium Atlas: petroleum geology of the central and northern North Sea. Geological Society, London.
- Coward, M.P., Dewey, J.F., Hempton, M. & Holroyd, J. 2003. *Tectonic evolution*. 17-33 In: Evans, D., Graham, C., Armour, A. & Bathurst, P. (eds) The Millennium Atlas: Petroleum Geology of the Central and Northern North Sea. Geological Society, London, 17–33.
- Fyfe, J. A., Gregersen, U., Jordt, H., Rundberg, Y., Eidvin, T., Evans, D., Stewart, D., Hovland, M, and Andresen, P. 2003. *Oligocene to Holocene*. In: Evans, D., Graham, C., Armour, A. and Bathurst, P. (eds.), The Millennium Atlas: Petroleum geology of the central and northern North Sea. The Geological Society of London, p. 279-287.
- Færseth, R. B., 1996. *Interaction of Permo-Triassic and Jurassic extensional fault-blocks during the development of the northern North Sea*. Journal of the Geological Society, 153(6), 931–944.
- Frost, R., Fitch, F. & Miller, J. 1981. *The age and nature of the crystalline basement of the North Sea Basin*. In Illing, L.V. & Hobson, G.D. (eds.): Petroleum Geology of the Continental Shelf of North-West Europe, Heyden and Son on behalf of The Institute of Petroleum, London, pp. 43–57.

- Glennie, K.W., 1995. *Permian and Triassic rifting in northwest Europe*. In: In: Boldy, S.A.R. (Ed.), Permian and Triassic Rifting in Northwest Europe, vol. 91. Geological Society Special Publication, pp. 1–5.
- Glennie, K.W. and Underhill, J.R. 1998. *Origin, Development and Evolution of Structural Styles*. In: Glennie, K.W. (ed): Petroleum Geology of the North Sea: Basic Concepts and Resent Advances, Fourth Edition. Blackwell Science Ltd, 42-84.
- Glennie, K.W., Higham, J., and Stemmerik, L. 2003. *Permian.* In: Evans. D., Graham, C., Armour, A. and Bathurst, P. (eds.): The Millennium Atlas: Petroleum Geology of the Central and Northern North Sea. London: The Geological Society of London, 91-103
- Gregersen, U. and Johannessen, P. N. 2007. *Distribution of the Neogene Utsira Sand and the succeeding deposits in the Viking Graben area,* North Sea. Marine and petroleum geology, v. 24, p. 591-606.
- Head, I. M., Larter, S. R., Gray, N. D., Sherry, A., Adams, J. J., Aitken, C. M., Jones, D. M., Rowan, A. K., Huang, H. and Roling, W. F. M., 2010. *Hydrocarbon Degradation in Petroleum Reservoirs*. In: Timmis K.N. (eds) Handbook of Hydrocarbon and Lipid Microbiology. Springer, Berlin, Heidelberg
- Horstad, I and Larter. S.R., 1997. *Petroleum migration, alteration and remigration within Troll Field, Norwegian North Sea*. AAPG Bulletin, 81, 222-248.
- Isaksen, D., and Tonstad, K., 1989. *A revised Cretaceous and Tertiary lithostratigraphic nomenclature for the Norwegian North Sea*: Norwegian Petroleum Directorate Bulletin, 5, 59.
- Jackson, C.A.L., Kane, K.E. and Larsen, E. 2010. *Structural evolution of minibasins on the Utsira High, northern North Sea; implications for Jurassic sediment dispersal and reservoir distribution*. Petroleum Geoscience 16, 105-120.
- Johnsen, J. R., Rutledal, H., and Nilsen, D. E., 1995. *Jurassic reservoirs; field examples from the Oseberg and Troll fields, Horda Platform area*. Norwegian Petroleum Society, Special Publications, v. 4, p. 199-234
- Knipe, R. J., 1992, Faulting processes and fault seal, in R. M. Larsen, H. Brekke, B. T. Larsen, and E. Talleras, eds., *Structural and tectonic modelling and its application to petroleum geology*. Amsterdam, Elsevier, p. 325–342.
- Moss, B., Barson, D., Rakhit, K., Dennis, H., and Swarbrick, R., 2003, *Formation pore pressures and formation waters.* In: Evans. D., Graham, C., Armour, A. and Bathurst, P. (eds.): The Millennium Atlas: Petroleum Geology of the Central and Northern North Sea. London: The Geological Society of London, 317-329.

- Lambeck, K., Purcell, A., Zhao, J. and Svensson, N., 2010. *The Scandinavian Ice Sheet: from MIS 4 to the end of the Last Glacial Maximum*. Boreas, 39(2), pp.410-435.
- Lie, J.E., Nilsen, E.H., Grandal, E., Grue, K. and Sørlie, R. 2016. *A Successful Geophysical Prediction of Fractured Porous Basement Reservoir - Rolvsnes Oil Discovery 2015, Utsira High*. 78th EAGE Conference and Exhibition 2016.
- Ligtenberg, J. 2005. *Detection of fluid migration pathways in seismic data: implications for fault seal analysis*. Basin Research, 17, 141-153.
- Lundmark, A., Sæther, T. and Sørlie, R., 2013. *Ordovician to Silurian magmatism on the Utsira High, North Sea: implications for correlations between the onshore and offshore Caledonides*. Geological Society, London, Special Publications, 390(1), pp.513-523.
- Mahmic, O., Dypvik, H. and Hammer, E., 2018. *Diagenetic influence on reservoir quality evolution, examples from Triassic conglomerates/arenites in the Edvard Grieg field, Norwegian North Sea*. Marine and Petroleum Geology, 93, pp.247-271.
- Nystuen, J.P., Kjemperud, A.V., Müller, R., Adestål, V. and Schomacker, E.R. 2014. *Late Triassic to Early Jurassic climatic change, northern North Sea region: impact on alluvial architecture, palaeosoils and clay mineralogy*. IAS Special Publications 46, 59-100.
- Norwegian Petroleum Directorate (NPD). (2019). *Small oil discovery south of the Edvard Grieg field - 16/5-8 S* [Press release]. 29 August. Available at: https://www.npd.no/en/facts/news/Exploration-drilling-results/2019/small-oil-discovery-south-of-the-edvard-grieg-field---165-8-s/ (Accessed: 18 November 2020).
- NPD. 2018. *NPD Factpages and Factmaps* [Online]. The Norwegian Petroleum Directorate. Available: www.npd.no (Accessed January 2021).
- Nøttvedt, A., Johannessen, E.P., and Surlyk, F. 2008. *The Mesozoic of Western Scandinavia and East Greenland*. Episodes 31(1), 59-65.
- Olsen, H., Briedis, N. and Renshaw, D., 2017. *Sedimentological Analysis And Reservoir Characterization Of A Multi-Darcy, Billion Barrel Oil Field – The Upper Jurassic Shallow Marine Sandstones Of The Johan Sverdrup Field, North Sea, Norway.* Marine and Petroleum Geology 84, 102-134
- Osborne, M. J. & Swarbrick, R. E. 1997. *Mechanisms for generating overpressure in sedimentary basins: A reevaluation*. AAPG bulletin, 81, 1023-1041.
- Quigley, T. M. & Mackenzie, A. S. 1988. *The temperatures of oil and gas formation in the sub-surface*. Nature, 333, 549.

- Roden, R.,Smith, T. A.,Santogrossi, P.,Sacrey, D. and Jones, G. 2017. *Seismic interpretation below tuning with multiattribute analysis*. The Leading Edge 2017, 36 (4), 330–339.
- Slagstad, T., Davidsen, B. & Daly, J.S. 2011: *Age and composition of crystalline basement rocks on the Norwegian continental margin: offshore extension and continuity of the Caledonian-Appalachian orogenic belt*. Journal of the Geological Society of London 168, 1167– 1185.
- Sorento, T., Stemmerik, L. and Olaussen, S., 2018. *Upper Permian Carbonates At The Northern Edge Of The Zechstein Basin, Utsira High, Norwegian North Sea*. Marine and Petroleum Geology 89, 634-652
- Stoddart, D, Jorstad, A, Rønnevik, H C, Fjeldskaar, W, Fjeldskaar Løtveit, I. 2015. *Recent glacial events in the Norwegian North Sea – implications towards a better understanding of charging/leakage of oil fields and its impact oil exploration.* Presentation.
- Surlyk, F, Dons, T, Clausen, C K, and Higham, J. 2003. *Upper Cretaceous*. 213-233 In: Evans, D., Graham, C., Armour, A. & Bathurst, P. (eds) The Millennium Atlas: petroleum geology of the central and northern North Sea. Geological Society, London.
- Riber, L., Dypvik, H. and Sørlie, R., 2015. *Altered Basement Rocks on The Utsira High And Its Surroundings, Norwegian North Sea*. Norwegian Journal of Geology Vol 95 Nr. 1
- Ungerer, P., Bessis, F., Chenet, P., Durand, B., Nogaret, E., Chiarelli, A., Oudin, J., and Perrin, J., 1984. *Geological and geochemical models in oil exploration; principles and practical examples*, in Demaison, G., and Murris, R. J., eds., Petroleum Geochemistry and Basin Evaluation, AAPG, Memoir, 35, p. 53-77.
- Vollset, J. & Doré, A.G. 1984. *A revised Triassic and Jurassic lithostra - tigraphic nomenclature for the Norwegian North Sea*. Norwegian Petroleum Directorate Bulletin 3, 53
- Waldo, G. S., Carlson, R.M.K., Moldowan, J.M., Peters, K.E. and Penner-hahn, J.E., 1990. *Sulfur speciation in heavy petroleums: Information from X-ray absorption near-edge structure*, Geochimica et Cosmochimica Acta, 55, pp. 801-814
- Watts, N., 1987, *Theoretical aspects of cap-rock and fault seals for single- and two-phase hydrocarbon columns*: Marine and Petroleum Geology , v. 4, p. 274–307.
- Whipp, P., Jackson, C., Gawthorpe, R., Dreyer, T., and Quinn, D., 2014, *Normal fault array evolution above a reactivated rift fabric; a subsurface example from the northern Horda Platform, Norwegian North Sea*: Basin Research, v. 26, p. 523-549.
- Wiprut, D., and Zoback, M. D., 2000, *Fault reactivation and fluid flow along a previously dormant normal fault in the northern North Sea*: Geology, v. 28, p. 595-598.

- Wiprut, D., and Zoback, M. D., 2002, *Fault reactivation, leakage potential, and hydrocarbon column heights in the northern North Sea*: Norwegian Petroleum Society, Special Publications, v. 11, p. 203-219
- Yielding, G., Freeman, B. and Needham D. T. 1997. *Quantitative Fault Seal Prediction*. AAPG Bulletin 1997, 81 (6), 897–917.
- Zanella, E. and Coward, M.P. 2003. *Structural framework*. In: Evans. D., Graham, C., Armour, A. and Bathurst, P. (eds.): The Millennium Atlas: Petroleum Geology of the Central and Northern North Sea. London: The Geological Society of London, 45-59.
- Ziegler, P.A., 1990. *Tectonic and palaeogeographic development of the North Sea rift system*. Tectonic Evolution of the North Sea Rifts (Ed. by D.J. Blundell & A.D. Gibbs). Oxford: Oxford University Press, 1– 36.
- Ziegler, P.A. 1992. *North Sea rift system*. Tectonophysics, 208, 55–75.